Functional Characterization of Serine Hydrolases Mediating Lipid Metabolism and Protein Depalmitoylation in Asexual Stage *Plasmodium Falciparum*

Jiapeng Liu

Dissertation submitted to the faculty of the Virginia Polytechnic Institute and State University in partial fulfillment of the requirements for the degree of

Doctor of Philosophy
In
Biochemistry

Michael Klemba, Chair
Kylie Allen
Brandon Jutras
Jinsong Zhu

April 28, 2023
Blacksburg, VA

Keywords: *Plasmodium falciparum*, malaria, serine hydrolase, depalmitoylase, lysophospholipases

Functional Characterization of Serine Hydrolases Mediating Lipid Metabolism and Protein Depalmitoylation in Asexual Stage *Plasmodium Falciparum*

Jiapeng Liu

ABSTRACT

Malaria is an infectious disease caused by *Plasmodium* parasites and transferred by *Anopheles* mosquitos. Due to Artemisinin resistance, new druggable targets identification and new drug development are urgently needed. Serine hydrolases (SHs) are one of the largest classes of enzymes having important roles in life processes. The deadliest malaria parasite, *P. falciparum*, encodes more than 50 SHs including proteases, lipases, esterase and others, while only several of them have been characterized. The study of uncharacterized SHs will shed light on future drug development to treat malaria. In this study, we applied chemical biology and genetic approaches to identify SHs important for the pathogenic asexual stage growth of *P. falciparum* parasites. We mainly focused on a depalmitoylase essential for merozoite invasion and lysophospholipases (LPLs) essential for acquiring fatty acids (FAs) from the host.

Identifying essential metabolic enzymes will benefit the treatment to malaria. We focused on metabolic SHs and identified two SHs were refractory to knock out. We studied a likely essential SH named PfABHD17A, which is a human depalmitoylase homolog. PfABHD17A is localized on the rhoptry, an organelle essential for invasion. We expressed the recombinant PfABHD17A, conducted inhibitor screen and discovered that human depalmitoylase inhibitor ML211 inhibits PfABHD17A *in vitro*. ML211 inhibits merozoite invasion but not egress, which together with the localization of PfABHD17A on the rhoptries, suggested that PfABHD17A is

essential in merozoite invasion. We also purified PfABHD17A and verified that PfABHD17A may exhibit depalmitoylase activity *in vitro*.

LPLs are important for asexual stage parasites acquiring FAs from the host. The *P. falciparum* genome includes 17 putative LPLs while LPLs responsible for hydrolyzing FA from lysophosphatidylcholine (LPC) in the asexual stage are currently unknown. Using a chemical biology approach, we identified serine hydrolase inhibitor AKU-010 inhibits LPC hydrolysis effectively. Using activity-based protein profiling (ABPP) and genetic approaches, we identified that AKU-010 inhibits a series of SHs including Exported Lipases (XLs), Exported Lipases Homolog (XLH) and *Plasmodium falciparum* prodrug activation and resistance esterase (PfPARE). We generated a series of knockout parasite lines on the AKU-010 targets and identified that red blood cell (RBC)-localized XL2 and cytosolic XLH4 contribute to most LPC hydrolysis activity in the asexual stage. XLs and XLHs are important for parasites using LPC for growth and contribute to detoxification from accumulated LPC. XL2 and XL4 together are essential for parasite growth under high LPC concentration medium, such as human serum. XL/XLH-deficient parasites could still acquire FA from LPC, which is mainly contributed by parasite membrane-localized PfPARE. PfPARE has little impact on parasite growth and LPC metabolism with the existence of XLs and XLHs but is important after the loss of XLs and XLHs. Parasites deficient in PfPARE, XLs and XLHs have little ability to release FA from LPC and cannot use LPC as FAs source for growth.

In summary, we identified metabolic SHs mediating protein depalmitoylation and lipid metabolism and in asexual stage *Plasmodium falciparum*, which may benefit future drug development to treat malaria.

Functional Characterization of Serine Hydrolases Mediating Lipid Metabolism and Protein Depalmitoylation in Asexual Stage *Plasmodium Falciparum*

Jiapeng Liu

GENERAL AUDIENCE ABSTRACT

Malaria is an infectious disease caused by *Plasmodium* parasites and transferred by mosquitos. New druggable target identification and drug development are urgently needed to deal with the malaria issue. We focused on an understudied enzyme superfamily termed serine hydrolase (SHs), which includes more than 50 members in the deadliest malaria parasite, *P. falciparum*. We identified that several druggable enzymes, which can mediate protein depalmitoylation and lipid metabolism, are important for parasite growth in the pathogenic stage.

Identifying essential metabolic enzymes will benefit the treatment to malaria. We screened eleven SHs and discovered that two of them are likely essential in the pathogenic stage. We focused on one human depalmitoylase homolog termed PfABHD17A. We screened the inhibitors on PfABHD17A and used the inhibitor to suggest that PfABHD17A is essential for the growth of pathogenic stage parasites.

We also identified lipases important for acquiring fatty acids (FAs) from the host. Using chemical biology and genetic approaches, we discovered that three lipases are important for acquiring FAs form the host in the pathogenic stage. Inhibiting these enzymes may kill the parasite in the host.

ACKNOWLEDGEMENTS

My last five years in the Virginia Tech Biochemistry department were fantastic and this experience will benefit me forever. I appreciate the people and the overall environment in Virginia Tech Biochemistry department.

First, I would like to give my appreciation to my advisor, Dr. Michael Klemba. I was lucky to do the projects that I really like and learned how to become a good scientist from my advisor. His skills on discovering scientific questions, designing experiments to verify the hypothesis and explaining data have greatly broaden my understanding on science. His attitude towards science and the patience in mentoring deserve me to study forever.

My gratitude also goes to my committee members, Dr. Jinsong Zhu, Dr. Brandon Jutras, Dr. Kylie Allen and the past committee member Dr. Glenda Gillaspy. They guided me on critical thinking and encouraged me to make progress in my research. They also gave me good advice to make success in academia and provided me the access to use facilities in their lab.

I would thank the current and past lab members, Katie Fike, Dr. AEM Rubayet Elahi, Christie Dapper and Fahd Mohamed. They helped me a lot on my research projects and gave useful suggestions in my daily life.

I would also thank Dr. Zachary Mackey, Dr. Jake Tu, Mr. Yumin Qi, people in Allen lab and Zhu lab in the Virginia Tech Biochemistry department by providing me the access to the facilities needed for my research. I would thank Virginia Tech and biochemistry department for providing the fantastic program and friendly atmosphere for

international students.

Finally, I would thank my parents. They provided the support for me to study in another country and encouraged me to face the difficulties both in life and career. I wouldn't be here without their help and love. I hope they will be proud when they talk about their only child.

ATTRIBUTIONS

Some of the work in my dissertation was conducted and written by my colleagues.

Chapter 2 "Identification of a putative depalmitoylase essential for merozoite invasion in asexual stage *Plasmodium falciparum*"

Dr. AEM Rubayet Elahi was a previous graduate student in Klemba lab, Department of Biochemistry, Virginia Tech. Dr. AEM Rubayet Elahi and I generated Pf3D7_1134500 gene disruption parasite line together presented in Table 2-1.

Fahd Mohamed was a previous undergraduate researcher mentored by Dr. Klemba and I in Klemba lab, Department of Biochemistry, Virginia Tech. Fahd Mohamed conducted the inhibitor screen on PfABHD17 recombinant proteins presented in Figure 2-5A and 2-S3.

Katie Fike is currently a Research Specialist in Klemba lab, Department of Biochemistry, Virginia Tech. Katie Fike determined the potency of ML211 on PfABHD17A inhibition presented in Figure 2-5B and conducted the DPP-5 hydrolysis assay presented in Figure 2-7B.

Dr. Michael Klemba is currently Associate Professor in the Department of Biochemistry, Virginia Tech. Dr. Klemba is principal investigator of the grant supporting the work, contributed to experimental design and data analysis.

Charpter 3 "Intracellular and exported lysophospholipases metabolize and detoxify lysophosphatidylcholine in *Plasmodium falciparum*-infected erythrocytes"

Christie Dapper was a previous Senior Laboratory Specialist in Klemba lab, Department of Biochemistry, Virginia Tech. Christie Dapper contributed to the set-up of fluorescent fatty acid uptake assay presented in Figure 3-1A and 3-1B and collaborated with me on the inhibitor screen of LPC hydrolysis presented in Figure 3-1C. Christie Dapper is a co-author of the manuscript.

Dr. Michael Klemba is currently Associate Professor in the Department of Biochemistry, Virginia Tech. Dr. Klemba is the principal investigator for the grant supporting the work and a co-author of the manuscript, contributed to experimental design, data analysis and manuscript writing.

Chapter 4 "*Plasmodium falciparum* prodrug activation and resistance esterase is involved in lysophosphatidylcholine metabolism"

Dr. Seema Dalal was a previous Research Scientist in Klemba lab, Department of Biochemistry, Virginia Tech. Dr. Seema Dalal generated PfPARE-YFP parasite line and conducted microscopy to determine the location of PfPARE presented in Figure 4-4.

Dr. Michael Klemba is currently Associate Professor in the Department of Biochemistry, Virginia Tech. Dr. Klemba is the principal investigator of the grant supporting the work, contributed to experimental design and data analysis.

TABLE OF CONTENTS

LIST OF FIGURES

Chapter 1

Chapter 2

Chapter 3

Chapter 4

LIST OF TABLES

Chapter 2

Chapter 3

Chapter 4

LIST OF ABBREVIATION

3HA	3-human influenza hemagglutinin
4-MUH	4-methylumbelliferyl heptanoate
ABHD	Alpha/beta hydrolase domain
ABPP	Activity-based protein profiling
ACS	Acyl-coenzyme A synthetase
ACT	Artemisinin-combination therapy
acyl-coA	Acyl-coenzyme A
APEH	Acylpeptide hydrolase
APT	Acyl-protein thioesterase
ARO	Armadillo repeats-only
aTC	Anhydrotetracycline
BSA	Bovine serum albumin
BTC	BODIPY-TR-ceramide
C1,C12-FA	BODIPY™ 500/510 C_1, C_{12}
C4,C9-FA	BODIPY™ 500/510 C_4, C_9
CCT	CTP:phosphocholine cytidylyltransferase
CDP	Cytidine diphosphate
CDP-Cho	Cytidine diphosphocholine
CDP-DAG	Cytidine diphosphate diacylglycerol
CDS	Coding sequence
CEPT	Choline/ethanolamine phosphotransferase
Cho	Choline

CK	Choline kinase
Clp	Caseinolytic-protease
DAG	Diacylglycerol
DAGL	Diacylglycerol lipase
DD	Destabilization domain
desthiobiotin-FP	desthiobiotin-fluorophosphonate
DGAT	Diacylglycerol O-acyltransferase
DiCre	Dimerizable Cre recombinase
DMSO	Dimethyl sulfoxide
DV	Digestive vacuole
E. coli	*Escherichia coli*
ECT	CTP:phosphoethanolamine cytidylyltransferase
EK	Ethanolamine kinase
ER	Endoplasmic reticulum
Etn	Ethanolamine
FA	Fatty acid
FAS	Fatty acid synthase
FAS II	Type II fatty acid synthesis
FFA	Free fatty acid
FP	Fluorophosphonate
FP-N_3	Fluorophosphonate-N_3
G3P	Glycerol 3-phosphate
G3PAT	Glycerol-3-phosphate acyltransferase

GD	Gene disruption
GDPD	Glycerophosphodiester phosphodiesterase
GPC	Glycerophosphocholine
GPI	Glycosylphosphatidylinositol
GSK	GlaxoSmithKline
HA	Homology arm
hABHD17	Human ABHD17
HPLC	High-performance liquid chromatography
IDFP	Isopropyl dodecylfluorophosphonate
IMC	Inner membrane complex
LPA	Lysophosphatidic acid
LPAAT	Lysophosphatidic acid acyltransferase
LPC	Lysophosphatidylcholine
LPL	Lysophospholipase
MAG	Monoacylglycerol
MAGL	Monoacylglycerol lipase
MGAT	Monoacylglycerol acyltransferase
MSP	Merozoite surface protein
OA	Oleic acid alkyne
P-Cho	Phosphocholine
P-Etn	Phosphoethanolamine
PA	Phosphatidic acid
PAP	Phosphatidic acid phosphatase

PAT	Palmitoyl acyl transferase
Pb PL	*Plasmodium berghei* phospholipase
PBLP	*Plasmodium* BEM46-like protein
PbPla1	*Plasmodium berghei* phosphatidic acid preferring phospholipase A1
PBS	Phosphate buffered saline
PC	Phosphatidylcholine
PE	Phosphatidylethanolamine
PEMT/PLMT	Phosphatidylethanolamine/Phospholipid N-methyltransferase
PfCERLI1	*Plasmodium falciparum* cytosolically exposed rhoptry leaflet Interacting protein 1
PfClpP	*Plasmodium falciparum* Clp protease
PfCRT	*Plasmodium falciparum* chloroquine resistance transporter
PfEH	*Plasmodium falciparum* epoxide hydrolase
PfMAGLLP	*Plasmodium falciparum* monoacylglycerol lipase-like protein
PfNSM	*Plasmodium falciparum* neutral sphingomyelinase
PfPARE	*Plasmodium falciparum* prodrug activation and resistance esterase
PfPATPL1	*Plasmodium falciparum* patatin-like phospholipase 1
PfSUB	*Plasmodium falciparum* subtilisin-like serine protease
PI	Phosphatidylinositol
PI3K	Phosphatidylinositol-3-kinase
PIMMS2	*Plasmodium* invasion of mosquito midgut screen candidate 2
PIS	Phosphatidylinositol synthase
PM	Plasma membrane

PMT	Phosphoethanolamine methyltransferase
PNPLA1	Patatin-like phospholipases 1
PNPLA6	Patatin like phospholipase domain containing 6
PPT	Palmitoyl-protein thioesterase
PS	Phosphatidylserine
PSD	Phosphatidylserine decarboxylase
PSS	Phosphatidylserine synthase
PV	Parasitophorous vacuole
PVM	Parasitophorous vacuole membrane
RAP	Rhoptry-associated protein
RBC	Red blood cell
RhopH3	High molecular weight rhoptry protein 3
ROM	Rhomboid proteases
rPfABHD17	recombinant PfABHD17
SDPM	Serine decarboxylase-phosphoethanolamine methyltransferase
SDS-PAGE	Sodium dodecyl sulfate–polyacrylamide gel electrophoresis
SERA6	Serine repeat antigen 6
SH	Serine hydrolase
SOPT	Subtilisin-like ookinete protein
TAG	Triacylglycerol
TAMRA-FP	Carboxytetramethylrhodamine-fluorophosphonate
TMP	Trimethoprim
UTR	Untranslated region

WHO	World Health Organization
wt	wild type
XL	Exported lipase
XLH	Exported lipase homolog
YFP	Yellow fluorescence protein

Chapter 1

Introduction

1.1 The malaria issue

Malaria is an infectious disease caused by *Plasmodium*. spp. and transferred by *Anopheles* mosquitos. Human malaria is caused by five species of *Plasmodium* parasites: *Plasmodium falciparum*, *Plasmodium vivax*, *Plasmodium malariae*, *Plasmodium ovale* and *Plasmodium knowlesi*. Of the five species, *Plasmodium falciparum* is the deadliest one and causes the most death. According to the world malaria report, there were an estimated of 619,000 deaths caused by 247 million malaria cases in 84 malaria-endemic countries in 2021[1]. About 95% global malaria cases and deaths happened in African region[1]. Children less than the age of 5 are the most vulnerable to malaria and account for more than 75% of the global deaths[1].

With the progresses of the artemisinin-based combination therapies (ACTs), insecticide-treated mosquito net campaigns, seasonal malaria chemoprevention and indoor residual spraying administrated by World Health Organization (WHO), great success has been witnessed in controlling malaria between 2000 and 2019 that the malaria cases incidence declined from 82 to 57 cases per 1000 population at risk[1]. However, the incidence increased to 59 per 1000 population at risk in 2020 and 2021 due to the disruption to services caused by the COVID-19 pandemic[1].

The history of malaria can be traced back to at least 2700 BC in China[2]. There was no treatment for malaria for a long time until the discovery of quinine from cinchona tree bark in 1820. In 1934, chloroquine was synthesized by Bayer Corporation in Germany and was the most successful antimalarial after the second world war until the occurrence of the widespread resistance driven by the mutation of *Plasmodium falciparum* chloroquine resistance transporter (PfCRT) on the digestive vacuole (DV) [3]. The natural function of

PfCRT is recently recognized as transporting peptides from DV to the cytosol so that PfCRT contributes to parasite metabolism and preventing osmotic stress[4]. Mutated PfCRT can transport chloroquine away from the DV to prevent its action[5]. Currently, the most efficacious tools to treat malaria are ACTs, which combine a short half-life artemisinin derivative with another longer half-life partner drug. Artemisinin was firstly isolated by Chinese scientists Tu Youyou from the sweet wormwood (*Artemisia annua*) in 1970s and then shown to be successful in clinical trials[6-8]. In 2006, ACTs were recommended in guidelines for the treatment of malaria by WHO[9].

However, artemisinin partial resistance has occurred because of PfKelch13 mutation[10]. PfKelch13 is essential for *P. falciparum* growth in the asexual stage and localizes on the endoplasmic reticulum (ER), intracellular vesicles and cytostomes[11-13]. Parasites with PfKelch13 mutation exhibit a lower proteotoxic stress level and disrupted hemoglobin catabolism, which may lead to a longer parasite clearance half-life under the treatment of artemisinin[12,14]. Currently PfKelch13 mutation is at such a high prevalence in Greater Mekong Subregion that one study found PfKelch13 mutation occurred in about 45% of the samples collected in Thailand between 2012 and 2016[1,15]. PfKelch13 mutation was also found in Africa region[16].

Vaccines are useful tools to deal with diseases. Currently, the most successful malaria vaccine is RTS,S/AS01 vaccine (Mosquirix™) developed by GlaxoSmithKline (GSK) and PATH's Malaria Vaccine Initiative. WHO has approved the use of RTS,S/AS01 for children living in malaria moderate to high transmission regions in October, 2021. However, the efficacy of the RTS,S/AS01 vaccine is less than 40% in children less than 17 months, according to a phase 3 test in 7 African countries from 2009 to 2014[17,18]. There

are other vaccine candidates in development or in clinical trial including R21/MatrixM, PfSPZ vaccine and others[1].

Due to the emerging artemisinin resistance and the low efficacy of the approved RTS,S/AS01 vaccine, new drug development is urgently needed to deal with the malaria issue.

1.2 The life cycle of *P. falciparum*

The life cycle of *P. falciparum* involves two hosts, human and mosquito. The life cycle in human starts from people being bitten by infected mosquitos. Sporozoites are injected into human, enter the blood stream, travel through sinusoidal barrier and infect the hepatocytes[19,20]. Sporozoites will develop in hepatocytes and generate merozoites in about 2-10 days[19]. Merozoites then are released into the blood, invade erythrocytes and begin the asexual stage development. After invasion, parasites will generate a parasitophorous vacuole membrane (PVM) and seal themselves in the parasitophorous vacuole (PV) [21]. After development in erythrocytes, schizogony starts and forms 16-32 merozoites. Then parasites egress, rupture the erythrocytes, release merozoites to the blood and start a new asexual cycle. Some parasites will start the gamecytogenesis and form gametocytes. Immature stage II to IV gametocytes are sequestered in the bone marrow until they mature[22], which takes about 10 days after sexual commitment. Stage V gametocytes (macrogametocytes and microgametocytes) appear in the peripheral blood vessels[23]. Gametocytes then are taken up by mosquitos when they bite an infected human.

In the midgut of mosquitos, macrogametocytes and microgametocytes will receive the signal from the environment such as the decrease of temperature and xanthurenic acid

to form gametes[24,25]. Male microgametocytes will undergo exflagellation and generate eight motile flagellar microgametes. Then microgametes will search for macrogametes and fuse the membrane with macrogametes to form zygotes[26]. Zygotes will transform to motile ookinetes and then invade the mosquito midgut epithelium. Ookinetes develop into oocysts and then release sporozoites. Sporozoites invade the mosquito salivary gland and will be injected to human during mosquitos' bite.

1.3 Lipid synthesis in asexual stage *Plasmodium*

Lipids are building blocks of biological membranes and can provide living organisms with energy. During the development of the pathogenic asexual stage *Plasmodium*, a drastic increase can be detected in phospholipids and neutral lipids but not cholosterol[27]. A 4 to 6-fold increase of phospholipids in the mature parasite-infected red blood cells (RBCs) can be observed because of the expansion of parasite plasma membrane (PM) as well as the synthesis of PVM and varieties of organelle membranes[28,29]. In asexual stage parasites, phosphatidylcholine (PC) and phosphatidylethanolamine (PE) are the most abundant phospholipids which constitutes 40-50% and 35-45% of the total phospholipids, respectively[30]. The 3rd and 4th most abundant phospholipids are phosphatidylinositol (PI) and phosphatidylserine (PS) constituting about 4-11% and 5%, respectively[29,30]. Infected RBCs exhibit higher levels of PC, PE and PI but a lower level of PS compared to uninfected RBCs[29]. Parasites also produce a significant amount of the neutral lipids mainly diacylglycerol (DAG) and triacylglycerol (TAG), which are deposited in lipid droplets and mobilized late in the replication cycle[29,31]. Thus, lipid biosynthesis is crucial for the development of asexual stage *Plasmodium* parasites.

Fatty acids (FAs) are the building blocks of phospholipids and neutral lipids. Fatty acid synthase (FAS) is responsible for FA *de novo* synthesis from acetyl-CoA and malonyl-CoA. The *Plasmodium* genome encodes prokaryotic type II fatty acid synthesis (FAS II) system which localizes to the apicoplast. However, the FASII system is only essential in the sporozoite and late liver stage[32,33]. Thus, in other stages, parasites have to scavenge FAs from the host[28,34]. In asexual stage *P. falciparum*, parasites can uptake the FAs from the plasma, or use FAs liberated from lysophosphatidylcholine (LPC) for their own lipid biosynthesis[35-37].

LPC hydrolysis catalyzed by lysophospholipases A1 is crucial for the lipid synthesis in asexual stage *Plasmodium* parasites by providing FAs and choline[36,38]. LPC hydrolysis releases FAs, which are converted into acyl-coenzyme A (acyl-coA) by acyl-coA synthetases (ACSs), and acyl-coA is then used for lipids synthesis[35-37]. LPC hydrolysis also releases glycerophosphocholine (GPC), which is then hydrolyzed by glycerophosphodiester phosphodiesterase (GDPD) and releases glycerol 3-phosphate (G3P) and choline[39], proving the main source of choline for PC synthesis[36,38].

PC has important roles as the structural molecule of the membranes in *Plasmodium* parasties[40]. PC was thought to have 3 origins[40,41]: 1) *de novo* synthesis from choline via the Kennedy pathway; 2) from ethanolamine via serine decarboxylase-phosphoethanolamine methyltransferase (SDPM) pathway; and 3) direct methylation from PE.

Most PC is synthesized via the Kennedy pathway in the asexual stage[38]. The *de novo* synthesis of PC via the Kennedy pathway starts from choline. Choline is phosphorylated by cytosolic choline kinase (CK), which results choline captured at a higher concentration in the cytosol[42-44]. Then phosphocholine (P-Cho) is converted to cytidine

diphosphocholine (CDP-Cho) by CTP:phosphocholine cytidylyltransferase (CCT) in the cytosol[44,45]. Finally CDP-Cho is converted into PC, with the participation of DAG, which is catalyzed by ER localized choline/ethanolamine phosphotransferase (CEPT) [44,46]. P-Cho can also be converted from phosphoethanolamine (P-Etn) through the SDPM pathway by three steps of methylation catalyzed by phosphoethanolamine methyltransferase (PMT), which is on the Golgi apparatus[47,48].

Methylation of PE was found in *Plasmodium knowlesi* and *Plasmodium falciparum*[49]. This reaction is catalyzed by Phosphatidylethanolamine/Phospholipid N-methyltransferase (PEMT/PLMT) in other eukaryotes[50-53]. However, the homologs of PEMT or PLMT are currently not known in any *Plasmodium*. spp[41].

PE is generated through *de novo* synthesis from ethanolamine (Etn) from the plasma and decarboxylated serine[54], or decarboxylation of PS by ER phosphatidylserine decarboxylase (PSD) [55,56]. In the *de novo* synthesis, Etn is phosphorylated to P-Etn by ethanolamine kinase (EK) in the cytosol[43]. CDP-ethanolamine is then generated by cytosolic CTP:phosphoethanolamine cytidylyltransferase (ECT) [44,57]. CDP-ethanolamine and DAG are converted to PE by CEPT[46].

Enzymes involved in the *de novo* synthesis of PC and PE from choline or ethanolamine may be potential drug targets. CEPT, CCT, ECT and CK are essential[44] while PMT is dispensable but knocking out PMT results in a great defect on parasite growth[58].

PS is exposed to the surface of infected RBCs and has important function in adherence of parasite to the RBCs[40,59]. The synthesis of PS starts form serine acquired from the host plasma or the digestion of hemoglobin[40]. Then phosphatidylserine synthase (PSS) catalyze the formation of PS in ER[60].

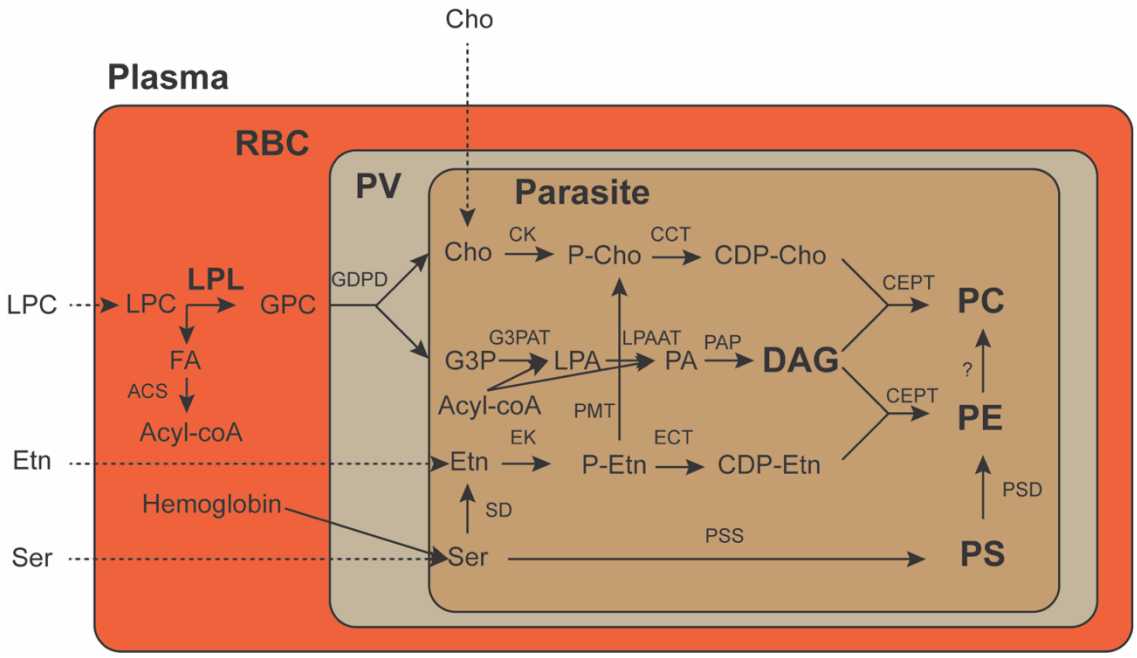

Figure 1-1. Scheme of current understanding of PC, PE and PS biosynthesis in *Plasmodium* parasite-infected erythrocytes. PC can be derived from *de novo* synthesis from choline (from LPC or the plasma) via the Kennedy pathway, ethanolamine via SDPM pathway or direct methylation from PE. PE can be synthesized from *de novo* synthesis from ethanolamine (from the plasma or decarboxylated serine) via the Kennedy pathway or decarboxylation from PS. PS is synthesized from serine (from the plasma or the digestion from hemoglobin). ACS, acyl-CoA synthetase; CCT, CTP:phosphocholine cytidylyltransferase; CDP-Cho, cytidine diphosphocholine; CDP-Etn, cytidine diphosphate ethanolamine; CEPT, choline/ethanolamine phosphotransferase; Cho, choline; CK, choline kinase; DAG, diacylglycerol; ECT, CTP:phosphoethanolamine cytidylyltransferase; EK, ethanolamine kinase; Etn, ethanolamine; FA, fatty acid; G3P, glycerol 3-phosphate; G3PAT, glycerol-3-phosphate acyltransferase; GDPD, glycerophosphodiester phosphodiesterase; GPC, glycerophosphocholine; LPA, lysophosphatidic acid; LPAAT, lysophosphatidic acid acyltransferase; LPC, lysophosphatidylcholine; LPL, lysophospholipase; P-Cho, phosphocholine; P-Etn, phosphoethanolamine; PA, phosphatidic acid; PAP, phosphatidic acid phosphatase; PC, phosphatidylcholine; PE, phosphatidylethanolamine; PMT, phosphoethanolamine methyltransferase; PS, phosphatidylserine; PSD, phosphatidylserine decarboxylase; PSS, phosphatidylserine synthase; PV, parasite vacuole; RBC, red blood cell; SD, serine decarboxylase; Ser, serine. Broken arrows indicate the transport processes. Question mark on the arrow from PE to PC represents the enzymes for this process are unknown.

Phosphatidic acid (PA) is an important metabolite for phospholipid biosynthesis. PA is synthesized from two step acylation on G3P and then lysophosphatidic acid (LPA) in eukaryotes, which are catalyzed by G3P acyltransferase (G3PAT) and LPA

acyltransferase (LPAAT), respectively. *Plasmodium* parasites encodes two G3PATs. One G3PAT is localized on the ER[61], which is predicted to be essential in the asexual stage[62]. The other G3PAT is on the apicoplast but is only essential in the liver stage[63,64]. Only one LPAAT homolog has been identified, which is localized on ER and is essential in the asexual stage[63].

PI has important functions as a structural component and the anchor for membrane proteins[40]. PI can also mediate signal transduction[40]. PI can be phosphorylated on the hydroxyl group by different kinases. Phosphatidylinositol-3-kinase (PI3K) was found to regulate hemoglobin trafficking[65]. PI can also be converted to glycosylphosphatidylinositol (GPI) which can anchor proteins on merozoites or other organelles[66]. The synthesis of PI is from PA, which is converted to cytidine diphosphate diacylglycerol (CDP-DAG) and then CDP-DAG is converted to PI catalyzed by phosphatidylinositol synthase (PIS) [67].

DAG and TAG are the main neutral lipids in asexual stage *plasmodium* while the abundance of monoacylglycerol (MAG) is low[68]. In most eukaryotes, DAG is generated by phosphatidic acid phosphatase (PAP) that dephosphorylates the phosphate from PA[69]. One type-2 PAP has been identified in *Plasmodium falciparum* and is essential in the asexual stage[70]. DAG can also be produced by monoacylglycerol acyltransferase (MGAT) from MAG in eukaryotes. However, no homolog of MGAT exists in the *Plasmodium* genome[41,71]. TAG is generated by the acylation of DAG catalyzed by diacylglycerol O-acyltransferase (DGAT) which has the maximal activity in late trophozoites[37].

1.4 Serine hydrolases in *Plasmodium*

Serine hydrolases (SHs) are enzymes using an active site serine to hydrolyze peptide bonds, ester, thioester or amide bonds in the substrates[72]. The hydrolysis activity

of SHs is achieved by SHs attacking the electrophilic bond of the substrates using the nucleophile serine to form a covalent acyl-enzyme intermediate and then cleaving the intermediate with the involvement of a water molecule, which will finally release the product and regenerate the SHs[73].

SH family is one of the largest enzyme classes including more than 200 enzymes in human[72]. SHs can be classified into 2 classes: serine proteases and metabolic SHs including lipases, esterases, amidases and others[74]. Serine proteases, which can cleave the peptide bonds of the substrate proteins, consists near one-third of all proteases with more than 100 members in the human genome[74,75]. Metabolic SHs can hydrolyze ester, amide or thioester bonds in small molecules and includes more than 110 members in the human genome[74]. The majority of metabolic SHs have an alpha/beta hydrolase domain (ABHD) that consists of 8 β-sheet in the center surrounded by 6 α-helicies[76,77]. SHs have important roles in life processes including metabolism, cellular signaling, immune response and others[78,79]. The *Plasmodium falciparum* genome encodes 56 serine hydrolases[80], while only a few of them have been studied.

Plasmodium falciparum serine proteases include 4 subtilisin proteases, 8 rhomboid proteases (ROMs) and 5 other serine proteases[80]. Two *P. falciparum* subtilisin proteases are essential in the asexual stage[81-83]. *Plasmodium falciparum* subtilisin-like protease (PfSUB) 1 is essential both in egress and invasion by mediating the maturation of a series of proteins including serine repeat antigen 6 (SERA6), merozoite surface protein (MSP) 1, MSP6, MSP7 and rhoptry associated protein (RAP) 1 in the asexual stage[81,82,84,85]. PfSUB1 is also essential for egress from hepatocytes[86]. PfSUB2 is an essential protease secreted to the parasite surface during the merozoite release and is important for RBC sealing after

invasion and intracellular parasite development[83,87]. PfSUB3 is dispensable in the asexual stage[62,88]. Subtilisin-like ookinete protein (SOPT) or named as *Plasmodium* invasion of mosquito midgut screen candidate 2 (PIMMS2) by another group, is dispensable in the asexual stage or gametocytes, but influences oocyst formation[89,90].

Four ROMs (ROM4, 6, 7 and 8) are refractory to knock out in the asexual stage[91]. Merozoite plasma membrane-localized PfROM4 is essential in invasion by cleaving erythrocyte binding-like antigens including erythrocyte binding antigen 175[92-94]. Little is known about other essential ROMs except that ROM7 is localized on the apicoplast[95]. ROM1 has little impact in the asexual stage, but influences liver stage development[91]. ROM3 is not essential in the asexual stage but is important for generating sporozoites[91].

Two serine protases are signal peptidases. Pf3D7_1320400 is a Type I signal peptidase[96]. PfSP21, is an ER signal peptidase which may impact parasite growth[97]. *Plasmodium falciparum* Clp protease (PfClpP), a component of apicoplast caseinolytic-protease (Clp) system, is essential for apicoplast biogenesis and parasite survival in the asexual stage[98]. PfDegP, a part of heat shock protein 70 complex, may be important for parasite to combat with host febrile illness[99].

Only a few metabolic SHs in *P. falciparum* have been characterized. The *P. falciparum* genome encodes 5 patatin-like phospholipases, having predicted sizes spanning from 78 to 283 kD. The 78 kD patatin-like phospholipase, termed patatin-like phospholipases 1 (PNPLA1) or *P. falciparum* patatin-like phospholipase 1 (PfPATPL1), has little effect in the asexual stage growth or gametocyte development[100,101]. PNPLA1-deficient leads to higher levels in phospholipids and a downregulation of genes involved in gametocytogenesis, thus having impact on gametocytogenesis[100]. However, another

group showed that PNPLA1 doesn't influence gametocytogenesis but rather gametocyte round-up, exflagellation and egress as well as oocyst formation in mosquitoes[99]. The 81 kD patatin-like phospholipase homolog in *Plasmodium berghei*, termed phosphatidic acid preferring phospholipase A1 (PbPla1), is not essential in the asexual and mosquito stages but influences merosome release in the liver stage[102]. The other 3 higher molecular weight patatin-like phospholipases remain unstudied in *P. falciparum*, but the homolog of the 238 kD patatin-like phospholipase in *Toxoplasma gondii* is localized on the apicoplast and is essential in tachyzoites[103].

The *P. falciparum* genome contains a large number of ABHDs. Seventeen of them are predicted to have lysophospholipases (LPLs) activity (Plasmodb.org[104]). Three of them (LPL1, 3 and 20) were verified to have lysophospholipase *in vitro* and can mediate lipid metabolism[105-107]. *P. falciparum* prodrug activation and resistance esterase (PfPARE) can activate an esterified prodrug by cleaving the ester bond and the mutations of PfPARE were found to be able to mediate drug resistant[108-110]. *P. falciparum* epoxide hydrolases (PfEH) 1 and 2 are dispensable epoxides hydrolases which are localized in the RBC in the asexual stage[111]. *P. berghei* phospholipase (Pb PL) localizes on the surface of sporozoites and can facilitate sporozoite passage through epithelial cell layers[112]. In the liver stage, Pb PL is on the PVM and are important in PVM rupture and egress[113]. *Plasmodium* BEM46-like protein (PBLP) has broad roles in the parasite life cycle including asexual stage schizogony, the development in oocysts and sporozoites as well as the infection in hepatocytes[114].

Human-derived SHs also have important roles on parasite growth. Acylpeptide hydrolase (APEH) is internalized by the parasites and is required for parasite growth in the asexual stage[115]. Acyl-protein thioesterase 1 (APT1) and patatin like phospholipase domain

containing 6（PNPLA6) were verified to impact parasite growth in the asexual stage using specific inhibitors[116].

Activity-based protein profiling (ABPP) is an effective approach for proteomic studies that uses chemical probes to label the active status of the proteins. Two ABPP studies were conducted on *Plasmodium* SHs[80,116]. Our lab applied desthiobiotin-fluorophosphonate (desthiobiotin-FP) and identified 21 SHs from the *P. falciparum* genome and 5 SHs from the human genome expressed in schizont stage parasites[80]. Another study used fluorophosphonate-N_3 (FP-N_3) and identified 25 *P. falciparum* and 8 human SHs in the asexual stage[116].

A large number of SHs in *P. falciparum* are still uncharacterized. Characterization of these SHs will expand the current understanding on parasite life processes and contribute to the discovery of new druggable targets and drugs to deal with the malaria issue. This process will be facilitated by a large number of chemical tools and inhibitors designed for human SHs.

1.5 Protein palmitoylation

Protein palmitoylation is a protein post-translational modification by transferring palmitic acid to proteins via covalent bond. Three types of palmitoylation have been identified: S-palmitoylation, N-palmitoylation and O-palmitoylation[117]. S-palmitoylation, which refers to the binding of palmitic acid to the cysteine residue through a thioester bond, is the most common type of palmitoylation and the only reversible one[117,118]. Palmitoylation can increase the hydrophobicity of the proteins, thus can regulate the subcellular localization of the proteins[119,120]. Protein palmitoylation can also regulate protein half-life and modify protein-protein interactions[121,122].

Protein S-palmitoylation can be a dynamic process maintained by palmitoyl acyl transferases (PATs) and depalmitoylases. The known depalmitoylases include acyl-protein thioesterases (APTs), palmitoyl-protein thioesterases (PPTs), ABHD10 and ABHD17A/B/C[117,123,124].

Protein palmitoylation is important for *Plasmodium* development. In the asexual stage, more than 400 proteins are palmitoylated and protein palmitoylation is the most abundant in schizonts[125,126]. Protein palmitoylation is found to be essential in rhoptry biogenesis, inner membrane complex (IMC) assembly, schizont development, microneme secretion and merozoite invasion in the asexual stage[125-130]. Besides, protein palmitoylation is also important for zygote to ookinete differentiation and the liver stage development[129,131].

The *P. falciparum* genome encodes 12 PATs and at least one PAT was identified to be essential in the asexual stage[132,133]. There is no homolog of human depalmitoylase APTs, PPTs or ABHD10 existing in the *P. falciparum* genome. But the *P. falciparum* genome encodes 4 hABHD17 homologs, which may function as depalmitoylases. PfABHD17s may have important functions during the life cycle of *Plasmodium* parasites.

REFERENCES

1 WHO. World malaria report 2022. (2022).

2 Cox, F. E. History of the discovery of the malaria parasites and their vectors. *Parasites & vectors* **3**, 1-9 (2010).

3 Fidock, D. A. *et al.* Mutations in the *P. falciparum* digestive vacuole transmembrane protein PfCRT and evidence for their role in chloroquine resistance. *Molecular Cell* **6**, 861-871 (2000).

4 Shafik, S. H. *et al.* The natural function of the malaria parasite's chloroquine resistance transporter. *Nature communications* **11**, 3922 (2020).

5 Martin, R. E. *et al.* Chloroquine transport via the malaria parasite's chloroquine resistance transporter. *Science* **325**, 1680-1682 (2009).

6 Qinghaosu, A. C. R. g. Antimalaria studies on Qinghaosu. *Chinese medical journal* **92**, 811-816 (1979).

7 Li, G. *et al.* Clinical trials of artemisinin and its derivatives in the treatment of malaria in China. *Transactions of the Royal Society of Tropical Medicine and Hygiene* **88**, 5-6 (1994).

8 Li, G. *et al.* Clinical studies on treatment of cerebral malaria with qinghaosu and its derivatives. *Journal of traditional Chinese medicine* **2** (1982).

9 Olumese, P. *Guidelines for the Treatment of Malaria* (2006).

10 Ariey, F. *et al.* A molecular marker of artemisinin-resistant *Plasmodium falciparum* malaria. *Nature* **505**, 50-55 (2014).

11 Birnbaum, J. *et al.* A genetic system to study *Plasmodium falciparum* protein function. *Nature Methods* **14**, 450-456 (2017).

12 Xie, S. C. *et al.* K13, the cytostome, and artemisinin resistance. *Trends in Parasitology* **36**, 533-544 (2020).

13 Gnädig, N. F. *et al.* Insights into the intracellular localization, protein associations and artemisinin resistance properties of *Plasmodium falciparum* K13. *PLoS Pathogens* **16**, e1008482 (2020).

14 Siddiqui, F. A. *et al.* Role of *Plasmodium falciparum* Kelch 13 protein mutations in *P. falciparum* populations from northeastern Myanmar in mediating artemisinin resistance. *MBio* **11**, e01134-01119 (2020).

15 Kobasa, T. *et al.* Emergence and spread of kelch13 mutations associated with artemisinin resistance in *Plasmodium falciparum* parasites in 12 Thai provinces from 2007 to 2016. *Antimicrobial agents and chemotherapy* **62**, e02141-02117 (2018).

16 Ndwiga, L. *et al.* A review of the frequencies of *Plasmodium falciparum* Kelch 13 artemisinin resistance mutations in Africa. *International Journal for Parasitology: Drugs and Drug Resistance* **16**, 155-161 (2021).

17 Laurens, M. B. RTS, S/AS01 vaccine (Mosquiri^{TM}): an overview. *Human vaccines & immunotherapeutics* **16**, 480-489 (2020).

18 Rts, S. Efficacy and safety of RTS, S/AS01 malaria vaccine with or without a booster dose in infants and children in Africa: final results of a phase 3, individually randomised, controlled trial. *The Lancet* **386**, 31-45 (2015).

19 Sinnis, P. & Coppi, A. A long and winding road: the *Plasmodium* sporozoite's journey in the mammalian host. *Parasitology International* **56**, 171-178 (2007).

20 Cowman, A. F. *et al.* Malaria: biology and disease. *Cell* **167**, 610-624 (2016).
21 Goldberg, D. E. & Zimmerberg, J. Hardly vacuous: The parasitophorous vacuolar membrane of malaria parasites. *Trends in Parasitology* **36**, 138-146 (2020).
22 Farfour, E. *et al.* The extravascular compartment of the bone marrow: a niche for *Plasmodium falciparum* gametocyte maturation? *Malaria journal* **11**, 1-4 (2012).
23 Talman, A. M. *et al.* Gametocytogenesis: the puberty of *Plasmodium falciparum*. *Malaria journal* **3**, 1-14 (2004).
24 Billker, O. *et al.* The roles of temperature, pH and mosquito factors as triggers of male and female gametogenesis of *Plasmodium berghei in vitro*. *Parasitology* **115**, 1-7 (1997).
25 Billker, O. *et al.* Identification of xanthurenic acid as the putative inducer of malaria development in the mosquito. *Nature* **392**, 289-292 (1998).
26 Bennink, S. *et al.* The development of malaria parasites in the mosquito midgut. *Cellular Microbiology* **18**, 905-918 (2016).
27 Vial, H. *et al.* Biosynthesis and dynamics of lipids in *Plasmodium*-infected mature mammalian erythrocytes. *Blood cells* **16**, 531-555 (1990).
28 Vial, H. J. & Ancelin, M. L. Malarial lipids: an overview. *Intracellular Parasites*, 259-306 (1992).
29 Gulati, S. *et al.* Profiling the essential nature of lipid metabolism in asexual blood and gametocyte stages of *Plasmodium falciparum*. *Cell Host & Microbe* **18**, 371-381 (2015).
30 Vial, H. J. *et al.* Phospholipids in parasitic protozoa. *Molecular and Biochemical Parasitology* **126**, 143-154 (2003).
31 Palacpac, N. M. Q. *et al.* Developmental-stage-specific triacylglycerol biosynthesis, degradation and trafficking as lipid bodies in *Plasmodium falciparum*-infected erythrocytes. *Journal of Cell Science* **117**, 1469-1480 (2004).
32 Vaughan, A. M. *et al.* Type II fatty acid synthesis is essential only for malaria parasite late liver stage development. *Cellular Microbiology* **11**, 506-520 (2009).
33 van Schaijk, B. C. *et al.* Type II fatty acid biosynthesis is essential for *Plasmodium falciparum* sporozoite development in the midgut of *Anopheles* mosquitoes. *Eukaryotic Cell* **13**, 550-559 (2014).
34 Vial, H. J. *et al.* Phospholipid Biosynthesis in Synchronous *Plasmodium falciparum* Cultures 1. *The Journal of protozoology* **29**, 258-263 (1982).
35 Vial, H. *et al.* Phospholipid metabolism in *Plasmodium*-infected erythrocytes: guidelines for further studies using radioactive precursor incorporation. *Parasitology* **98**, 351-357 (1989).
36 Brancucci, N. M. *et al.* Lysophosphatidylcholine regulates sexual stage differentiation in the human malaria parasite *Plasmodium falciparum*. *Cell* **171**, 1532-1544. e1515 (2017).
37 Vielemeyer, O. *et al.* Neutral lipid synthesis and storage in the intraerythrocytic stages of *Plasmodium falciparum*. *Molecular and Biochemical Parasitology* **135**, 197-209 (2004).
38 Wein, S. *et al.* Contribution of the precursors and interplay of the pathways in the phospholipid metabolism of the malaria parasite. *Journal of Lipid Research* **59**, 1461-1471 (2018).

39 Denloye, T. *et al.* Characterization of a glycerophosphodiesterase with an unusual tripartite distribution and an important role in the asexual blood stages of *Plasmodium falciparum*. *Molecular and Biochemical Parasitology* **186**, 29-37 (2012).
40 Kilian, N. *et al.* Role of phospholipid synthesis in the development and differentiation of malaria parasites in the blood. *Journal of Biological Chemistry* **293**, 17308-17316 (2018).
41 Déchamps, S. *et al.* Glycerophospholipid acquisition in *Plasmodium*–A puzzling assembly of biosynthetic pathways. *International Journal for Parasitology* **40**, 1347-1365 (2010).
42 Choubey, V. *et al.* Molecular characterization and localization of *Plasmodium falciparum* choline kinase. *Biochimica et Biophysica Acta (BBA)-General Subjects* **1760**, 1027-1038 (2006).
43 Alberge, B. *et al.* Comparison of the cellular and biochemical properties of *Plasmodium falciparum* choline and ethanolamine kinases. *Biochemical Journal* **425**, 149-163 (2010).
44 Déchamps, S. *et al.* The Kennedy phospholipid biosynthesis pathways are refractory to genetic disruption in *Plasmodium berghei* and therefore appear essential in blood stages. *Molecular and Biochemical Parasitology* **173**, 69-80 (2010).
45 Yeo, H. J. *et al.* Molecular cloning of CTP: phosphocholine cytidylyltransferase from *Plasmodium falciparum*. *European Journal of Biochemistry* **233**, 62-72 (1995).
46 Vial, H. J. *et al.* Cholinephosphotransferase and ethanolaminephosphotransferase activities in *Plasmodium knowlesi*-infected erythrocytes: Their use as parasite-specific markers. *Biochimica et Biophysica Acta (BBA)-Lipids and Lipid Metabolism* **795**, 372-383 (1984).
47 Pessi, G. *et al.* A pathway for phosphatidylcholine biosynthesis in *Plasmodium falciparum* involving phosphoethanolamine methylation. *Proceedings of the National Academy of Sciences of the United States of America* **101**, 6206-6211 (2004).
48 Witola, W. H. *et al.* Localization of the phosphoethanolamine methyltransferase of the human malaria parasite *Plasmodium falciparum* to the Golgi apparatus. *Journal of Biological Chemistry* **281**, 21305-21311 (2006).
49 Moll, G. N. *et al.* Phospholipid uptake by *Plasmodium knowlesi* infected erythrocytes. *FEBS Letters* **232**, 341-346 (1988).
50 Ridgway, N. D. & Vance, D. E. Purification of phosphatidylethanolamine N-methyltransferase from rat liver. *Journal of Biological Chemistry* **262**, 17231-17239 (1987).
51 Kodaki, T. & Yamashita, S. Yeast phosphatidylethanolamine methylation pathway. Cloning and characterization of two distinct methyltransferase genes. *Journal of Biological Chemistry* **262**, 15428-15435 (1987).
52 Summers, E. F. *et al. Saccharomyces cerevisiae* cho2 mutants are deficient in phospholipid methylation and cross-pathway regulation of inositol synthesis. *Genetics* **120**, 909-922 (1988).

53 Keogh, M. R. *et al.* Functional characterization of phospholipid N-methyltransferases from Arabidopsis and soybean. *Journal of Biological Chemistry* **284**, 15439-15447 (2009).
54 Elabbadi, N. *et al.* Phospholipid metabolism of serine in *Plasmodium*-infected erythrocytes involves phosphatidylserine and direct serine decarboxylation. *Biochemical Journal* **324 (Pt 2)**, 435-445 (1997).
55 Choi, J. Y. *et al.* Characterization of *Plasmodium* phosphatidylserine decarboxylase expressed in yeast and application for inhibitor screening. *Molecular Microbiology* **99**, 999-1014 (2016).
56 Choi, J.-Y. *et al.* Identification of gene encoding *Plasmodium knowlesi* phosphatidylserine decarboxylase by genetic complementation in yeast and characterization of *in vitro* maturation of encoded enzyme. *Journal of Biological Chemistry* **287**, 222-232 (2012).
57 Maheshwari, S. *et al.* Biochemical characterization of *Plasmodium falciparum* CTP: phosphoethanolamine cytidylyltransferase shows that only one of the two cytidylyltransferase domains is active. *Biochemical Journal* **450**, 159-167 (2013).
58 Witola, W. H. *et al.* Disruption of the *Plasmodium falciparum* PfPMT gene results in a complete loss of phosphatidylcholine biosynthesis via the serine-decarboxylase-phosphoethanolamine-methyltransferase pathway and severe growth and survival defects. *Journal of Biological Chemistry* **283**, 27636-27643 (2008).
59 Eda, S. & Sherman, I. Cytoadherence of malaria-infected red blood cells involves exposure of phosphatidylserine. *Cellular Physiology and Biochemistry* **12**, 373-384 (2002).
60 Anwar, M. O. *et al.* Defining ER-mitochondria contact dynamics in *Plasmodium falciparum* by targeting component of phospholipid synthesis pathway, phosphatidylserine synthase (PfPSS). *Mitochondrion* **65**, 124-138 (2022).
61 Santiago, T. C. *et al.* The *Plasmodium falciparum* PfGatp is an endoplasmic reticulum membrane protein important for the initial step of malarial glycerolipid synthesis. *Journal of Biological Chemistry* **279**, 9222-9232 (2004).
62 Zhang, M. *et al.* Uncovering the essential genes of the human malaria parasite *Plasmodium falciparum* by saturation mutagenesis. *Science* **360** (2018).
63 Lindner, S. E. *et al.* Enzymes involved in plastid‐targeted phosphatidic acid synthesis are essential for *Plasmodium yoelii* liver‐stage development. *Molecular Microbiology* **91**, 679-693 (2014).
64 Shears, M. J. *et al.* Characterization of the *Plasmodium falciparum* and *P. berghei* glycerol 3‐phosphate acyltransferase involved in FASII fatty acid utilization in the malaria parasite apicoplast. *Cellular Microbiology* **19**, e12633 (2017).
65 Vaid, A. *et al.* PfPI3K, a phosphatidylinositol-3 kinase from *Plasmodium falciparum*, is exported to the host erythrocyte and is involved in hemoglobin trafficking. *Blood, The Journal of the American Society of Hematology* **115**, 2500-2507 (2010).
66 Sanders, P. R. *et al.* A set of glycosylphosphatidyl inositol-anchored membrane proteins of *Plasmodium falciparum* is refractory to genetic deletion. *Infection and Immunity* **74**, 4330-4338 (2006).

67 Wengelnik, K. & Vial, H. J. Characterisation of the phosphatidylinositol synthase gene of *Plasmodium* species. *Research in Microbiology* **158**, 51-59 (2007).
68 Holz Jr, G. G. Lipids and the malarial parasite. *Bulletin of The World Health Organization* **55**, 237 (1977).
69 Lykidis, A. Comparative genomics and evolution of eukaryotic phospholipid biosynthesis. *Progress in lipid research* **46**, 171-199 (2007).
70 Kumar Sah, R. *et al.* Phosphatidic acid homeostasis regulated by a type-2 phosphatidic acid phosphatase represents a novel druggable target in malaria intervention. *Cell death discovery* **5**, 107 (2019).
71 Vial, H. J. & Ben Mamoun, C. *Plasmodium* lipids: metabolism and function. *Molecular approaches to malaria*, 327-352 (2005).
72 Sieber, S. A. *et al.* Small Molecules as Versatile Tools for Activity-Based Protein Profiling Experiments. *Journal: Comprehensive Natural Products II*, 629-674 (2010).
73 Engel, P. Enzymatic reaction mechanisms: By C Walsh. pp 978. WH Freeman & Co, Oxford. 1979.£ 18.30. (1981).
74 Simon, G. M. & Cravatt, B. F. Activity-based proteomics of enzyme superfamilies: serine hydrolases as a case study. *Journal of Biological Chemistry* **285**, 11051-11055 (2010).
75 Hedstrom, L. Serine protease mechanism and specificity. *Chemical reviews* **102**, 4501-4524 (2002).
76 Nardini, M. & Dijkstra, B. W. Alpha/beta hydrolase fold enzymes: the family keeps growing. *Current Opinion in Structural Biology* **9**, 732-737 (1999).
77 Ollis, D. L. *et al.* The α/β hydrolase fold. *Protein Engineering, Design and Selection* **5**, 197-211 (1992).
78 Shahiduzzaman, M. & Coombs, K. M. Activity based protein profiling to detect serine hydrolase alterations in virus infected cells. *Frontiers in Microbiology* **3**, 308 (2012).
79 Lu, M. *et al.* A novel α/β hydrolase domain protein derived from *Haemonchus contortus* acts at the parasite-host interface. *Frontiers in Immunology* **11**, 1388 (2020).
80 Elahi, R. *et al.* Functional annotation of serine hydrolases in the asexual erythrocytic stage of *Plasmodium falciparum*. *Scientific reports* **9**, 1-11 (2019).
81 Koussis, K. *et al.* A multifunctional serine protease primes the malaria parasite for red blood cell invasion. *The EMBO journal* **28**, 725-735 (2009).
82 Yeoh, S. *et al.* Subcellular discharge of a serine protease mediates release of invasive malaria parasites from host erythrocytes. *Cell* **131**, 1072-1083 (2007).
83 Collins, C. R. *et al.* The malaria parasite sheddase SUB2 governs host red blood cell membrane sealing at invasion. *Elife* **9**, e61121 (2020).
84 Silmon de Monerri, N. C. *et al.* Global identification of multiple substrates for *Plasmodium falciparum* SUB1, an essential malarial processing protease. *Infection and Immunity* **79**, 1086-1097 (2011).
85 Thomas, J. A. *et al.* A protease cascade regulates release of the human malaria parasite *Plasmodium falciparum* from host red blood cells. *Nature microbiology* **3**, 447-455 (2018).

86 Tawk, L. *et al.* A key role for *Plasmodium* subtilisin-like SUB1 protease in egress of malaria parasites from host hepatocytes. *Journal of Biological Chemistry* **288**, 33336-33346 (2013).
87 Harris, P. K. *et al.* Molecular identification of a malaria merozoite surface sheddase. *PLoS Pathogens* **1**, e29 (2005).
88 Alam, A. *et al.* Proteolytic activity of *Plasmodium falciparum* subtilisin-like protease 3 on parasite profilin, a multifunctional protein. *Molecular and Biochemical Parasitology* **191**, 58-62 (2013).
89 Ukegbu, C. V. *et al. Plasmodium berghei* PIMMS2 promotes ookinete invasion of the *Anopheles gambiae* mosquito midgut. *Infection and Immunity* **85**, e00139-00117 (2017).
90 Armistead, J. S. *et al. Plasmodium falciparum* subtilisin-like ookinete protein SOPT plays an important and conserved role during ookinete infection of the *Anopheles stephensi* midgut. *Molecular Microbiology* **109**, 458-473 (2018).
91 Lin, J. w. *et al.* Loss-of-function analyses defines vital and redundant functions of the *Plasmodium* rhomboid protease family. *Molecular Microbiology* **88**, 318-338 (2013).
92 O'Donnell, R. A. *et al.* Intramembrane proteolysis mediates shedding of a key adhesin during erythrocyte invasion by the malaria parasite. *The Journal of cell biology* **174**, 1023-1033 (2006).
93 Baker, R. P. *et al.* Two *Plasmodium* rhomboid proteases preferentially cleave different adhesins implicated in all invasive stages of malaria. *PLoS Pathogens* **2**, e113 (2006).
94 Gandhi, S. *et al.* Designed parasite-selective rhomboid inhibitors block invasion and clear blood-stage malaria. *Cell Chemical Biology* **27**, 1410-1424. e1416 (2020).
95 Boucher, M. J. *et al.* Integrative proteomics and bioinformatic prediction enable a high-confidence apicoplast proteome in malaria parasites. *PLoS Biology* **16**, e2005895 (2018).
96 Sharma, S. *et al.* Isolation and characterization of type I signal peptidase of different malaria parasites. *Journal of Biomedicine and Biotechnology* **2005**, 301-309 (2005).
97 Tuteja, R. *et al. Plasmodium falciparum* signal peptidase is regulated by phosphorylation and required for intra-erythrocytic growth. *Molecular and Biochemical Parasitology* **157**, 137-147 (2008).
98 Florentin, A. *et al.* Plastid biogenesis in malaria parasites requires the interactions and catalytic activity of the Clp proteolytic system. *Proceedings of the National Academy of Sciences of the United States of America* **117**, 13719-13729 (2020).
99 Sharma, S. *et al.* A secretory multifunctional serine protease, DegP of *Plasmodium falciparum*, plays an important role in thermo-oxidative stress, parasite growth and development. *The FEBS Journal* **281**, 1679-1699 (2014).
100 Flammersfeld, A. *et al.* A patatin-like phospholipase functions during gametocyte induction in the malaria parasite *Plasmodium falciparum*. *Cellular Microbiology* **22**, e13146 (2020).
101 Singh, P. *et al.* Role of a patatin-like phospholipase in *Plasmodium falciparum* gametogenesis and malaria transmission. *Proceedings of the National Academy of Sciences of the United States of America* **116**, 17498-17508 (2019).

102 Srivastava, P. N. & Mishra, S. Disrupting a *Plasmodium berghei* putative phospholipase impairs efficient egress of merosomes. *International Journal for Parasitology* (2022).
103 Lévêque, M. F. *et al.* TgPL2, a patatin-like phospholipase domain-containing protein, is involved in the maintenance of apicoplast lipids homeostasis in *Toxoplasma*. *Molecular Microbiology* **105**, 158-174 (2017).
104 Aurrecoechea, C. *et al.* PlasmoDB: a functional genomic database for malaria parasites. *Nucleic Acids Research* **37**, D539-D543 (2009).
105 Asad, M. *et al.* An essential vesicular-trafficking phospholipase mediates neutral lipid synthesis and contributes to hemozoin formation in *Plasmodium falciparum*. *BMC Biology* **19**, 1-22 (2021).
106 Sheokand, P. K. *et al.* GlmS mediated knock-down of a phospholipase expedite alternate pathway to generate phosphocholine required for phosphatidylcholine synthesis in *Plasmodium falciparum*. *Biochemical Journal* **478**, 3429-3444 (2021).
107 Sheokand, P. K. *et al.* A *Plasmodium falciparum* lysophospholipase regulates host fatty acid flux via parasite lipid storage to enable controlled asexual schizogony. *Cell Reports* (2023).
108 Butler, J. H. *et al.* Resistance to some but not other dimeric lindenane sesquiterpenoid esters is mediated by mutations in a *Plasmodium falciparum* esterase. *ACS Infectious Diseases* **6**, 2994-3003 (2020).
109 Istvan, E. S. *et al.* Esterase mutation is a mechanism of resistance to antimalarial compounds. *Nature communications* **8**, 1-8 (2017).
110 Sindhe, K. M. *et al. Plasmodium falciparum* resistance to a lead benzoxaborole due to blocked compound activation and altered ubiquitination or sumoylation. *MBio* **11**, e02640-02619 (2020).
111 Spillman, N. J. *et al.* Exported epoxide hydrolases modulate erythrocyte vasoactive lipids during *Plasmodium falciparum* infection. *MBio* **7**, e01538-01516 (2016).
112 Bhanot, P. *et al.* A surface phospholipase is involved in the migration of *Plasmodium* sporozoites through cells. *Journal of Biological Chemistry* **280**, 6752-6760 (2005).
113 Burda, P.C. *et al.* A *Plasmodium* phospholipase is involved in disruption of the liver stage parasitophorous vacuole membrane. *PLoS Pathogens* **11**, e1004760 (2015).
114 Groat-Carmona, A. M. *et al.* A *Plasmodium* α/β-hydrolase modulates the development of invasive stages. *Cellular Microbiology* **17**, 1848-1867 (2015).
115 Elahi, R. *et al.* Internalization of erythrocyte acylpeptide hydrolase is required for asexual replication of *Plasmodium falciparum*. *Msphere* **4**, e00077-00019 (2019).
116 Davison, D. *et al.* Activity-based protein profiling of human and *plasmodium* serine hydrolases and interrogation of potential antimalarial targets. *Iscience* **25**, 104996 (2022).
117 Liu, Z. *et al.* Emerging roles of protein palmitoylation and its modifying enzymes in cancer cell signal transduction and cancer therapy. *International Journal of Biological Sciences* **18**, 3447-3457 (2022).
118 Malgapo, M. I. P. & Linder, M. E. Substrate recruitment by zDHHC protein acyltransferases. *Open biology* **11**, 210026 (2021).

119 Eisenberg, S. *et al.* The role of palmitoylation in regulating Ras localization and function. *Biochemical Society Transactions* **41**, 79-83 (2013).
120 Guan, X. & Fierke, C. A. Understanding protein palmitoylation: Biological significance and enzymology. *Science China Chemistry* **54**, 1888-1897 (2011).
121 Dallavilla, T. *et al.* Model-driven understanding of palmitoylation dynamics: regulated acylation of the endoplasmic reticulum chaperone calnexin. *PLoS Computational Biology* **12** (2016).
122 Bachert, C. & Linstedt, A. D. Dual anchoring of the GRASP membrane tether promotes trans pairing. *Journal of Biological Chemistry* **285**, 16294-16301 (2010).
123 Won, S. J. *et al.* Protein depalmitoylases. *Critical Reviews in Biochemistry and Molecular Biology* **53**, 83-98 (2018).
124 Lin, D. T. S. & Conibear, E. ABHD17 proteins are novel protein depalmitoylases that regulate N-Ras palmitate turnover and subcellular localization. *eLife* **4**, e11306 (2015).
125 Jones, M. L. *et al.* Analysis of protein palmitoylation reveals a pervasive role in *Plasmodium* development and pathogenesis. *Cell Host & Microbe* **12**, 246-258 (2012).
126 Siddiqui, M. A. *et al.* Protein S-Palmitoylation is responsive to external signals and plays a regulatory role in microneme secretion in *Plasmodium falciparum* merozoites. *ACS Infectious Diseases* **6**, 379-392 (2020).
127 Cabrera, A. *et al.* Dissection of minimal sequence requirements for rhoptry membrane targeting in the malaria parasite. *Traffic* **13**, 1335-1350 (2012).
128 Beck, J. R. *et al.* A *Toxoplasma* palmitoyl acyl transferase and the palmitoylated armadillo repeat protein TgARO govern apical rhoptry tethering and reveal a critical role for the rhoptries in host cell invasion but not egress. *PLoS Pathogens* **9**, e1003162 (2013).
129 Wang, X. *et al.* A protein palmitoylation cascade regulates microtubule cytoskeleton integrity in *Plasmodium*. *The EMBO journal* **39**, e104168 (2020).
130 Qian, P. *et al.* Inner membrane complex proteomics reveals a palmitoylation regulation critical for intraerythrocytic development of malaria parasite. *Elife* **11**, e77447 (2022).
131 Hopp, C. S. *et al.* Palmitoyl transferases have critical roles in the development of mosquito and liver stages of *Plasmodium*. *Cellular Microbiology* **18**, 1625-1641 (2016).
132 Santos, J. M. *et al.* The *Plasmodium* palmitoyl-S-acyl-transferase DHHC2 is essential for ookinete morphogenesis and malaria transmission. *Scientific reports* **5**, 16034 (2015).
133 Frénal, K. *et al.* Global analysis of apicomplexan protein S-acyl transferases reveals an enzyme essential for invasion. *Traffic* **14**, 895-911 (2013).

Chapter 2

Identification of a putative depalmitoylase essential for merozoite invasion in asexual stage *Plasmodium falciparum*

Jiapeng Liu, Katie Fike, Fahd Mohamed, Rubayet Elahi and Michael Klemba

Department of Biochemistry, Virginia Tech

Running Head: *P. falciparum* ABHD17A

2.1 ABSTRACT

Due to artemisinin resistance, new druggable target identification and drug development are urgently needed to deal with the malaria issue. Metabolic serine hydrolases (SHs), which use a catalytic nucleophile serine to hydrolyze ester, thioester or amide bonds in small molecules, are druggable but remain understudied in malaria parasites. Determining the essentiality and functional characterization of these metabolic SHs are beneficial for understanding the life processes of malaria parasites and will shed light on future drug development to treat malaria. We identified 2 metabolic SHs that are refectory to gene disruption (GD) in the asexual stage and focused on a putative essential depalmitoylase termed PfABHD17A. PfABHD17A is localized on the rhoptries and exhibits depalmitoylase activity *in vitro.* Using human depalmitoylase inhibitor ML211, which can inhibit recombinant PfABHD17A *in vitro*, we suggested that PfABHD17A is essential in merozoite invasion but not egress. In conclusion, we discovered a rhoptry depalmitoylase PfABHD17A likely required for merozoite invasion.

KEYWORDS: *Plasmodium*, malaria, serine hydrolase, depalmitoylase, ABHD17, rhoptry, merozoite invasion

2.2 INTRODUCTION

Malaria caused about 619,000 deaths in 2021 according to the world malaria report[1]. The life cycle of the deadliest malaria parasite, *Plasmodium falciparum*, involves two hosts, mosquito and human. The infection of malaria started from human bitten by infected mosquitos, which releases sporozoites to infect human hepatocytes. After the development in the hepatocytes, merozoites will be released to the blood stream and infect human red blood cells (RBCs) to start their development in the asexual stage. Parasites utilize the nutrients from the host, develop into schizonts, rupture the RBCs, release the new merozoites to the blood and start their next cycle replication. Some asexual stage parasites will develop into gametocytes, which can be taken up by mosquitos and will finally develop into sporozoites to start their infection on human again. The asexual stage is the pathogenic stage of malaria, which may cause anemia, fever and chills because of the rupture of RBCs[2]. Infected RBCs may also trigger inflammatory response or hypoxia by blocking capillaries[3,4]. Thus, stopping the growth of malaria parasites in the asexual stage is important for the treatment of malaria.

Serine hydrolases (SHs) are one kind of enzymes using nucleophile serine to catalyze hydrolysis reactions and can be classified into serine proteases and metabolic SHs. Metabolic SHs have important roles in life processes and several drugs towards SHs including rivastigmine, Orlistat and others have been approved in clinical use[5]. The *P. falciparum* genome encodes 39 active metabolic SHs[6] while only a few of them have been studied. Characterization of the unstudied SHs will help us to gain a better understanding on the biology of *Plasmodium* and shed light on future drug development.

Recently, a saturation mutagenesis study was applied in asexual stage *Plasmodium falciparum* parasites and about 60% genes were identified to be potential essential in the asexual stage[7]. Taking advantage of this mutagenesis study[7] and our proteomic study on the asexual stage SHs[6], we identified 2 metabolic SHs are refractory to gene disruption (GD). We focused on one likely essential SH termed PfABHD17A, which is homologous to human ABHD17s. We found that PfABHD17A localizes on the rhoptries, exhibits depalmitoylase activity and is likely essential in merozoite invasion.

2.3 RESULTS

Identification of metabolic serine hydrolases essential in the asexual stage

The *P. falciparum* genome encodes 39 putatively active metabolic SHs including 34 alpha/beta hydrolases (ABHDs) and 5 putative patatin-like phospholipases[6]. Only a few metabolic SHs have been studied. Three Lysophospholipases (LPL1, 3 and 20) were verified to have lysophospholipase activities *in vitro* and mediate lipid metabolism[8-10]. *Plasmodium falciparum* prodrug activation and resistance esterase (PfPARE) can cleave an esterified prodrug and its mutation can mediate drug resistance of the parasites[11-13]. *P. falciparum* epoxide hydrolase (PfEH) 1 and 2 are dispensable RBC-localized epoxides hydrolases that can hydrolyze erythrocyte epoxide signaling lipids[14]. *P. berghei* phospholipase (Pb PL) is not essential in all stages of the parasites but can facilitate sporozoites passing through epithelial cell layers and mediate parasitophorous vacuole membrane (PVM) rupture and egress[15,16]. *Plasmodium* BEM46-like protein (PBLP) has broad roles in parasite life cycle including regulating asexual stage schizogony, development in oocysts and sporozoites, and infection in hepatocytes[17]. Patatin-like

phospholipases 1 (PNPLA1) or *P. falciparum* patatin-like phospholipase 1 (PfPATPL1), is found to have little effect in the asexual stage growth or gametocyte development[18,19]. *Plasmodium berghei* phosphatidic acid preferring phospholipase A1 (PbPla1), is not essential in the asexual or mosquito stages but can influence merozoite release in the liver stage[20]. The homolog of a 238 kD patatin-like phospholipase in *Toxoplasma gondii*, is essential in tachyzoites and regulates lipid metabolism[21].

We started from identifying potential essential metabolic SHs in the asexual stage based on our previous proteomic study[6] and the mutagenesis study[7] (Table 2-1 and Figure 2-1). In our previous proteomics study, Elahi *et al* utilized a desthiobiotin-fluorophosphonate (desthiobiotin-FP) affinity probe to capture active SHs and identified 21 parasite SHs expressed in schizont stage *P. falciparum*[6]. Seven SHs in this study[6], having a low mutagenesis index score according to the mutagenesis study[7], are identified as potential essential, including Pf3D7_0403800, Pf3D7_0728700, Pf3D7_1001600, Pf3D7_1120400, Pf3D7_1134500, Pf3D7_1143000 and Pf3D7_ 1252600. Three SHs, Pf3D7_0218600, Pf3D7_0629300 and Pf3D7_1358000, have low mutant fitness scores and are annotated as non-essential but impacting parasite growth[7]. We also included PF3D7_0924000, a patatin-like phospholipase which did not appear in our previous study but is indicated to influence parasite growth[6,7].

We determined the essentiality of these SHs by examining if these genes are tolerant to truncation using a selection-link integration method[22] (Figure 2-1A). In this method, homologous recombination occurs in front of the catalytic domain or the catalytic amino acids, which will generate an inactive, truncated protein. The vector plasmid which carries a human dihydrofolate reductase (DHFR) cassette is used to introduce WR99210

resistance for the selection of the plasmids. After homologous recombination, the neomycin resistance gene is in frame with the target gene and is translated under the target gene promoter. The expression of neomycin resistance protein is also mediated by a skip peptide so that neomycin resistance protein is translated as a separate product instead of a fusion protein with the target gene. Thus, only gene disrupted parasites can survive under G418 selection.

Table 2-1. Identification of essential serine hydrolases in the asexual stage.
Gene ID, Name/PlasmoDB annotation and molecular weight were obtained from PlasmoDB.org[23]. The gene essentiality is determined by the results of generating GD single clone parasites verified by diagnostic PCR. Y indicates that GD line was not generated successfully from two independent biological replicates with two technical replicates each time. N indicates that gene disruption single clone parasite lines were generated successfully.

Gene ID Pf3D7_	Name/PlasmoDB Annotation	Molecular Weight (kD)	Essentiality
0218600	Patatin-like phospholipase, putative	283.6	N
0403800	Alpha/beta hydrolase, putative	83.4	Y
0629300	Phospholipase	99.2	N
0728700	Alpha/beta hydrolase, putative	84.8	N
0924000	Patatin-like phospholipase, putative	151.5	N
1001600	Exported lipase 2	88.6	N
1120400	Alpha/beta hydrolase, putative	44.7	N
1134500	Alpha/beta hydrolase, putative	210.5	Y
1143000	Alpha/beta hydrolase, putative	48.8	N
1252600	Esterase, putative	52.9	N
1358000	Patatin-like phospholipase, putative	238.2	N

Nine GD single clone parasite lines were generated successfully after drug selection, single-cell cloning and diagnostic PCR analysis (Table 2-1), which is not surprising

because lots of genes that are predicted to be essential according to the transposon mutagenesis study are in fact dispensable[17,24]. Two genes, Pf3D7_0403800 and Pf3D7_1134500, were refractory to GD. Thus, Pf3D7_0403800 and Pf3D7_1134500 were identified as likely essential in the asexual stage.

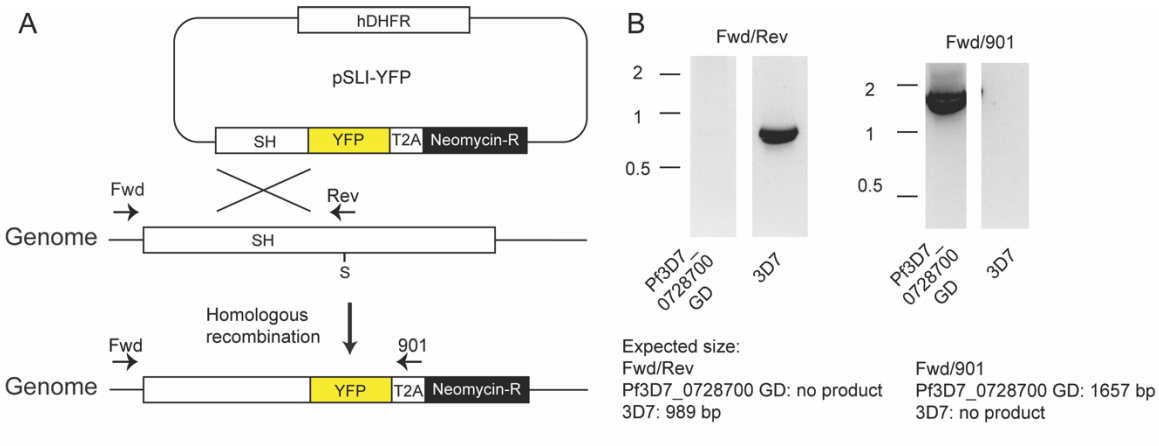

Figure 2-1. Generation of serine hydrolases gene disruption parasite lines to identify essential serine hydrolases in the asexual stage. (A) Strategy for disruption of SH coding sequence through single-crossover homologous recombination and selection-linked integration. The position of the catalytic serine (S) is indicated. SH, serine hydrolase. YFP, yellow fluorescent protein. T2A, *Thosea asigna* virus 2A self-cleaving peptide. Neomycin-R, neomycin resistance gene. Fwd and Rev, gene-specific primers used for diagnostic PCR. (B) An example of diagnostic PCR result of a dispensable serine hydrolase (Pf3D7_0728700). Diagnostic PCR results of other dispensable serine hydrolases are not shown. Sizes of markers are indicated in kilobases.

Phylogenetic analysis and schematic structure of PfABHD17A

We focused on one likely essential SH, Pf3D7_0403800, a human ABHD17 (hABHD17) homolog in *P. falciparum*. The only known function of hABHD17 is depalmitoylase mediating protein localization[25-27]. We conducted a phylogenetic analysis on *P. falciparum* and some human metabolic SHs including human depalmitoylase acyl-protein thioesterases (APTs) and ABHD10 (Figure 2-2A). The *P. falciparum* genome

includes 4 hABHD17 homologs, termed PfABHD17A/B/C/D (Table 2-2), which are closed related to hABHD17s but not APTs or ABHD10 (Figure 2-2A). PfABHD17B/C were identified as dispensable in our study according to the result of identification of essential SHs in the asexual stage (Table 2-1), while PfABHD17D is tolerant to the transposon insertion on the coding sequence in the mutagenesis study[7], thus PfABHD17A is the only essential PfABHD17 in the asexual stage.

We conducted an analysis of protein order and disorder on PfABHD17A using IUPred2A[28] (Figure 2-2B). The N-terminus of PfABHD17 which contains catalytic domain is predicted to be highly ordered. The N-terminus also includes a myristylation site, which is refractory to mutation in the asexual stage[29]. The C-terminus is predicted to be less ordered with multiple phosphorylation sites (Plasmodb.org[23]), which may regulate the activity of PfABHD17A.

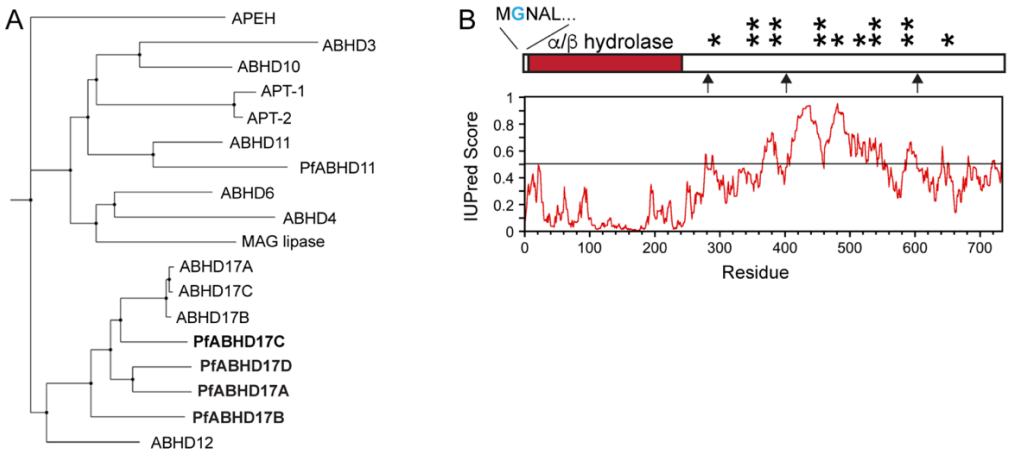

Figure 2-2. Phylogenetic analysis of selected human and *P. falciparum* metabolic serine hydrolases and schematic structure of PfABHD17A. (A) Maximum likelihood tree of selected human serine hydrolases and PfABHD17s. *P. falciparum* genome encodes 4 hABHD17 homologs. (B) Schematic of PfABHD17A as well as order and disorder analysis via IUPred2. The myristylation site is labeled in cyan and the phosphorylation sites are labeled as asterisks.

Table 2-2. Four *P. falciparum* ABHD17 homologs and the predicted molecular weights. Gene ID and molecular weight were obtained from PlasmoDB.org[23].

Gene ID Pf3D7_	Name	Molecular Weight (kD)
0403800	PfABHD17A	83.4
0728700	PfABHD17B	84.8
1120400	PfABHD17C	44.7
0805000	PfABHD17D	28.5

PfABHD17A is localized to the rhoptries

We determined the location of PfABHD17A to gain insights into the functions of PfABHD17A. We generated a C-terminal yellow fluorescent protein (YFP) tagged parasite line through selection-linked integration[22] (Figure 2-S1). Using immunofluorescence assay (IFA, Figure 2-3), we discovered that PfABHD17A was exclusively expressed in schizont stage and co-localized with the rhoptry marker protein rhoptry associated protein (RAP) 1. Rhoptries are secretary organelles in the merozoites and exist as two club-shaped organelles attached to the apical end of the merozoites[30,31]. During merozoite invasion, proteins from the rhoptries are released from the merozoites, which can facilitate the invasion[31]. Rhoptry proteins are also found to be important for the parasite development after invasion[32]. Thus, we hypothesized that rhoptry localized PfABHD17A may be essential in merozoite invasion or parasite development after invasion.

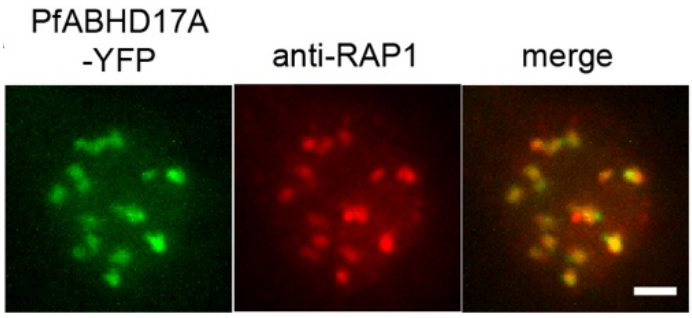

Figure 2-3. PfABHD17A localizes to the merozoite rhoptries. Colocalization of PfABHD17A (pseudocolored with green) with RAP1 via immunofluorescence assay in mature schizonts. Scale bar, 2 μm.

Generating PfABHD17A conditional knockdown parasite lines

We generated conditional knockdown parasite lines to verify the essentiality of PfABHD17A in the asexual stage and investigate its function. We applied a destabilization domain (DD) method[33] by introducing YFP and an *Escherichia coli* (*E. coli*) DHFR DD tag on the C-terminus of PfABHD17A to manipulate the steady-state level of PfABHD17A (Figure 2-4A and 2-S2A). The expression of PfABHD17A can be controlled by trimethoprim (TMP) in the medium. Without TMP, PfABHD17A-YFP-DD fusion protein is not stable on the C-terminus and will be degraded. After the addition of TMP, PfABDH17A-YFP-DD will be stabilized and the expression of PfABHD17A will be recovered. We generated PfABHD17A-YFP-DD parasite lines and conducted a growth assay after removing TMP. However, parasites were still viable growing in the absence of TMP (Figure 2-4B), which might be due to the residual activity of PfABHD17A. The knockout down efficiency was determined using microscopy. Most parasites in the absence of TMP exhibited no fluorescence while a small proportion of parasites exhibited weak fluorescence on the rhoptries (data not shown). This result suggested that PfABHD17A

was knocked down, but the knockdown was not complete. Viability in the absence of TMP might be due to the remaining expression of PfABHD17A.

We also applied the TetR-DOZI method[34], which have been successfully used to study essential genes in asexual stage *P. falciparum* parasites (Figure 2-4C). In this method, an aptamer sequence which can bind to the fusion protein TetR-DOZI, was installed on the 3' untranslated region (UTR) of PfABHD17A using CRISPR/Cas9 editing. The expression of the target gene can be regulated by DOZI, a *Plasmodium* RNA helicase that represses translation[35]. In the absence of ligand, TetR will bind to the aptamer sequence[36], which guides DOZI to suppress translation. When anhydrotetracycline (aTC) exists in the parasites, aTC will compete with TetR for the aptamer binding and reverse the inhibition[36]. We tagged PfABHD17A with 3-human influenza hemagglutinin (3HA) at the C-terminus for future knockdown efficiency examination. We conducted the growth assay after removing aTC and determined the knockdown efficiency. Similarly, parasites were still viable probably due to the residual activity of PfABHD17A as verified by IFA.

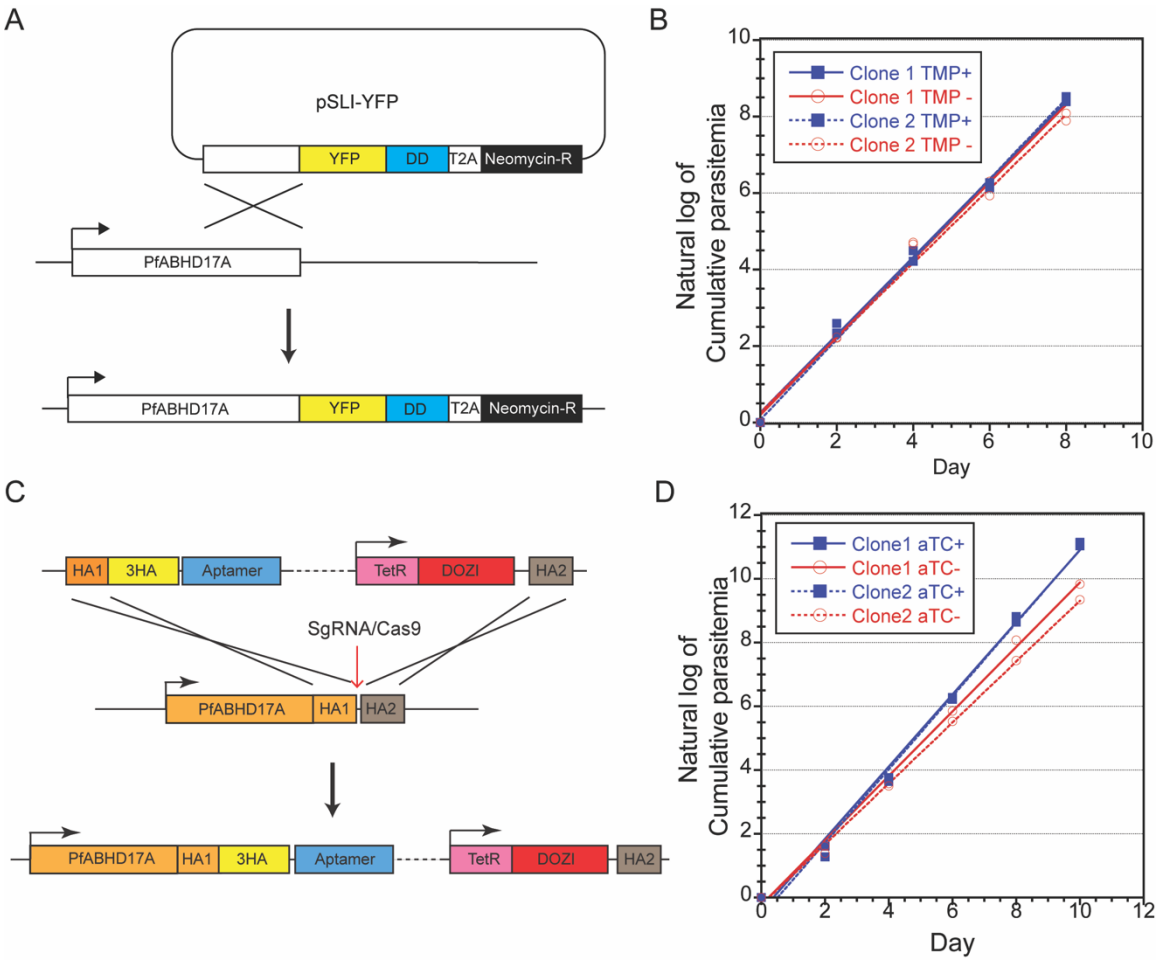

Figure 2-4. Generation of PfABHD17A conditional knockdown parasite lines to determine the essentiality of PfABHD17A. (A) Strategy for generating PfABHD17-YFP-DD parasite lines. YFP, yellow fluorescent protein. DD, destabilization domain. T2A, *Thosea asigna* virus 2A self-cleaving peptide. Neomycin-R, neomycin resistance gene. (B) PfABHD17A-YFP-DD parasites are still viable after removing the ligand. Two single clones were used to generate the growth curve. (C) Strategy for generating PfABHD17 TetR-DOZI parasite lines. The homologous recombination occurs on both 3' coding region and 3' UTR so that the aptamer and TetR-DOZI fusion protein cassette are inserted on the 3' UTR of PfABHD17A. HA, homology arm. 3HA, 3-human influenza hemagglutinin. (D) PfABHD17A TetR-DOZI on PfABHD17B GD background parasites are still viable after removing the ligand. Two single clones were used to generate the growth curve.

We then wondered if the expression of other PfABHD17 homologs could complement the effect of loss of PfABHD17A. Among the other 3 PfABHD17 homologs, PfABHD17B is the most similar to PfABHD17A with respect to size (~84 kD), protein

structure (N-terminus catalytic domain and myristylation site as well as a disordered C-terminus regulatory region) and expression profile on RNA level (high expression in schizonts and early rings but low expression in trophozoites)[37,38]. We generated PfABHD17A TetR-DOZI parasites on PfABHD17B GD background (Figure 2-S2B) and conducted a growth assay after removing aTC. Similarly, parasites were still viable (Figure 2-4D) with an incomplete knockdown efficiency verified by IFA (data not shown). Because of the remaining activity of PfABHD17A, other methods such as DiCre (dimerizable Cre recombinase)[39] are needed to determine if PfABHD17A is essential in the asexual stage.

Human depalmitoylase inhibitor ML211 inhibits recombinant PfABHD17A *in vitro*

We then used inhibitors to study the function of PfABHD17A. We expressed the catalytic domain of PfABHD17A in *E. coli*. The activity of recombinant PfABHD17A (rPfABHD17A) was verified by activity-based protein profiling (ABPP) using TAMRA-fluorophosphonate[6,40] (TAMRA-FP, Figure 2-5A), which can label the active site serine of SHs. We screened a panel of commercially available human depalmitoylase inhibitors (Table 2-S2) on rPfABHD17A (Figure 2-5A). We also included lipases inhibitors (Table 2-S2) since human depalmitoylases APT1/2 were reported to have lysophospholipase activity[41,42]. ML211[43], a human depalmitoylase APT1/2 inhibitor, could inhibit rPfABHD17A *in vitro*. To test the off-target effects of ML211, we expressed recombinant PfABHD17B/C/D (rPfABHD17B/C/D) in *E. coli* and determined if they can be inhibited by ML211 (Figure 2-S3). ML211 showed inhibition on rPfABHD17C but not rPfABHD17B or rPfABHD17D (Figure 2-S3). ML211 was also reported to have an off-target, human ABHD11, so we tested the control probe ML226, which can inhibit human

ABHD11 but not ABHD17[43]. ML226 had no inhibition on rPfABHD17A (Figure 2-5A). Both ML211 and ML226 inhibit the target SHs by forming covalent bond with the active site serine to block the catalytic activity of the targets[43]. Besides, rPfABHD17A could also be inhibited by pan-lipase inhibitor Isopropyl Dodecylfluorophosphonate (IDFP)[44] and monoacylglycerol lipase (MAGL) inhibitor JJKK046[45], which suggests that PfABHD17A may also have lipase activity (Figure 2-5A).

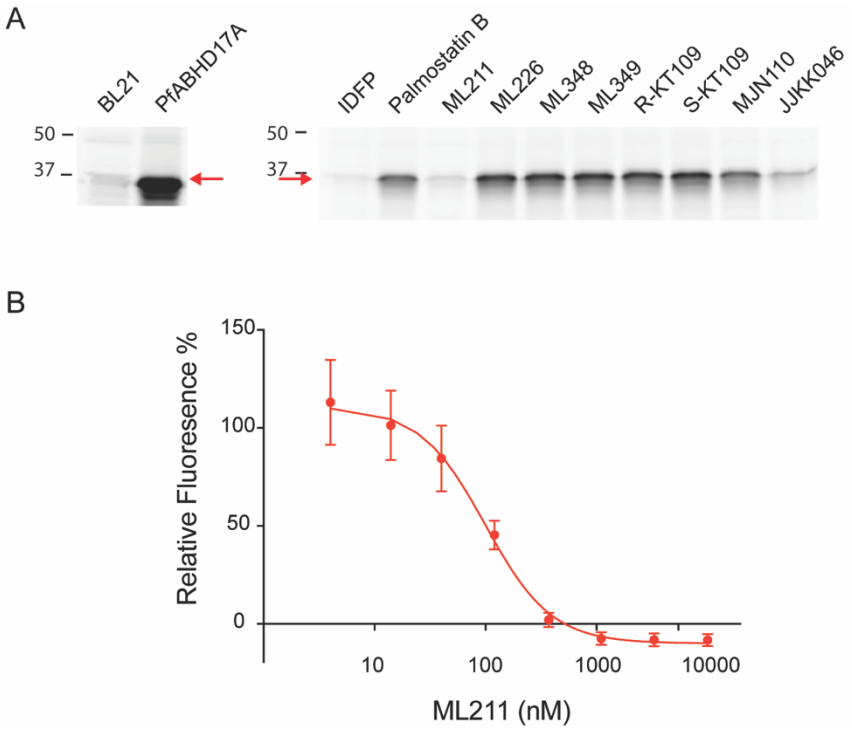

Figure 2-5. Human depalmitoylase inhibitor ML211 inhibits rPfABHD17A *in vitro*. (A) Recombinant protein expression of PfABHD17A in BL21 *E. coli* labeled with TAMRA-FP (left) and inhibitor screen on rPfABHD17A *in vitro* via ABPP (right). Inhibitors were added at 10 μM. Red arrows, rPfABHD17A. Sizes of markers are indicated in kD. (B) Determination of the potency of ML211 inhibition of rPfABHD17A *in vitro* via a solution-based 4-MUH hydrolysis assay. Data are normalized to DMSO-treated rPfABHD17A. Means and standard deviations are from three independent experiments.

We determined the potency of ML211 inhibition of rPfABHD17A using a solution-based 4-methylumbelliferyl-heptanoate (4-MUH) hydrolysis assay[46]. 4-MUH can be

hydrolyzed by lipases to generate a highly fluorescent compound 4-methylumbelliferone[46]. The IC_{50} of ML211 inhibition of recombinant PfABHD17A was 100 ± 11 nM (Figure 2-5B).

ML211 inhibits merozoite invasion *in vivo*

We investigated the roles of PfABHD17A in the asexual stage growth using ML211. At the end of schizont stage, two processes termed egress and invasion are important for parasite development. Egress is the process of parasite rupture of the parasitophorous vacuolar and RBC membranes resulting the release of merozoites to the blood stream. Invasion is the process whereby parasite merozoites enter RBCs to begin their development. As PfABHD17A is localized on the rhoptry (Figure 2-3), we hypothesized that PfABHD17A may be important for merozoite invasion. We therefore examined the functions of PfABHD17A on egress and invasion using ML211. Schizont stage parasites were labeled with dimethyl sulfoxide (DMSO), ML211 or ML226 and the parasitemia was determined by flow cytometry after 0, 4, 8 and 20 hours (Figure 2-6). In DMSO or ML226-treated parasites, schizont stage parasitemia decreased and the ring stage parasitemia increased as expected. In ML211-treated parasites, schizont stage parasitemia decreased similarly, which suggested that PfABHD17A had no effect on egress. However, ring stage parasitemia of ML211-treated parasites did not increase. This result suggested that PfABHD17A are essential for merozoite invasion but not egress, however, the off-target effect of ML211 cannot be excluded.

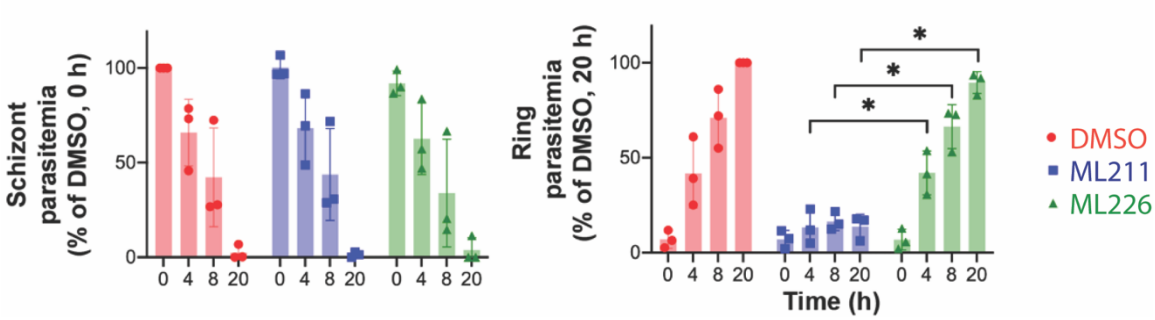

Figure 2-6. PfABHD17A inhibitor ML211 inhibits merozoite invasion but not egress. Data are normalized to DMSO-treated parasites at 0 h. Inhibitors were added at 10 μM. Significance relative to DMSO-treated parasites was assessed using student's *t*-test. *, $p < 0.01$.

Assessment of PfABHD17A as a depalmitoylase *in vitro*

We then assessed the enzymatic function of PfABHD17A as a depalmitoylase using a depalmitoylase substrate DPP-5[47], which contains a pre-fluorophore linked to an S-acylated peptide via a carbamate linkage. The hydrolysis of the thioester bond by depalmitoylases will trigger a reaction cascade and will finally release a fluorescent compound[47]. We purified the rPfABHD17A via immobilized metal affinity chromatography and gel filtration chromatography (Figure 2-7A). We then discovered that the purified rPfABHD17A can hydrolyze DPP-5 *in vitro* (Figure 2-7B), which is consistent with PfABHD17A having depalmitoylase activity.

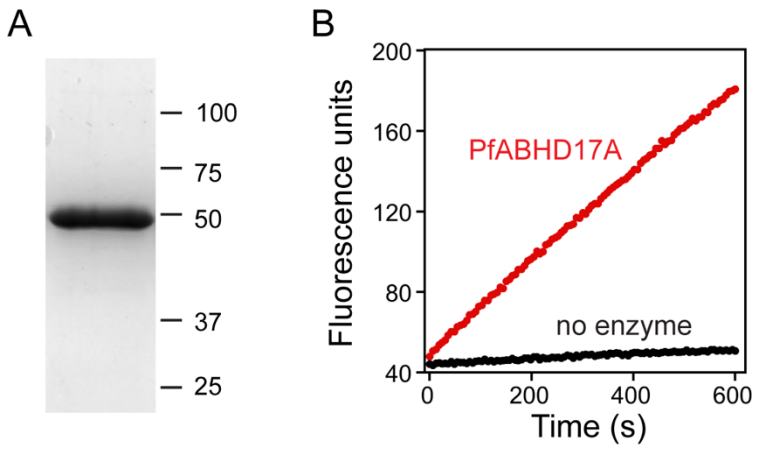

Figure 2-7. PfABHD17A can hydrolyze a depalmitoylase substrate *in vitro*. (A) Coomassie blue stain of purified rPfABHD17A. Sizes of markers are indicated in kD. (B) Purified rPfABHD17A can hydrolyze depalmitoylase substrate DPP-5.

2.4 DISCUSSION

The *P. falciparum* genome encodes 39 active metabolic SHs while most of them remain unstudied. Functional characterization of these unknown SHs will not only broaden our understanding on the metabolic processes of *Plasmodium* parasites, but will also provide insight for future drug development. Here, we determined the essentiality of metabolic SHs in asexual stage *Plasmodium falciparum* parasites and discovered that PfABHD17A may be an essential depalmitoylase involved in merozoite invasion.

Protein palmitoylation is important for protein function and activity, thus has a broad impact on life processes. Protein palmitoylation is essential in several processes in asexual stage *P. falciparum* parasites, including rhoptry biogenesis, inner membrane complex (IMC) assembly, schizont development, microneme secretion and merozoite invasion[48-53]. In the asexual stage, more than 400 proteins are palmitoylated and protein palmitoylation is the most abundant in schizonts[50,54]. The *P. falciparum* genome encodes 12 palmitoylases termed palmitoyl acyl transferases (PATs), which have been verified to have important roles in maintaining the life cycle of the parasites[54-57]. However, among the

known human depalmitoylases (APTs, palmitoyl-protein thioesterases (PPTs), ABHD10 and ABHD17s), the *P. falciparum* genome only includes ABHD17 homologs. Our study showed that PfABHD17A is likely the only essential one of the four PfABHD17s in the asexual stage. The other PfABHD17s may have roles as depalmitoylases in other stages of the parasite.

We concluded PfABHD17A is essential in the asexual stage because of the failure in generating GD parasites. However, the essentiality of PfABHD17A via conditional knockdown methods was not verified successfully, likely due to the residue expression of PfABHD17A. Instead, we identified and applied a PfABHD17A inhibitor to study its function. Human depalmitoylase APT1/2 inhibitor ML211 inhibited PfABHD17A *in vitro* and merozoite invasion, with an off-target of PfABHD17C. However, another study reported that ML348, which inhibits APT1 but not rPfABHD17A, had impact on parasite growth in the asexual stage[58], which raises the question whether ML211 inhibits parasite growth by APT1 or by PfABHD17A[58]. A method with enhanced knockdown or knockout efficiency is needed to verify the essentiality PfABHD17A in the asexual stage. DiCre method[39], which can control gene expression on genomic DNA level, has been wildly used to determine the essentiality of genes in *Plasmodium* and was reported to have a high conditional knockout efficacy. The application of DiCre method on PfABHD17A may provide a higher knockout efficacy for better characterization of the function of PfABHD17A.

Together, our data suggest that PfABHD17A may be essential for regulating the palmitoylation status of rhoptry proteins during merozoite invasion. Several rhoptry palmitoylated protein were identified, including armadillo repeats-only (ARO), rhoptry-

associated protein (RAP) 1/2/3, rhoptry neck protein 2, high molecular weight rhoptry protein 3 (RhopH3) and *Plasmodium falciparum* cytosolically exposed rhoptry leaflet interacting protein 1 (PfCERLI1) [50,57,59]. Palmitoylation status was verified to be important for the localization of PfARO[57]. Although the function of PfARO hasn't been studied, the homolog of PfARO in *Toxoplasma gondii* TgARO mediates the apical localization of the rhoptries and is essential for invasion[60,61]. TgARO was also verified to be a substrate of a *Toxoplasma gondii* depalmitoylase, which is a human APTs homolog[62]. Human APTs and other known human depalmitoylase homologs are absent in the *P. falciparum* genome, which suggests that PfABHD17A may mediate invasion by regulating the localization of PfARO.

PfABHD17A can be inhibited by lipases inhibitors, which suggests that PfABHD17A may also include lipase activity. Rhoptry is consisted of a lipid deficient neck and a lipid rich bulb region, with distinct protein composition on each compartment[63]. The lipase activity of PfABHD17A may be important for rhoptry function by maintaining the different lipid content between neck and bulb regions.

2.5 MATERIAL AND METHODS

Materials

IDFP, ML211, ML226, ML348, ML349, MAFP, anhydrotetracycline and blasticidin S were purchased from Cayman Chemical. R-KT109, S-KT109, MJN-110, Palmostatin B and Trimethoprim were purchased from Millipore Sigma. SYTO™ 11, ProLong™ Diamond Antifade Mountant with DAPI and Goat anti-Mouse Secondary Antibody, Alexa Fluor™ 594 were purchased from ThermoFisher. HisTALON™ Column was purchased

from Clonetech. Superdex 200 10/300 GL was purchased from Cytiva. JJKK-046 inhibitor described in Aaltonen *et al*[45] was provided by Dr. T. Nevalainen, University of Eastern Finland. The following reagent was obtained through BEI Resources, NIAID, NIH: DSM1, MRA-1161. WR99210 was a gift from D. Jacobus (Jacobus Pharmaceuticals). DPP-5[47] was a gift from Dr. Bryan Dickinson from the University of Chicago. Mouse anti-RAP1 was a gift from Dr. Alan Cowman, The Walter and Eliza Hall Institute of Medical Research.

Parasite culture

P. falciparum clone 3D7 was routinely cultured in human O^+ erythrocytes (Interstate Blood Bank) at 2% hematocrit in RPMI 1640 medium supplemented with 0.37 mM hypoxanthine, 0.5% Albumax I (Gibco), 11 mM glucose, 27 mM sodium bicarbonate and 10 μg/mL gentamicin. Cultures were incubated at 37 °C in a 5% CO_2 incubator and were synchronized by treatment with 5% (w/v) sorbitol.

Generation of plasmids and parasite transfection

Oligonucleotides for plasmid construction and parasite line validation are listed in **Table 2-S1**. Diagnostic PCR analysis was conducted using 10 ng of parasite genomic DNA in 15 μL reactions amplified by Taq polymerase (New England Biolabs).

Generation of SHs GD parasites, C-terminal YFP tagged PfABHD17A parasites and PfABHD17A-YFP-DD parasites were achieved by single cross over homologous recombination using selection-linked integration method[22]. The L3-2xFKBP-L4-GFP sequence between *Avr*II and *Sal*I sites of pSLI-2×FKBP-GFP was replaced by yellow fluorescent protein allele Citrine (without stop codon) to generate pSLI-YFP. A stop codon

followed by homology sequence at about 800 bp in front of the catalytic domain predicted by Plasmodb.org[23] or the conserved catalytic amino acids (asparagine, serine or histidine identified by BLAST search) was inserted into *Not*I and *Avr*II sites of pSLI-YFP to generate GD parasites. A stop codon followed by homology sequence at about 800 bp in front of the target gene stop codon was inserted into *Not*I and *Avr*II sites of pSLI-YFP to generate C-terminal YFP tagged PfABHD17A parasites. Destabilization domain sequence[33] was inserted into the *Sal*I site of pSLI-PfABHD17A-YFP to generate pSLI-PfABHD17A-YFP-DD parasite line. Ring stage *P. falciparum* clone 3D7 parasites were transfected with 100 µg plasmid by electroporation[64] and were treated with 5 nM WR99210 48 hours after transfection. For SHs GD parasites and C-terminal YFP tagged PfABHD17A parasites, WR99210 resistance parasites were treated with 400 µg/mL of G418 for 12 days for selection of parasites with single crossover homologous recombination. For PfABHD17A-YFP-DD parasites, WR99210 resistance parasites were treated with 5 µM TMP for 6 days and then selected with 400 µg/mL of G418 with the existence of TMP for 12 days. Single clone parasite lines were isolated by limiting dilution in 96-well plate.

Generation of PfABHD17A TetR-DOZI parasites was achieved by CRISPR/Cas9 editing[34]. Cas9 small guide RNAs targeting the parasite genome were selected from the database generated by Ribeiro *et al*[65] and were inserted on the BtgZ1 site of pUF-Cas9-pre-sgRNA[66]. For homology repair plasmid, two homology arm sequences at about 350 bp on the 3' CDS and 3' UTR of PfABHD17A were PCR amplified by primer 1210/1211 and 1212/1213, respectively. Both PCR products were merged into one product by overlapping PCR using oligo 1211/1212. The meagered product was insert between *AscI* and *AatII* sites of pKD^{PfAUBL}. For transfection, 75 µg pUF-Cas9-pre-sgRNA plasmid and 75 µg homology

repair plasmid (lineralized by EcorV) were co-transfected into ring stage parasites. Parasites were incubated with 0.5 μM anhydrotetracycline after transfection. After 48 hours, parasites were treated with 1.5 μM DSM-1 and 2.5 μg/ml blasticidin S with 0.5 μM anhydrotetracycline for 7 days.

Recombinant protein expression of PfABHD17s was achieved using pET-45b plasmid. The catalytic domains of PfABHD17A and PfABHD17C were inserted into *BamHI* and *XhoI* sites of pET-45b. The pET-45b plasmids with codon optimized PfABHD17B and PfABHD17D catalytic domain were purchased from GenScript.

Immunofluorescence assay

PfABHD17A-YFP parasite culture with >5% parasitemia was pelleted, washed with phosphate buffered saline (PBS) and fixed with 4% paraformaldehyde and 0.0075% glutaraldehyde in PBS for 30 minutes. Fixed parasites were washed with PBS and treated with 0.1% Triton X-100 for 10 minutes. Parasites were then washed and treated with sodium borohydride for 10 minutes. Parasites were blocked with 3% bovine serum albumin (BSA) for 1 hour. Parasites were labeled with 1:200 mouse anti-RAP1 antibody for 1 hour and washed for 3 times with PBS. Parasites were incubated with 1:1000 Goat anti-Mouse Secondary Antibody, Alexa Fluor™ 594 for 30 minutes. Parasites were washed 3 times with PBS, mounted with ProLong™ Diamond Antifade Mountant with DAPI, sealed for overnight and examined via microscopy. YFP and RAP1 signal were collected using Zeiss AxioImager by Zeiss filter set 46 and Chroma HcRed1 filter set, respectively.

Growth assay for PfABHD17A conditional knockdown parasites

Synchronized ring-stage parasite cultures (0-16 h post-invasion) growing with ligand were washed and divided into 2 groups (with ligand and without ligand). Parasites were cultured at 2% hematocrit in complete RPMI medium containing 5% Albumax I at 37 °C in a 5% CO_2 incubator. Over 8 to 10 days period, parasitemia was counted from Giemsa-stained smears and parasites were subcultured to 0.7% or 1% parasitemia every two days.

Recombinant protein expression of PfABHD17s

Constructed or purchased pET-45b-PfABHD17 plasmids were transformed into BL21 Rosetta Competent Cells. Transformed *E. coli* were inoculated into Luria-Bertani liquid medium and cultured at 37°C on an incubator shaker. Protein expression was induced with 1 mM Isopropyl β-D-1-thiogalactopyranoside at OD600=0.6 and cultured at 20°C on an incubator shaker for 16 hours. *E. coli* was pelleted and frozen at – 80 °C. *E. coli* was thawed, resuspended in PBS containing 1mg/mL hen egg white lysozyme (1 mL PBS for per 50 mL *E. coli* at OD600=1) and incubated for 30 minutes on ice. *E. coli* suspension was lysed by sonication three times using a microtip at 70% maximum power. The supernatant after centrifugation at 12,000 x*g* at 4 °C was snap frozen in liquid nitrogen and stored at – 80 °C.

Inhibitor screen on PfABHD17s via activity-based protein profiling

19.6 µL recombinant PfABHD17 *E. coli* lysates were incubated with 0.2 µL of 1 mM inhibitor (or DMSO) at 30 °C for 30 minutes. Then 0.2 µL of 100 µM TAMRA-FP

was added to the reaction and incubated at 30 °C for 30 minutes. At the end of labeling, the reaction was quenched by adding 20 µL of 2X sodium dodecyl sulfate–polyacrylamide gel electrophoresis (SDS-PAGE) loading buffer and incubated at 95 °C for 5 minutes. Labeled reaction were resolved on SDS-PAGE gels and the signal was collected on a Typhoon RGB flatbed scanner using the 532 nm laser and a 570/20 bandpass filter.

Potency measurement of ML211 inhibition of rPfABHD17A

IC_{50} values for ML211 of rPfABHD17A inhibition were determined using a 4-MUH hydrolysis assay[46] with modification. 1 µL rPfABHD17A or BL21 *E. coli* lysate were added with 19 µL PBS and incubated with 0.2 µL of ML211 (400 nM to 1 mM) or DMSO at 30 °C for 30 minutes. The reaction was added with 180 µL of 138.5 µM 4-MUH in PBS in 96-well plates. The fluorescence was detected every 10 seconds in 3 minutes period at room temperature using Molecular Devices SpectraMax M5 with excitation and emission wavelength bands at 355 and 460 nm, respectively. rPfABHD17A activity was calculated after subtracting the activity of BL21 lysate. Fluorescence values were expressed as a fraction of the DMSO control and the IC50 values were determined using four-parameter sigmoidal non-linear regression.

Determining the effect of PfABHD17A on egress and invasion using inhibitors

0.2 mg/mL heparin-treated synchronized 5% parasitemia schizont stage parasites (40-44 h post-invasion) were pelleted, washed and resuspended in compete RPMI medium with 0.5% Albumax I at 1% hematocrit. Parasites were incubated with 10 µM ML211, ML226 or 0.1% DMSO, aliquoted and cultured in 96 well plate at 37 °C in a 5% CO_2

incubator for 0.5 hour. After 0, 4, 8 and 16 hours, parasites were pelleted, washed with PBS and fixed in 0.1% (v/v) glutaraldehyde in PBS. Fixed parasites were washed with PBS, pelleted, incubated with 3 μM SYTO11 in PBS for 15 minutes and analyzed via Guava easyCyte™ flow cytometer.

Recombinant PfABHD17A protein purification

Recombinant PfABHD17A was expressed in 500 mL *E. coli* culture. The culture was harvested by centrifugation and frozen at – 80 °C. The pellet was thawed and resuspended with 15 mL lysis buffer (20 mM $NaHPO_4$, 500 mM NaCl and 10 mM imidazole, pH at 7.4) containing 1 mg/mL hen egg white lysozyme. The suspension was incubated on ice for 30 minutes. The suspension was sonicated using a large tip at 80% maximum power for 3 times. The lysate was centrifuged at 25,000 x*g* and the supernatant was transferred to a beaker. The supernatant was added with 2 mL lysis buffer containing 16 mg/mL protamine sulfate on ice with gentle stirring. The suspension was centrifuged at 25,000 x*g* and the supernatant was loaded on HisTALON™ Column. The column was washed with lysis buffer, eluted and collected in the mixture of lysis buffer and elution buffer (20 mM $NaHPO_4$, 500 mM NaCl and 500 mM imidazole, pH at 7.4) with linear gradient on a Waters 600 High-performance liquid chromatography (HPLC) system. The fractions with recombinant PfABHD17A were detected by coomassie staining, pooled and dialyzed in gel filtration buffer (50 mM Tris and 200 mM NaCl). Then the protein was purified by gel filtration using Superdex 200 10/300 GL. Fractions with rPfABHD17A were pooled. The protein solution was supplemented with 50% glycerol, aliquoted and stored in – 20 °C.

In vitro DPP-5 hydrolysis assay

2 μL of purified rPfABHD17A (~110 ng/μL) or 50% glycerol in gel filtration buffer was added to 98 μL of 50 μM DPP-5 in PBS in 96-well half-area plates. The fluorescence was detected every 6 seconds in 10 minutes period at room temperature using Molecular Devices SpectraMax M5 with excitation and emission wavelength bands at 380 and 480 nm, respectively.

ACKNOWLEDGEMENTS

We are grateful to Dr. Bryan Dickinson (The University of Chicago) for providing the DPP-5 compound described in Qiu *et al*[47], to Dr. Josh Beck (University of Iowa) for the CRISPR/Cas9 plasmids and to Dr. Sean Prigge (Johns Hopkins University) for the TetR-DOZI plasmids described in Rajaram *et al*[34]. M. K. discloses support for this work from National Institutes of Health grant AI133136 and from USDA National Institute of Food and Agriculture HATCH project VA-160082.

REFERENCES

1 WHO. World malaria report 2022. (2022).

2 Haldar, K. & Mohandas, N. Malaria, erythrocytic infection, and anemia. *ASH Education Program Book*, 87-93 (2009).

3 Baron, S. Medical microbiology. (1996).

4 Cowman, A. F. *et al.* Malaria: biology and disease. *Cell* **167**, 610-624 (2016).

5 Bachovchin, D. A. & Cravatt, B. F. The pharmacological landscape and therapeutic potential of serine hydrolases. *Nature Reviews Drug Discovery* **11**, 52-68 (2012).

6 Elahi, R. *et al.* Functional annotation of serine hydrolases in the asexual erythrocytic stage of *Plasmodium falciparum*. *Scientific reports* **9**, 1-11 (2019).

7 Zhang, M. *et al.* Uncovering the essential genes of the human malaria parasite *Plasmodium falciparum* by saturation mutagenesis. *Science* **360**, eaap7847 (2018).

8 Asad, M. *et al.* An essential vesicular-trafficking phospholipase mediates neutral lipid synthesis and contributes to hemozoin formation in *Plasmodium falciparum*. *BMC Biology* **19**, 1-22 (2021).

9 Sheokand, P. K. *et al.* GlmS mediated knock-down of a phospholipase expedite alternate pathway to generate phosphocholine required for phosphatidylcholine synthesis in *Plasmodium falciparum*. *Biochemical Journal* **478**, 3429-3444 (2021).

10 Sheokand, P. K. *et al.* A *Plasmodium falciparum* lysophospholipase regulates host fatty acid flux via parasite lipid storage to enable controlled asexual schizogony. *Cell Reports* (2023).

11 Butler, J. H. *et al.* Resistance to some but not other dimeric lindenane sesquiterpenoid esters is mediated by mutations in a *Plasmodium falciparum* esterase. *ACS Infectious Diseases* **6**, 2994-3003 (2020).

12 Istvan, E. S. *et al.* Esterase mutation is a mechanism of resistance to antimalarial compounds. *Nature communications* **8**, 1-8 (2017).

13 Sindhe, K. M. *et al. Plasmodium falciparum* resistance to a lead benzoxaborole due to blocked compound activation and altered ubiquitination or sumoylation. *MBio* **11**, e02640-02619 (2020).

14 Spillman, N. J. *et al.* Exported epoxide hydrolases modulate erythrocyte vasoactive lipids during *Plasmodium falciparum* infection. *MBio* **7**, e01538-01516 (2016).

15 Burda, P.C. *et al.* A *Plasmodium* phospholipase is involved in disruption of the liver stage parasitophorous vacuole membrane. *PLoS Pathogens* **11**, e1004760 (2015).

16 Bhanot, P. *et al.* A surface phospholipase is involved in the migration of *Plasmodium* sporozoites through cells. *Journal of Biological Chemistry* **280**, 6752-6760 (2005).

17 Groat-Carmona, A. M. *et al.* A *Plasmodium* α/β-hydrolase modulates the development of invasive stages. *Cellular Microbiology* **17**, 1848-1867 (2015).

18 Flammersfeld, A. *et al.* A patatin-like phospholipase functions during gametocyte induction in the malaria parasite *Plasmodium falciparum*. *Cellular Microbiology* **22**, e13146 (2020).

19 Singh, P. *et al.* Role of a patatin-like phospholipase in *Plasmodium falciparum* gametogenesis and malaria transmission. *Proceedings of the National Academy of Sciences of the United States of America* **116**, 17498-17508 (2019).

20 Srivastava, P. N. & Mishra, S. Disrupting a *Plasmodium berghei* putative phospholipase impairs efficient egress of merosomes. *International Journal for Parasitology* (2022).
21 Lévêque, M. F. *et al.* TgPL2, a patatin-like phospholipase domain-containing protein, is involved in the maintenance of apicoplast lipids homeostasis in *Toxoplasma*. *Molecular Microbiology* **105**, 158-174 (2017).
22 Birnbaum, J. *et al.* A genetic system to study *Plasmodium falciparum* protein function. *Nature Methods* **14**, 450-456 (2017).
23 Aurrecoechea, C. *et al.* PlasmoDB: a functional genomic database for malaria parasites. *Nucleic Acids Research* **37**, D539-D543 (2009).
24 Frénal, K. *et al.* Global analysis of apicomplexan protein S-acyl transferases reveals an enzyme essential for invasion. *Traffic* **14**, 895-911 (2013).
25 Lin, D. T. S. & Conibear, E. ABHD17 proteins are novel protein depalmitoylases that regulate N-Ras palmitate turnover and subcellular localization. *eLife* **4**, e11306 (2015).
26 Won, S. J. *et al.* Protein depalmitoylases. *Critical Reviews in Biochemistry and Molecular Biology* **53**, 83-98 (2018).
27 Yokoi, N. *et al.* Identification of PSD-95 Depalmitoylating Enzymes. *Journal of Neuroscience* **36**, 6431-6444 (2016).
28 Erdős, G. & Dosztányi, Z. Analyzing protein disorder with IUPred2A. *Current Protocols in Bioinformatics* **70**, e99 (2020).
29 Schlott, A. C. *et al.* Inhibition of protein N-myristoylation blocks *Plasmodium falciparum* intraerythrocytic development, egress and invasion. *PLoS Biology* **19**, e3001408 (2021).
30 Hanssen, E. *et al.* Electron tomography of *Plasmodium falciparum* merozoites reveals core cellular events that underpin erythrocyte invasion. *Cellular Microbiology* **15**, 1457-1472 (2013).
31 Liffner, B. *et al.* The ins and outs of *Plasmodium* rhoptries, focusing on the cytosolic side. *Trends in Parasitology* **37**, 638-650 (2021).
32 Ghosh, S. *et al.* The *Plasmodium* rhoptry associated protein complex is important for parasitophorous vacuole membrane structure and intraerythrocytic parasite growth. *Cellular Microbiology* **19**, e12733 (2017).
33 Muralidharan, V. *et al.* Asparagine repeat function in a *Plasmodium falciparum* protein assessed via a regulatable fluorescent affinity tag. *Proceedings of the National Academy of Sciences of the United States of America* **108**, 4411-4416 (2011).
34 Rajaram, K. *et al.* Redesigned TetR-aptamer system to control gene expression in *Plasmodium falciparum*. *MSphere* **5**, e00457-00420 (2020).
35 Tarique, M. *et al. Plasmodium falciparum* DOZI, an RNA helicase interacts with eIF4E. *Gene* **522**, 46-59 (2013).
36 Ramos, J. L. *et al.* The TetR family of transcriptional repressors. *Microbiology and Molecular Biology Reviews* **69**, 326-356 (2005).
37 Otto, T. D. *et al.* New insights into the blood-stage transcriptome of *Plasmodium falciparum* using RNA-Seq. *Molecular Microbiology* **76**, 12-24 (2010).
38 Josling, G. A. *et al.* A *Plasmodium Falciparum* Bromodomain Protein Regulates Invasion Gene Expression. *Cell Host & Microbe* **17**, 741-751 (2015).

39 Knuepfer, E. *et al.* Generating conditional gene knockouts in *Plasmodium*–a toolkit to produce stable DiCre recombinase-expressing parasite lines using CRISPR/Cas9. *Scientific reports* **7**, 1-12 (2017).
40 Patricelli, M. P. *et al.* Direct visualization of serine hydrolase activities in complex proteomes using fluorescent active site-directed probes. *Proteomics* **1**, 1067-1071 (2001).
41 Hirano, T. *et al.* Thioesterase activity and subcellular localization of acylprotein thioesterase 1/lysophospholipase 1. *Biochimica et Biophysica Acta* **1791**, 797-805 (2009).
42 Manna, J. D. *et al.* Identification of the major prostaglandin glycerol ester hydrolase in human cancer cells. *Journal of Biological Chemistry* **289**, 33741-33753 (2014).
43 Adibekian, A. *et al.* Optimization and characterization of a triazole urea dual inhibitor for lysophospholipase 1 (LYPLA1) and lysophospholipase 2 (LYPLA2). *Probe Reports from the NIH Molecular Libraries Program* (2013).
44 Nomura, D. K. *et al.* Activation of the endocannabinoid system by organophosphorus nerve agents. *Nature Chemical Biology* **4**, 373-378 (2008).
45 Aaltonen, N. *et al.* Piperazine and piperidine triazole ureas as ultrapotent and highly selective inhibitors of monoacylglycerol lipase. *Chemistry & Biology* **20**, 379-390 (2013).
46 Saunders, R. & Heltved, F. Fluorimetric assay of lipase in rice bran, and its application to determination of conditions for rice bran stabilization. *Journal of Cereal Science* **3**, 79-86 (1985).
47 Qiu, T. *et al.* A Fluorescent Probe with Improved Water Solubility Permits the Analysis of Protein S-Depalmitoylation Activity in Live Cells. *Biochemistry* **57**, 221-225 (2018).
48 Cabrera, A. *et al.* Dissection of minimal sequence requirements for rhoptry membrane targeting in the malaria parasite. *Traffic* **13**, 1335-1350 (2012).
49 Beck, J. R. *et al.* A *Toxoplasma* palmitoyl acyl transferase and the palmitoylated armadillo repeat protein TgARO govern apical rhoptry tethering and reveal a critical role for the rhoptries in host cell invasion but not egress. *PLoS Pathogens* **9**, e1003162 (2013).
50 Jones, M. L. *et al.* Analysis of protein palmitoylation reveals a pervasive role in *Plasmodium* development and pathogenesis. *Cell Host & Microbe* **12**, 246-258 (2012).
51 Siddiqui, M. A. *et al.* Protein S-Palmitoylation Is Responsive to External Signals and Plays a Regulatory Role in Microneme Secretion in *Plasmodium falciparum* Merozoites. *ACS Infectious Diseases* **6**, 379-392 (2020).
52 Wang, X. *et al.* A protein palmitoylation cascade regulates microtubule cytoskeleton integrity in *Plasmodium*. *The EMBO journal* **39**, e104168 (2020).
53 Qian, P. *et al.* Inner membrane complex proteomics reveals a palmitoylation regulation critical for intraerythrocytic development of malaria parasite. *Elife* **11**, e77447 (2022).
54 Siddiqui, M. A. *et al.* Protein S-Palmitoylation is responsive to external signals and plays a regulatory role in microneme secretion in *Plasmodium falciparum* merozoites. *ACS Infectious Diseases* **6**, 379-392 (2020).

55 Wang, X. *et al.* A protein palmitoylation cascade regulates microtubule cytoskeleton integrity in *Plasmodium*. *The EMBO journal* **39**, e104168 (2020).
56 Wetzel, J. *et al.* The role of palmitoylation for protein recruitment to the inner membrane complex of the malaria parasite. *Journal of Biological Chemistry* **290**, 1712-1728 (2015).
57 Cabrera, A. *et al.* Dissection of minimal sequence requirements for rhoptry membrane targeting in the malaria parasite. *Traffic* **13**, 1335-1350 (2012).
58 Davison, D. *et al.* Activity-based protein profiling of human and *plasmodium* serine hydrolases and interrogation of potential antimalarial targets. *Iscience* **25**, 104996 (2022).
59 Liffner, B. *et al.* PfCERLI1 is a conserved rhoptry associated protein essential for *Plasmodium falciparum* merozoite invasion of erythrocytes. *Nature communications* **11**, 1411 (2020).
60 Beck, J. R. *et al.* A *Toxoplasma* palmitoyl acyl transferase and the palmitoylated armadillo repeat protein TgARO govern apical rhoptry tethering and reveal a critical role for the rhoptries in host cell invasion but not egress. *PLoS Pathogens* **9**, e1003162 (2013).
61 Mueller, C. *et al.* The *Toxoplasma* protein ARO mediates the apical positioning of rhoptry organelles, a prerequisite for host cell invasion. *Cell Host & Microbe* **13**, 289-301 (2013).
62 Child, M. A. *et al.* Small-molecule inhibition of a depalmitoylase enhances *Toxoplasma* host-cell invasion. *Nature Chemical Biology* **9**, 651-656 (2013).
63 Counihan, N. A. *et al. Plasmodium* rhoptry proteins: why order is important. *Trends in Parasitology* **29**, 228-236 (2013).
64 Fidock, D. A. & Wellems, T. E. Transformation with human dihydrofolate reductase renders malaria parasites insensitive to WR99210 but does not affect the intrinsic activity of proguanil. *Proceedings of the National Academy of Sciences of the United States of America* **94**, 10931-10936 (1997).
65 Ribeiro, J. M. *et al.* Guide RNA selection for CRISPR-Cas9 transfections in *Plasmodium falciparum*. *International Journal for Parasitology* **48**, 825-832 (2018).
66 Garten, M. *et al.* EXP2 is a nutrient-permeable channel in the vacuolar membrane of *Plasmodium* and is essential for protein export via PTEX. *Nature Microbiology* **3**, 1090-1098 (2018).

SUPPLEMENTARY INFORMATION

Table 2-S1. Oligonucleotides used in this study for plasmid construction and diagnostic PCR. Abbreviations: CDS, coding sequence; GD, gene disruption; UTR, untranslated region; SLI, selection-linked integration; YFP, yellow fluorescent protein; HA, homology arm.

Oligo Number	Sequence	Function	Sequence
985	PfABHD17A CDS	pSLI-PfABHD17A-GD	TGACACTATAGAATACTCGCGGCCGCTAAGGGAATGCATTGAACCAACTAATCTTC
986	PfABHD17A CDS	pSLI-PfABHD17A-GD	TTGAAAATATAAATTTTCCCTAGGAGTAAATTTTAATCTTAATTTTACACG
987	PfABHD17B CDS	pSLI-PfABHD17B-GD	TGACACTATAGAATACTCGCGGCCGCTAATATGATGATGAATTGAAAAATCTTGTATAC
988	PfABHD17B CDS	pSLI-PfABHD17B-GD	TTGAAAATATAAATTTTCCCTAGGATAAGAAGAATAAGTAAAATAATCTTC
1029	PfABHD17B CDS	Diagnostic PCR, wild-type and PfABHD17B GD integration	GTCCAATTCAACCCTATTCCGC
1230	PfABHD17B 3' UTR	Diagnostic PCR, wild-type	TGAATAATTTCATCTTCTTTACCATG
901	pSLI	Diagnostic PCR	ATCCATCTTGTTCAATCATTGGTCC
1037	PfABHD17A CDS	pSLI-PfABHD17A-YFP	TGACACTATAGAATACTCGCGGCCGCTAAAATAGTATGTCCTTAAATATGAAAACG
1038	PfABHD17A CDS	pSLI-PfABHD17A-YFP	TTGAAAATATAAATTTTCCCTAGGATCGAGAAATTCTTTTTTGGAAGTTTCC
1063	PfABHD17A CDS	Diagnostic PCR, wild-type and PfABHD17A-YFP/YFP-DD/TetR-DOZI integration	ATATTCCCCAAATAAAGTGACAAG
1064	PfABHD17A 3' UTR	Diagnostic PCR, wild-type	CATGCTCCTCCCTCCTTCTAC

209	YFP	Diagnostic PCR, PfABHD17A-YFP-DD integration	TCAACAAGAATTGGGACAACTCC
1206	PfABHD17A CDS	sgRNA	TAAGTATATAATATTATTAAATA GTAGAAGGAGGGGTTTTAGAGCT AGAA
1207	PfABHD17A CDS	sgRNA	TTCTAGCTCTAAAACCCCTCCTTC TACTATTTAATAATATTATATACT TA
1210	PfABHD17A CDS	HA1, CRISPR repair	GATATCGTCCACCTGGATATCCA ACACTCGTTATGTATCTTGTG
1211	PfABHD17A CDS	HA1, CRISPR repair	CATAAGGATAGACGTCATCGAGA AATTCTTTTTTGGAAGTTTC
1212	PfABHD17A 3' UTR	HA2, CRISPR repair	CCCTTTCCGGGCGCGCCTTAGAA GAATTTGTAGGAAATATAC
1213	PfABHD17A 3' UTR	HA2, CRISPR repair	GATATCCAGGTGGACGATATCTA TGTGTGTGCCTTAAGAATTTTC
HSPR1	HSPR1	Diagnostic PCR, TetR-DOZI integration	TATATATGTATATTGGGGTGATG
1015	PfABHD17A CDS	Recombinant protein expression	ACGACGACAAGAGTCCGGAAAA CCTGTATTTTCAGAGCAATGCAT TGAACCAACTAATCTTCAG
1016	PfABHD17A CDS	Recombinant protein expression	GCGGTTTCTTTACCAGACTTATG GAATTTTATTGTTAATAATAACTT TCTC
1021	PfABHD17C CDS	Recombinant protein expression	ACGACGACAAGAGTCCGGAAAA CCTGTATTTTCAGAGCCGCATGG TGAAAAAAATGGCCTTTG
1022	PfABHD17C CDS	Recombinant protein expression	GCGGTTTCTTTACCAGACTTATG ATAAGAACTCACCTAATTTATGA TA

Table 2-S2. Chemical structures for probes and inhibitors used in this study.

Chemical name	Structure	Function
TAMRA-FP[1]	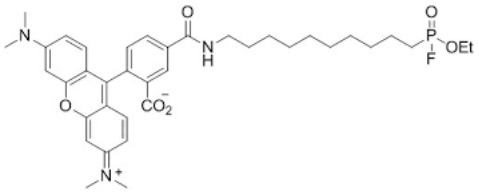	ABPP probe for SHs
IDFP[2]		Pan-lipase inhibitor
Palmostatin B[3]	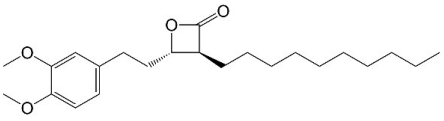	APT1 inhibitor
ML211[4]	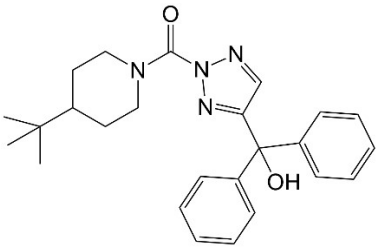	APT1/2 inhibitor
ML226[4]	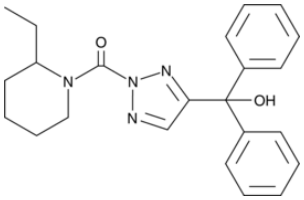	ABHD11 inhibitor
ML348[5]	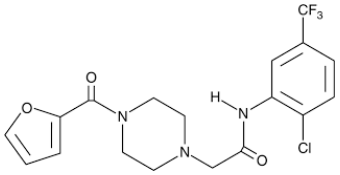	APT1 inhibitor
ML349[5]	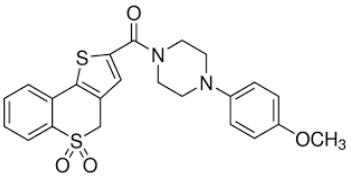	APT2 inhibitor

R/S-KT109[6]	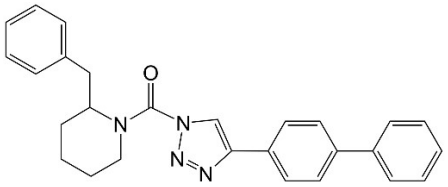	Diacylglycerol lipase (DAGL) inhibitor
MJN110[7]	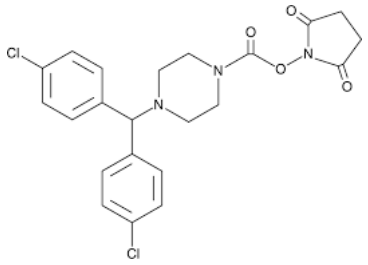	MAGL inhibitor
JJKK-046[8]	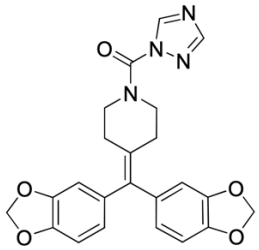	MAGL inhibitor
MAFP[9]	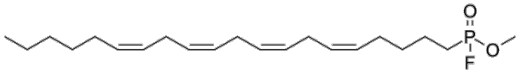	Calcium-dependent and calcium-independent cytosolic phospholipase A_2 inhibitor
DPP-5[10]	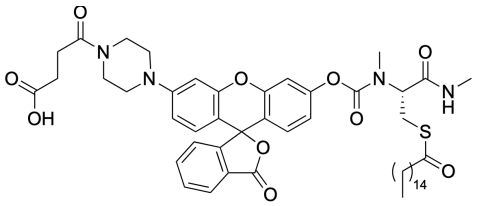	Depalmitoylase substrate
4-MUH	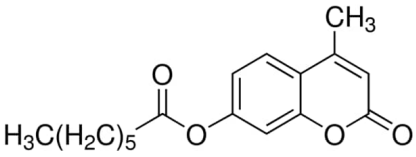	Lipase substrate

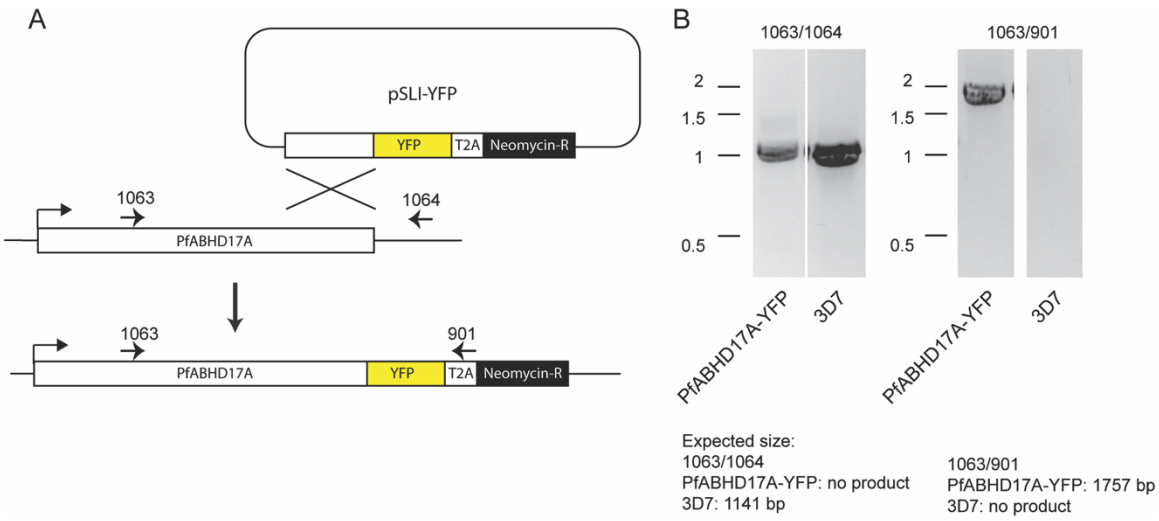

Figure 2-S1. Generation of PfABHD17A-YFP parasite line. (A) Strategy for generating PfABHD17A-YFP parasite line through single-crossover homologous recombination and selection-linked integration. YFP, yellow fluorescent protein. T2A, *Thosea asigna* virus 2A self-cleaving peptide. Neomycin-R, neomycin resistance gene. (B) Diagnostic PCR result of PfABHD17A-YFP. PfABHD17A-YFP parasite line was generated with some remaining wild type parasites. Primer 1063 and 1064 were used to examine the remaining wild type parasites. Primer 1063 and 901 were used to examine integrated parasites. Sizes of markers are indicated in kilobases.

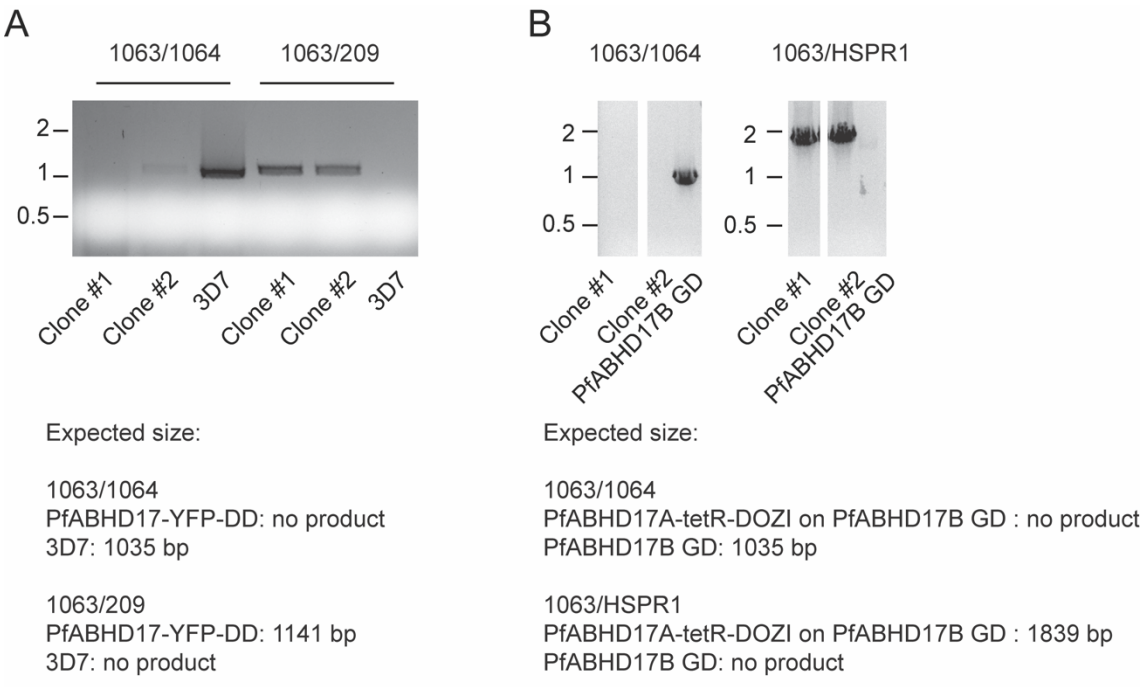

Figure 2-S2. Diagnostic PCR results of PfABHD17A conditional knockdown parasite lines. (A) Diagnostic PCR result of PfABHD17-YFP-DD parasite line. Primer 1063 and 1064 were used to examine the remaining wild type parasites. Primer 1063 and 209 were used to examine the integrated parasites. Sizes of markers are indicated in kilobases. (B) Diagnostic PCR result of PfABHD17A-tetR-DOZI on PfABHD17B GD background. Primer 1063 and 1064 were used to examine the remaining wild type parasites. Primer 1063 and HSPR1 were used to examine the integrated parasites. Sizes of markers are indicated in kilobases.

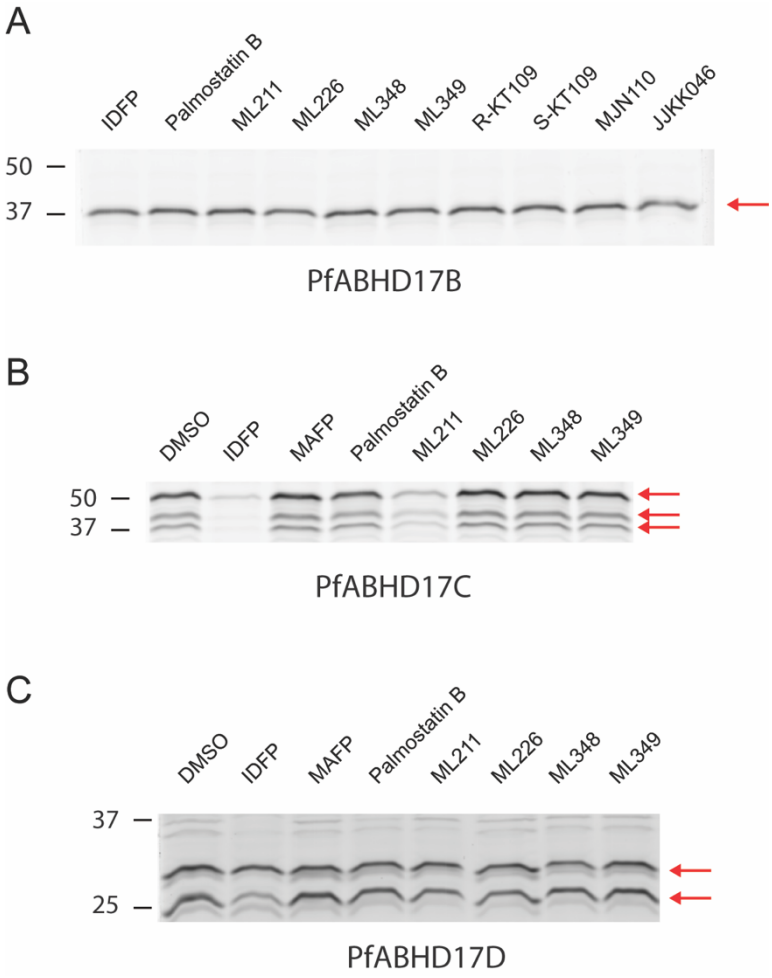

Figure 2-S3. Inhibitor screen on rPfABHD17B/C/D. (A) Inhibitor screen on rPfABHD17B. (B) Inhibitor screen on rPfABHD17C. (C) Inhibitor screen on rPfABHD17D. Red arrow, rPfABHD17B/C/D. rPfABHD17B is single product, while PfABHD17C and PfABHD17D are 3 products and 2 products, respectively. Inhibitors were added at 10 μM. Sizes of markers are indicated in kD.

SUPPLEMENTARY REFERENCES

1 Patricelli, M. P. *et al.* Direct visualization of serine hydrolase activities in complex proteomes using fluorescent active site-directed probes. *Proteomics* **1**, 1067-1071 (2001).

2 Nomura, D. K. *et al.* Activation of the endocannabinoid system by organophosphorus nerve agents. *Nature Chemical Biology* **4**, 373-378 (2008).

3 Dekker, F. J. *et al.* Small-molecule inhibition of APT1 affects Ras localization and signaling. *Nature Chemical Biology* **6**, 449-456 (2010).

4 Adibekian, A. *et al.* in *Probe Reports from the NIH Molecular Libraries Program* (2010).

5 Adibekian, A. *et al.* Characterization of a selective, reversible inhibitor of lysophospholipase 2 (LYPLA2). *Probe Reports from the NIH Molecular Libraries Program* (2014).

6 Hsu, K.L. *et al.* DAGLβ inhibition perturbs a lipid network involved in macrophage inflammatory responses. *Nature Chemical Biology* **8**, 999-1007 (2012).

7 Chang, J. W. *et al.* Proteome-wide reactivity profiling identifies diverse carbamate chemotypes tuned for serine hydrolase inhibition. *ACS Chemical Biology* **8**, 1590-1599 (2013).

8 Aaltonen, N. *et al.* Piperazine and piperidine triazole ureas as ultrapotent and highly selective inhibitors of monoacylglycerol lipase. *Chemistry & Biology* **20**, 379-390 (2013).

9 Huang, Z. *et al.* Methyl arachidonyl fluorophosphonate, a potent irreversible cPLA2 inhibitor, blocks the mobilization of arachidonic acid in human platelets and neutrophils. *Mediators Inflamm* **3**, 307-308 (1994).

10 Qiu, T. *et al.* A Fluorescent Probe with Improved Water Solubility Permits the Analysis of Protein S-Depalmitoylation Activity in Live Cells. *Biochemistry* **57**, 221-225 (2018).

Chapter 3

Intracellular and exported lysophospholipases metabolize and detoxify lysophosphatidylcholine in *Plasmodium falciparum*-infected erythrocytes

Jiapeng Liu, Christie Dapper and Michael Klemba

Department of Biochemistry, Virginia Tech

Running Head: *P. falciparum* lysophospholipases

(This chapter is available on BioRxiv preprint server with some modifications at https://doi.org/10.1101/2023.04.17.537066)

3.1 ABSTRACT

Host lysophosphatidylcholine (LPC) is a major source of fatty acids during intraerythrocytic replication of *Plasmodium falciparum*. Here, we combine chemical biology and genetic approaches to identify two serine hydrolases, exported lipase (XL) 2 and exported lipase homolog (XLH) 4, as the dominant lysophospholipase activities in parasite-infected erythrocytes. While XL2 and XLH4 were individually dispensable with little effect on LPC hydrolysis *in situ*, loss of both enzymes resulted in a marked reduction in the ability to scavenge fatty acids from LPC and an enhanced sensitivity to LPC toxicity. The parasite ensures efficient LPC hydrolysis by directing the two enzymes to distinct locations: XL2 is exported to the host erythrocyte, while XLH4 is retained within the parasite. When XL2 and XLH4 activities were ablated by genetic or pharmacologic means, parasites were unable to proliferate in human serum, revealing the essentiality of LPC hydrolysis in the host environment.

KEYWORDS: *Plasmodium*, malaria, serine hydrolase, lysophosphatidylcholine, lysophospholipase, exported lipase

3.2 INTRODUCTION

Malaria counts among the most devastating infectious diseases in the world today. An estimated 247 million cases and 619,000 deaths were attributed to malaria in 2021[1]. Continued development of new anti-malarial strategies will be required to mitigate the effects of eventual drug resistance against current frontline therapies[2].

During the pathogenic, asexual stage of the human malaria parasite *Plasmodium falciparum* within erythrocytes, high rates of phospholipid synthesis are required to support the expansion of parasite membranes[3]. Parasites also produce the neutral lipids diacylglycerol (DAG) and triacylglycerol (TAG), which are deposited in lipid droplets and mobilized late in the replication cycle[4,5]. Although the *P. falciparum* genome encodes enzymes for *de novo* fatty acid (FA) synthesis, these are dispensable in the asexual stage[6]. Thus, the intraerythrocytic parasite is dependent on exogenous sources of fatty acids to support its vigorous anabolic activity. Host serum contains two abundant fatty acid sources: free fatty acids and lysophosphatidylcholines (LPC) [7]. Studies with isotope-labeled LPC have demonstrated that LPC-derived fatty acids are readily incorporated into parasite lipids[8,9]. LPC catabolism also provides choline[9,10], an important precursor for phosphatidylcholine (PC) biosynthesis. While the metabolites supplied by LPC catabolism support asexual growth, the depletion of this host lipid plays a regulatory role by enhancing commitment to gametocytogenesis[9].

Although it has long been evident that asexual *P. falciparum* expresses high levels of lysophospholipase activity[11], the identities of the enzyme(s) that catalyze exogenous LPC hydrolysis are unknown. This is due in part to the large number of possible candidates and the likelihood of functional redundancy: the *P. falciparum* genome encodes 17

members of the serine hydrolase superfamily that are annotated as "lysophospholipase" through either EC number or InterPro domain assignments (data from Plasmodb.org[12]). While two of these, termed PfLPL1 and PfLPL20, have been shown to have lysophospholipase activity *in vitro*[13,14], their contributions to the hydrolysis of exogenous LPC have not been examined. Elucidating the repertoire of enzymes responsible for exogenous LPC hydrolysis is a formidable challenge that is unlikely to yield to a piecemeal approach.

To expedite the discovery of key parasite lysophospholipases, we have pursued complementary chemical biology and genetic approaches focused on the serine hydrolase superfamily. We first developed an assay for *in situ* LPC hydrolysis that enabled identification of inhibitors that blocked the release of fatty acids form LPC (here, *in situ* refers to processes in intact, infected erythrocytes in culture). Candidate lysophospholipases were interrogated by activity-based protein profiling, leading to a serine hydrolase subgroup consisting of four paralogs. Single and multigenic knockout parasite lines were generated to characterize their roles individually and in combination. Two of these four enzymes were revealed to be the source of nearly all LPC hydrolysis activity in asexually-replicating parasites. The consequences of the loss of these activities on parasite fitness was investigated, revealing a critical role for LPC hydrolysis for parasite survival in the presence of human serum.

3.3 RESULTS

Parasite serine hydrolases catalyze LPC hydrolysis *in situ*

We first sought to identify serine hydrolase-directed, small-molecule inhibitors of LPC hydrolysis *in situ* by adapting an intact-cell assay for the incorporation of a fluorescent fatty acid analog, BODIPY™ 500/510 C_4, C_9 (C4,C9-FA), into parasite neutral lipids[15]. We reasoned that unlabeled fatty acids derived from LPC hydrolysis would compete with C4,C9-FA for incorporation into parasite lipids and thus reduce lipid-associated fluorescence. To test this, C4,C9-FA labeling of the neutral lipids diacylglycerol (DAG) and triacylglycerol (TAG) in cultured parasites was examined in the presence of exogenous LPC (Figure 3-1A). LPC 18:1 reduced C4,C9-FA incorporation in a concentration-dependent manner, with 30 and 60 μM suppressing C4,C9-FA incorporation by >90%. LPC 16:0 was less effective, and lyso-platelet activating factor (lyso-PAF), a non-hydrolysable LPC analog, had no effect (Figure 3-1A). We therefore conducted *in situ* LPC hydrolysis assays with 30 μM LPC 18:1 (Figure 3-1B).

We tested a panel of serine hydrolase inhibitors for the ability to inhibit *in situ* LPC hydrolysis as reflected by a gain in C4,C9-FA labeling of DAG and TAG. These inhibitors included: 1) isopropyldodecyl fluorophosphonate (IDFP), a monoacylglycerol isostere and potent lipase inhibitor[16] that we have previously employed to identify putative *P. falciparum* lipases[17]; 2) JW642, a monoacylglycerol lipase inhibitor[18] that inhibits an abundant *P. falciparum* serine hydrolase and putative lipase termed "prodrug activating a resistance esterase", (PfPARE) [17]; and 3) a panel of highly potent, structurally-diverse, monoacylglycerol lipase inhibitors that are based on a piperazine- or piperadine-urea scaffold[19]. All inhibitors act through a competitive-covalent mechanism by reacting with

the active site serine residue and were assayed at 10 μM concentration. IDFP treatment resulted in a strong recovery of C4,C9-FA lipid labeling (Figure 3-1C), indicating that serine hydrolase-family enzymes are major contributors to LPC hydrolysis *in situ*. Of the other inhibitors, only one, AKU-010[19], was as effective as IDFP. The structurally-related inhibitors AKU-005 and AKU-006 exhibited modest and no inhibition of LPC hydrolysis, respectively, and JW642 did not inhibit LPC hydrolysis (see Figure 3-1D and Figure 3-S1 for compound structures). Thus, compounds AKU-010/005/006/JW642 define an inhibition "signature", or profile, for major *P. falciparum* lysophospholipase activities.

To identify candidate lysophospholipases, we profiled the inhibitor sensitivities of parasite and host serine hydrolases using activity-based probe TAMRA-fluorophosphonate (TAMRA-FP) [20]. To ensure that all enzymes within the infected erythrocyte were included in this analysis, parasitized erythrocytes (infected RBC, or iRBC) were highly enriched by "magnetic activated cell sorting", or MACS[21]. Profiling of iRBC lysate revealed multiple enzyme species that matched the *in situ* inhibition profile (Figure 3-1E). In contrast, while the host erythrocyte possesses a number of serine hydrolases that are susceptible to IDFP inhibition, none was inhibited by AKU-010 (Figure 3-1F), which points to parasite-encoded enzymes being the key catalysts for LPC hydrolysis in infected erythrocytes.

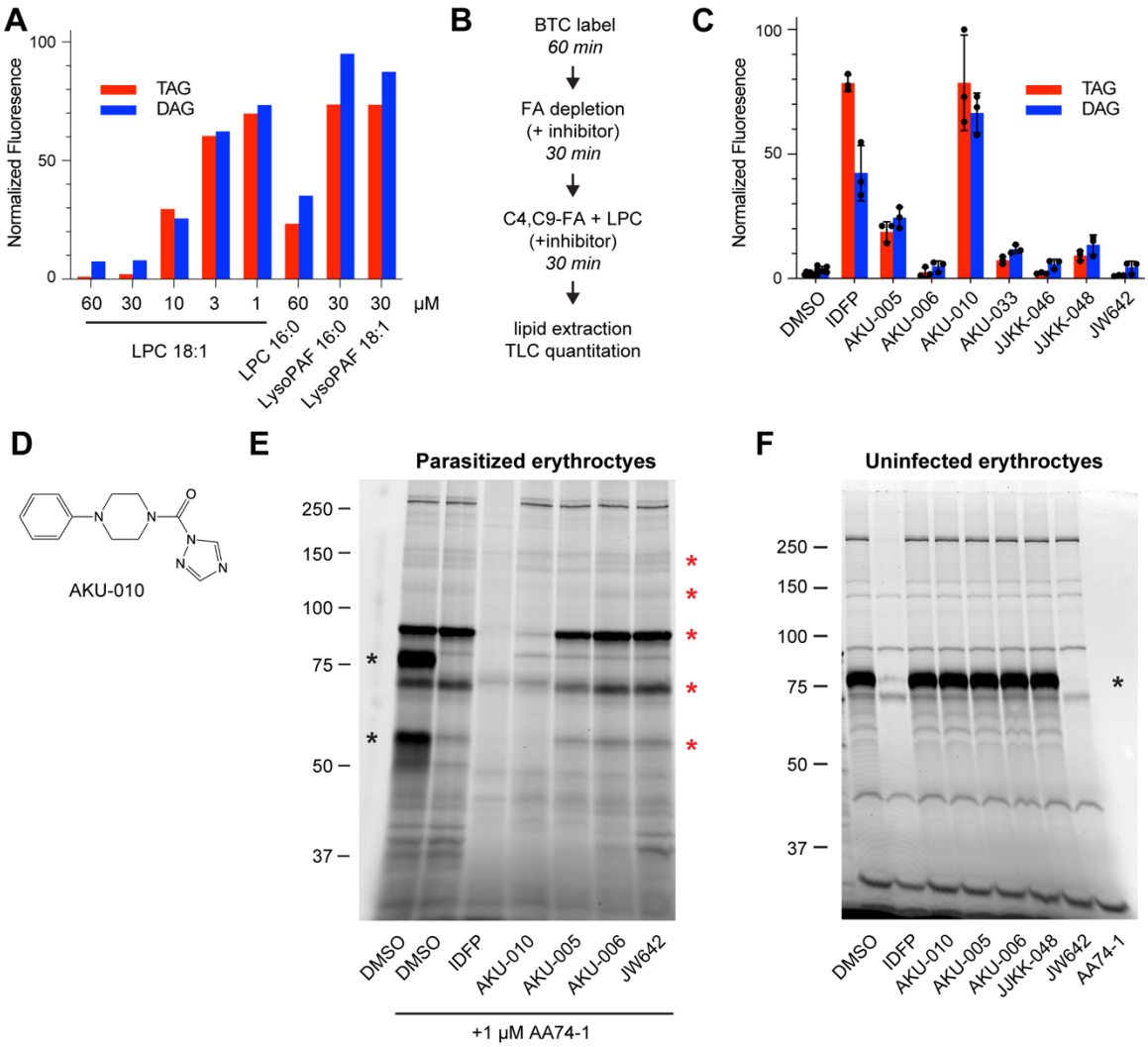

Figure 3-1. Serine hydrolase inhibitors block LPC hydrolysis *in situ*. (A) Fatty acids derived from LPC hydrolysis reduce C4,C9-FA incorporation into parasite neutral lipids. LPC or the non-hydrolysable LPC analog lyso-PAF were co-incubated with C4,C9-FA and incorporation of the probe into DAG and TAG was quantified and normalized to a no-LPC control (set to 100). (B) C4,C9-FA/LPC competition assay for identifying inhibitors of *in situ* LPC hydrolysis. (C) Serine hydrolase inhibitors (10 µM) define an inhibition profile for *in situ* LPC hydrolysis. C4,C9-FA fluorescence volumes were normalized to a no-LPC, no inhibitor control (set to 100). Means and standard deviations are from three independent experiments. (D) Structure of the AKU-010. (E) Inhibition of serine hydrolases in lysates of MACS-enriched, *P. falciparum*-infected erythrocytes as assessed by TAMRA-FP profiling. AA74-1 was included to suppress the strong signal from erythrocyte acylpeptide hydrolase (APEH), which was present at 80 and 55 kDa species (far left lane, black asterisks). Red asterisks indicate species with the inhibition profile AKU-010 > AKU-005 >> AKU-006, JW642. (F) TAMRA-FP profiling of uninfected erythrocytes. Inhibition of erythrocyte serine hydrolases was only observed with IDFP and AA74-1. Black asterisk, APEH. Sizes of markers are indicated in kDa.

Two exported serine hydrolases are targets of AKU-010

To gain insight into candidates for these activities, we consulted our previous proteomic analysis of serine hydrolase-family lipases in *P. falciparum*[17]. Of the seven putative lipases identified in that study, one stood out as a top candidate: PF3D7_1001600, previously termed "exported lipase 2" (XL2) based on its export to the host erythrocyte cytosol[22]. A paralog of XL2, termed "exported lipase 1" (XL1; PF3D7_1001400), is also exported to the erythrocyte[22]. To determine whether XL1 and XL2 correspond to the AKU-010-sensitive activities, we generated single- and double-knockout parasite lines, targeting the entire coding sequence for deletion using a markerless CRISPR-Cas9 strategy (Figure 3-S2A and 3-S2B). The ΔXL1 line appeared to have undergone telomere shortening or "healing" (Figure 3-S2C), a phenomenon that can occur when double-stranded DNA breaks are made in subtelomeric regions[23]. The XL2 single knockout and the ΔXL1/2 double knockout contained the expected gene deletion events (Figure 3-S2D and Figure 3-S2E).

Inhibitor profiling of the knockout lines revealed that XL2 is a highly-expressed enzyme that corresponds to three of the AKU-010-sensitive species (Figure 3-2B), the two smaller species likely generated by limited proteolytic cleavage. XL1 is expressed at a much lower level and corresponds to the AKU-010-sensitive activity at ~110 kDa (Figure 3-2A). Both proteins are absent from the ΔXL1/2 line (Figure 3-S2F). To establish that endogenous XL1 and XL2 are exported, MACS-enriched wild-type parasites were fractionated into a supernatant fraction that contains soluble erythrocyte proteins and a pellet fraction that contains intraparasitic proteins (Figure 3-2C). Both enzymes were

recovered exclusively in the supernatant, confirming efficient export, whereas the intracellular enzyme PfPARE was located in the parasite pellet.

To assess the effects of loss of XL1 and/or 2 on LPC hydrolysis *in situ*, we modified our fatty acid probe-competition assay by replacing C4,C9-FA with a terminal alkyne analog of oleic acid (oleate alkyne, OA), a probe that more closely resembles a physiological fatty acid. Parasites were labeled with 30 μM OA with or without 30 μM LPC 18:1 for 40 minutes. Lipids were extracted from saponin-isolated parasites and alkyne-containing lipids were rendered fluorescent by click addition of 3-azido-7-hydroxycoumarin and resolved by thin-layer chromatography as previously described[24]. For the parental 3D7 line, LPC reduced OA labeling to ~30-60% of that in its absence (Figure 3-2D and 3-2E). In ΔXL1, ΔXL2 and ΔXL1/2 parasites, no significant changes in OA labeling were observed for PE, DAG or TAG compared to 3D7 (Figure 3-2E). In contrast, PC labeling was somewhat elevated in ΔXL2 and ΔXL1/2 lines. Overall, these studies revealed that parasites retained the ability to efficiently release fatty acids from LPC.

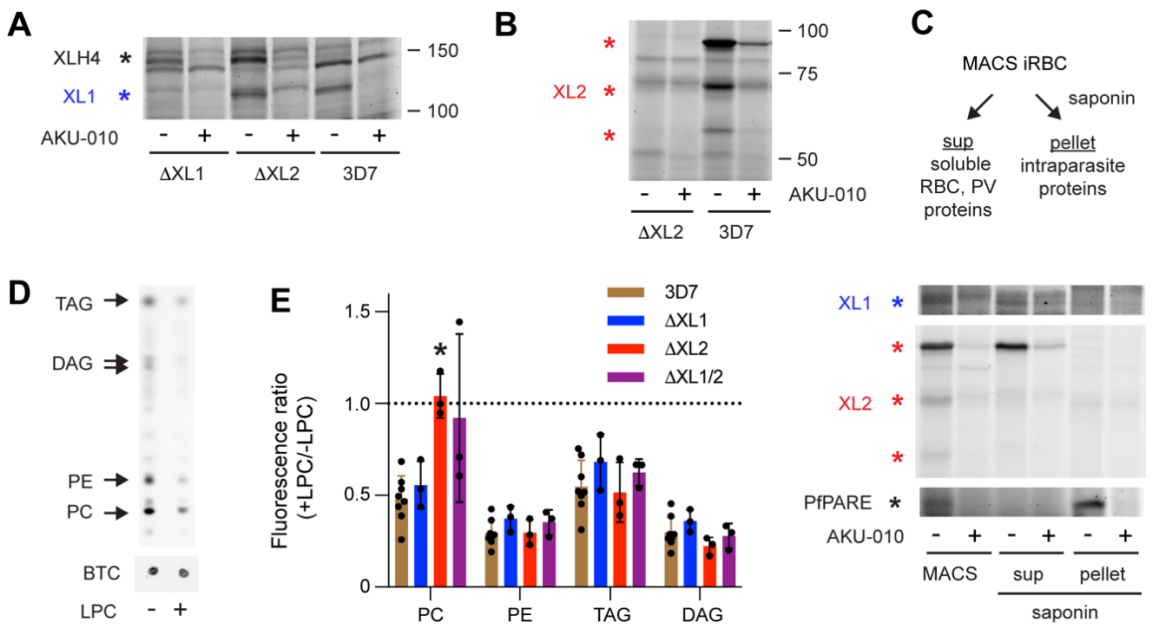

Figure 3-2. Two exported serine hydrolases are targets of AKU-010. (A) TAMRA-FP profiling of XL1 expression (blue asterisk) in MACS-enriched ΔXL1, ΔXL2 and parental 3D7 iRBCs. An additional, high molecular weight, AKU-010-inhibited species, later identified as XLH4, is indicated with a black asterisk. (B) TAMRA-FP profiling of XL2 expression in MACS-enriched ΔXL2 and 3D7 iRBCs. Three AKU-010-inhibited species corresponding to XL2 are indicated with red asterisks. (C) XL1 and XL2 are exported to the host cell. TAMRA-FP profiling of MACS-enriched 3D7 parasites and of saponin supernatant and pellet fractions. XL1 and XL2 appear predominantly in the saponin supernatant containing soluble erythrocyte proteins, whereas the intracellular serine hydrolase PfPARE appears exclusively in the pellet. (D) LPC reduces incorporation of the fatty acid probe oleate alkyne (OA) into parasite phospholipids (PC, PE) and neutral lipids (DAG, TAG). The two DAG species are 1,2- and 1,3-isomers. BTC, BODIPY-TR-ceramide internal standard. (E) Oleate alkyne/LPC competition profiling of single and double XL1/XL2 knockout lines. Ratios below 1 (dotted line) indicate suppression of OA incorporation in the presence of LPC. Means and standard deviations are from at least three independent experiments. Significance relative to 3D7 was assessed within lipid groups using a two-tailed Welch's *t*-test. *, $p < 0.05$; no asterisk, $p \geq 0.05$.

Intracellular and exported lysophospholipases contribute to efficient LPC hydrolysis

We reasoned that additional AKU-010-sensitive serine hydrolases were responsible for exogenous LPC hydrolysis in ΔXL1/2 parasites. We focused our attention on two enzymes that have been identified as XL1/2 paralogs in the PlasmoDB database: PF3D7_0731800 and PF3D7_1328500. Neither sequence contains a canonical PEXEL

host targeting motif[25] for export to the host erythrocyte (PlasmoDB.org); thus, we refer to these as "exported lipase homolog" (XLH) 3 and 4, respectively.

We first attempted to identify XLH3 in the TAMRA-FP profile of iRBC serine hydrolases by generating a knockout line by marker-free CRISPR/Cas9 deletion (Figure 3-S3A and 3-S3B). We also generated a yellow fluorescent protein (YFP)-tagged line by single crossover homologous recombination and selection-linked integration[26] (Figure 3-S4A and 3-S4B). TAMRA-FP profiling of MACS-enriched iRBCs of the ΔXLH3 and XLH3-YFP parasite lines failed to reveal a labeled species that could be attributed to XLH3, suggesting that the protein is not expressed in asexual stages or is expressed below the detection threshold of our assay. Preliminary OA/LPC competition experiments yielded results essentially identical to those obtained with 3D7; thus, we did not characterize this single-knockout line in detail.

We next generated a parasite line expressing an endogenous XLH4-YFP fusion (Figure 3-S4C). TAMRA-FP profiling revealed a ~30 kDa increase in molecular mass associated with a ~150 kDa serine hydrolase that is partially inhibited by 10 μM AKU-010 *in vitro* (Figure 3-3A). Live-cell fluorescence microscopy revealed a diffuse cytosolic distribution of XLH4-YFP in the parasite (Figure 3-3B), which indicates that XLH4 is not exported to the host cell. To assess the contribution of XLH4 to LPC hydrolysis, we generated parasite lines in which the XLH4 coding sequence was truncated by homologous recombination to render the enzyme non-functional, yielding single (ΔXLH4), double (ΔXL2/XLH4) and triple (ΔXL1/2/XLH4) knockout lines (Figure 3-S3C, 3-S3D and 3-S3E). Finally, we introduced an XLH3 coding sequence deletion on the ΔXL1/2/XLH4 background to produce a parasite line devoid of all four XL/XLH coding sequences (Figure

3-S3F). The resulting ΔXL1/2/XLH3/4 line is referred to as "quadruple knockout", or QKO. We confirmed the loss of XLH4 in two independently-generated lines (ΔXL2/XLH4 and QKO) by TAMRA-FP profiling (Figure 3-3C and 3-S3G).

We conducted OA/LPC competition assays to determine the contribution of XLH4 to *in sit*u LPC hydrolysis. While loss of XLH4 alone had a minimal effect, deletion of XLH4 on a ΔXL2 background (*i.e.*, ΔXL2/XLH4, ΔXL1/2/XLH4, and QKO lines) was associated with a strong reduction of LPC hydrolysis as reflected by increased OA incorporation into DAG, TAG and PE (Figure 3-3D; a ratio of 1 indicates no competition). To our surprise, a ~10-fold increase in the fluorescence ratio for PC was observed with ΔXL1/2/XLH4 and QKO lines over the parental 3D7 line. This increase was also observed with LPC 16:0, but not when LPC was replaced with LPE, LPS or the non-hydrolysable LPC analog lyso-PAF (all with 18:1 fatty acyl groups; Figure 3-S5). One explanation for this finding is that unhydrolyzed LPC is directly acylated to PC through the activity of an LPC acyltransferase. Because erythrocytes possess LPC acyltransferase activity for the purpose the phospholipid remodeling (*i.e.*, the Lands cycle)[27], we asked whether PC is efficiently formed from OA and LPC in uninfected erythrocytes. While a very small amount of PC synthesis was observed, this was insignificant compared to that in QKO parasites (Figure 3-3E). Finally, we complemented the QKO line with an XL2 expression cassette delivered on a *piggybac* transposon (Figure 3-S6). TAMRA-FP profiling indicated that the complemented parasite line, termed QKO/XL2c, expressed XL2 at a level essentially identical to that of parental 3D7 parasites (Figure 3-3F). XL2 complementation fully restored the capacity of parasites to efficiently hydrolyze LPC (Figure 3-3D).

XL2 and XLH4 catalyze LPC hydrolysis *in vitro*

To determine whether XL/XLH enzymes directly contribute to LPC metabolism through catalysis of hydrolysis of the fatty acyl ester (*i.e.*, A1-type lipase activity), we developed an *in vitro* lysophospholipase activity that employs a fluorescent LPC analog, TopFluor-LPC (Figure 3-S7). Lysates of MACS-enriched 3D7, ΔXL2, ΔXL2/XLH4, QKO and QKO/XL2c parasites, as well as uninfected RBC (uRBC), were generated at equivalent cell densities. Serial 3-fold dilutions were then assayed for hydrolysis of TopFluor-LPC, with substrate and product (TopFluor-oleic acid) resolved by TLC and quantified by fluorescence scanning.

Consistent with a previous report[11], lysophospholipase (LPL) activity was greatly elevated in 3D7-infected cells over that in uRBC (Figure 3-3G). A substantial drop in LPL activity in the ΔXL2 lysate indicates that much of that activity can be attributed to XL2. Interpolating the dilutions required for 10% hydrolysis activity, we estimate that loss of XL2 effected a ~6-fold reduction in LPL activity. Comparison of ΔXL2 and ΔXL2/XLH4 lysates revealed an additional ~3-fold drop in LPL activity upon loss of XLH4. No further reduction of LPL activity was observed in QKO parasites, suggesting that neither XL1 nor XLH3 contributed appreciably to LPL activity in asexual stages. The level of LPL activity was slightly above that of uRBC, which suggests that a small amount of residual LPL activity remains in QKO parasites. XL2 complementation of QKO restored LPL activity to wild-type levels. These results indicate that XL2 and XL4 are authentic lysophospholipases and constitute the bulk of LPC-hydrolyzing activity in infected erythrocytes.

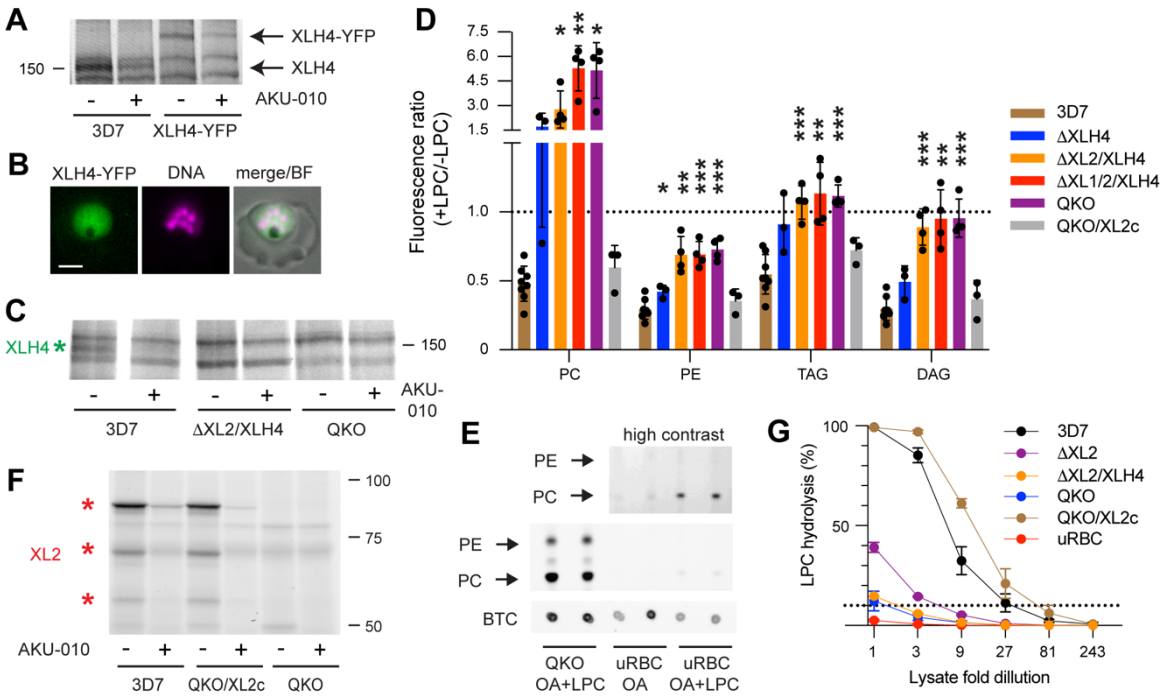

Figure 3-3. Exported XL2 and intraparasitic XLH4 govern the metabolism of exogenous LPC in asexual parasites. (A) TAMRA-FP profiling of MACS-enriched parental 3D7 and XLH4-YFP-expressing parasites. YFP tagging of XLH4 results in a mass increase of ~30 kDa. (B) A live parasitized erythrocyte exhibiting intraparasitic XLH4-YFP fluorescence. Hoechst 33342 fluorescence (DNA) is pseudocolored magenta. BF, brightfield. Scale bar, 3 µm. (C) TAMRA-FP profiling demonstrates the loss of XLH4 in MACS-enriched double (ΔXL2/XLH4) and quadruple (QKO) knockout lines. Full gel images are shown in Figure 3-S3G. (D) Oleate alkyne/LPC competition profiling of XLH4 single and XL/XLH multiple knockout lines. A ratio of 1 (dotted line) indicates no competition from LPC hydrolysis. Means and standard deviations are from at least three independent experiments. Significance relative to 3D7 was assessed within lipid groups using a two-tailed Welch's *t*-test. *, $p < 0.05$; **, $p < 0.01$; ***, $p < 0.001$; no asterisk, $p \geq 0.05$. (E) Enhanced PC synthesis in QKO parasites is not due to erythrocyte acyltransferase activity. Equivalent numbers of MACS-enriched QKO iRBC or uninfected erythrocytes (uRBC) were labeled with OA with or without LPC as indicated, in duplicate. Phospholipids were resolved by TLC. (F) TAMRA-FP profiling of MACS-enriched parasites reveals comparable expression in the complemented QKO parasite (QKO/XL2c) and parental 3D7 lines. (G) *In vitro* lysophospholipase activity in lysates of equivalent numbers of MACS-enriched iRBC or uRBC. Percent of TopFluor LPC hydrolysis is shown for serial three-fold dilutions of lysates. The dotted line indicates 10% substrate hydrolysis. Means and standard deviations are from three independent experiments.

XL/XLH-deficient parasites cannot efficiently use exogenous LPC as a source of fatty acids and are hypersensitive to LPC toxicity

We predicted that the depletion of LPL activities in QKO parasites would impact their ability to scavenge fatty acids from exogenous LPC. To test this, we washed synchronized ring-stage parasites into media containing two LPC species, 16:0 and 18:1, as sole sources of fatty acids ("2LPC medium") at concentrations from 5 to 50 μM each. Parasites were also cultured with the two corresponding free fatty acids, palmitate and oleate (30 μM each; "2FFA medium"), and with 5% Albumax I, as growth controls. Prior studies have reported that palmitate and oleate are sufficient to support parasite growth over multiple generations[28,29]; however, we found that only one complete cycle could be sustained in 2LPC or 2FFA medium. Thus, we evaluated parasite proliferation by comparing second-cycle parasitemias, normalizing 2LPC values to those in 2FFA or Albumax-containing media.

Growth of wild-type 3D7 parasites was optimal at LPC concentrations between 15 and 25 μM each, at which the replication efficiency was essentially identical to that in 2FFA medium, but somewhat lower than in Albumax-containing medium (Figure 3-4A). Second-cycle parasitemias declined at higher LPC concentrations, presumably due to the adverse effects of elevated LPC concentrations, which have been reported perturb erythrocyte membranes[30,31]. QKO parasites exhibited a similar concentration response in 2LPC medium, however their ability to proliferate in this medium was substantially diminished compared to that in 2FFA or Albumax (Figure 3-4A). Notably, XL2 complementation of the QKO line restored robust growth in 2LPC medium (Figure 3-4A).

The studies in 2LPC medium suggested that parasite lysophospholipases may fulfill two critical roles: generating fatty acids for lipid synthesis and protecting against LPC toxicity. To evaluate the latter role, we supplemented Albumax-containing medium (which is rich in free fatty acids; see Discussion) with LPC 18:1 at concentrations up to 240 μM and evaluated the growth of 3D7, QKO and QKO/XL2c parasites over one cycle. QKO parasites were substantially more sensitive to LPC toxicity compared to the wild-type 3D7 line (Figure 3-4B), with EC_{50} values of 33 ± 3 μM and 72 ± 5 μM, respectively. This sensitivity was reversed by XL2 complementation (Figure 3-4B).

Human serum is an abundant source of both free fatty acids and LPC, with concentrations of both in the range of 200-300 μM[7]. Given the enhanced sensitivity of QKO parasites to LPC, we were interested in assessing their ability to proliferate in the presence of a physiologically-relevant, complex source of exogenous fatty acids. Strikingly, QKO parasites were unable to replicate in RPMI medium containing 10% serum. This phenotype was replicated with ΔXL2/XLH4 parasites but not the single ΔXL2 or ΔXLH4 lines (although the ΔXLH4 line exhibited a reduced growth rate), indicating that loss of both enzymes prevented parasite growth in serum. Complementation of the QKO line with XL2 fully restored growth in serum (Figure 3-4C). Notably, all parasite lines exhibited comparable growth rates in Albumax-containing medium (Figure 3-4C).

Given the inability of XL2/XLH4-deficient parasites to flourish in the presence of human serum, we predicted that wild-type 3D7 parasites would exhibit enhanced sensitivity to AKU-010 in serum-containing medium. This was indeed the case (Figure 3-4D). In Albumax-containing medium, parasites were insensitive to AKU-010 concentrations below 10 μM. In contrast, parasite growth in serum-containing medium was

inhibited with an EC_{50} value of 1.3 ± 0.4 µM, representing a >10-fold increase in sensitivity to AKU-010, an effect that is likely driven by enhanced LPC toxicity upon inhibition of LPL activity.

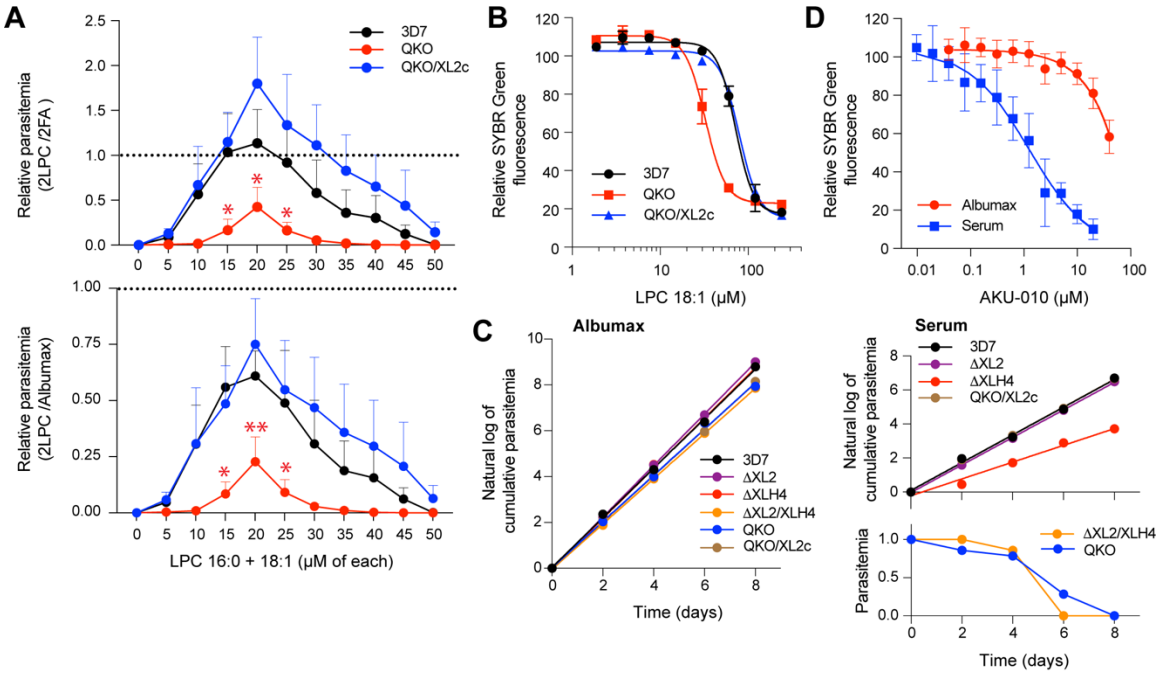

Figure 3-4. Loss of XL2 and XLH4 activities impairs fatty acid scavenging from LPC, exacerbates LPC toxicity and abrogates growth in serum. (A) QKO parasites have diminished ability to use LPC as a sole source of fatty acids. Parasites were grown for one generation in a minimal-lipid medium containing either two LPC ("2LPC") or two fatty acid species ("2FA"), or in medium containing Albumax. Parasitemias in 2LPC medium were normalized to those in 2FA medium (upper panel), or in Albumax (lower panel). Means and standard deviations are shown for three independent experiments. Significance relative to 3D7 was assessed for 15-25 uM concentrations using a two-tailed Welch's *t*-test. *, $p < 0.05$; **, $p < 0.01$. (B) QKO parasites are hypersensitive to LPC toxicity. 3D7, QKO or QKO/XL2c parasites were cultured for 48 h in complete RPMI supplemented with LPC 18:1 (1.95 to 240 µM) and parasite growth was quantified using SYBR Green. Data are from two (3D7, QKO) or one (QKO/XL2c) independent experiments. (C) Parasites lacking XL2 and XLH4 do not proliferate in medium containing human serum. The indicated parasite lines were grown in RPMI medium supplemented with either 0.5% Albumax I or 10 % pooled human serum. Where parasite growth was observed, data were natural-log transformed and fitted by linear regression. One of two independent experiments with similar results is shown. (D) Growth in serum sensitizes wild-type 3D7 parasites to AKU-010. Parasites were incubated with AKU-010 (80 nM - 40 µM for Albumax and 10 nM - 20 µM for serum) for 60 h and parasitemia was quantified on Giemsa-stained smears. Cumulative parasitemia is the parasitemia on day X multiplied by

the total dilution up to that point. Means and standard deviations are shown for three independent experiments.

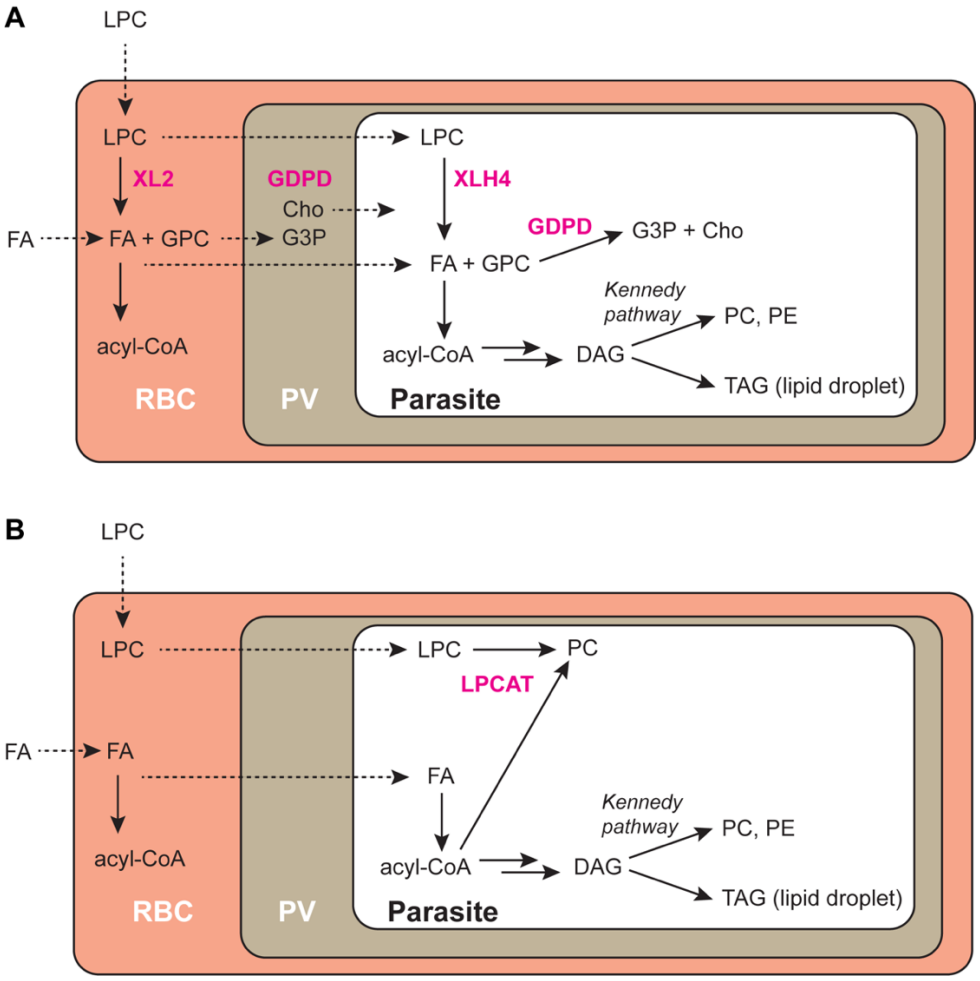

Figure 3-5. LPC metabolism in *P. falciparum* and metabolic consequences of the loss of XL2/XLH4 activities. (A) LPC is hydrolyzed to fatty acids and glycerophosphocholine (GPC) either in the host erythrocyte by XL2 or within the parasite by XLH4. In both cases, GPC can be hydrolyzed to glycerol-3-phosphate (G3P) and choline (Cho) by glycerophosphocholine phosphodiesterase (GDPD). The resulting fatty acids (FA) serve as precursors for lipid synthesis. Exogenous fatty acids can also be taken up and incorporated into parasite lipids. Solid arrows indicate metabolic reactions with the corresponding enzymes in magenta. Broken arrows indicate transport processes. RBC, red blood cell; PV, parasitophorous vacuole. (B) Loss of XL2 and XL4H greatly diminishes the rate of hydrolysis of LPC (a low level of hydrolysis is likely occurring but is not depicted). LPC accumulating in the infected erythrocyte may be directly acylated to PC through the activity of an LPC acyltransferase (LPCAT), with acyl-CoA serving as co-substrate.

3.4 DISCUSSION

We have identified two enzymes, XL2 and XLH4, that are each capable of efficient hydrolysis of exogenous LPC in asexual *P. falciparum*-infected erythrocytes (Figure 3-5A). Knockout of either enzyme individually had a negligible effect on the ability of parasites to scavenge fatty acids from LPC; however, deletion of both enzymes greatly reduced parasite lysophospholipase activity *in vitro* and *in situ*, diminished the ability to scavenge fatty acids from LPC, and hypersensitized parasites to LPC toxicity (Figure 3-5B). A low level of residual LPL activity in QKO parasites likely accounts for their ability to replicate to a limited extent in 2LPC medium.

We propose that XL2 catalyzes the hydrolysis of LPC in the erythrocyte cytosol, yielding fatty acids and glycerophosphocholine (GPC). These fatty acids may serve as substrates for parasite-exported acyl-CoA synthetases[32] and must also be able to enter the parasite, given the ability of XL2 complementation of the QKO line to fully restore LPC hydrolysis and growth in 2LPC medium. XL2 is not conserved across *Plasmodium* spp., but rather is restricted to the *Laverania* subgenus consisting of human and ape parasites. This may reflect an adaptation to the mature erythrocyte environment, as these host cells have a limited capacity for lipid metabolism. XLH4 is a cytosolic enzyme that is found in human- and ape-infecting *Plasmodium* species (including the non-Laveranian species *vivax, knowlesi, malariae* and *ovale*) but is absent from rodent parasites (PlasmoDB.org). We speculate that XLH4 catalyzes the hydrolysis of LPC that either escapes hydrolysis in the erythrocyte or that diffuses into the parasite through points of contact between host cell and parasite membranes[33,34]. Clearly, XLH4 can compensate for the absence of extensive LPC hydrolysis in the host erythrocyte, as indicated by the minimal impact of deleting XL1

and XL2. Fatty acids generated through XLH4 activity can directly enter the parasite acyl-CoA pool and be used for parasite lipid synthesis.

A surprising finding was the ~10-fold elevation in OA-labeled PC observed in OA/LPC competition assays with parasite lines lacking both XL2 and XLH4, with more modest elevations in the ΔXL2 and ΔXLH4 lines. The most likely explanation for this phenomenon is direct LPC acylation, *i.e.*, acyl transfer to LPC from an acyl-CoA donor, a ubiquitous reaction in eukaryotes that has not previously been described in P. *falciparum*. According to this model (Figure 3-5), intracellular LPC levels are elevated in the absence of XL2 and XLH4, leading to increased flux through an existing LPC acylation pathway that presumably makes a minor contribution to PC synthesis in wild-type parasites. Further investigation will be required to identify the relevant acyltransferase(s) and to evaluate the physiological significance of an LPC acylation pathway in a wild-type genetic background.

Parasite LPC metabolism appears to have a dual role: acquisition of fatty acids and reduction of LPC toxicity. All XL/XLH-deficient parasites generated in this study replicated at comparable rates in medium containing Albumax, an enriched bovine serum albumin product that is relatively rich in free fatty acids (FFA) and poor in LPC. Based on literature values for the FFA and LPC content of Albumax[35], we estimate that our standard formulation of 0.5% Albumax (w/v) in RPMI provided ~66 μM FFA and ~11 μM LPC. In contrast, serum contains high levels of both free fatty acids and LPC. A detailed analysis of the human serum metabolome revealed total FFA and LPC concentrations of 220 and 280 μM, respectively (Table 11 in Psychogios *et al*[7]). In medium with 10% (v/v) human serum, the LPC concentration would be ~28 μM. Thus, we speculate that the elevated LPC concentrations in serum compared to Albumax were responsible for the lack of growth of

ΔXL2/XLH4 and QKO parasites in the former. Consistent with this interpretation, wild-type parasites were sensitized to AKU-010 in serum-containing medium. Together, these findings highlight the importance of XL/XLH-mediated LPC catabolism for parasite proliferation in high-LPC environments such as that found in the host circulation and validate the co-inhibition of XL2 and XLH4 as viable anti-malarial strategy.

3.5 ONLINE METHODS

Materials

BODIPY™ 500/510 C_4, C_9 (C4,C9-FA) and BODIPY-TR-ceramide (BTC) were obtained from ThermoFisher. LPC 18:1 and 16:0, Lyso-PAF 18:1 and 16:0, (*Z*)-octadec-9-en-17-ynoic acid (oleic acid alkyne), TopFluor® LPC, TopFluor® oleic acid, and palmitic and oleic acids were obtained from Avanti Polar Lipids. IDFP and JW642 were purchased from Cayman Chemical. 3-azido-7-hydroxycoumarin was acquired from Abcam. Piperazine-based MAGL inhibitors described in Aaltonen *et al*[19] were provided by Dr. T. Nevalainen, University of Eastern Finland. The following reagent was obtained through BEI Resources, NIAID, NIH: DSM1, MRA-1161. WR99210 was a gift from D. Jacobus (Jacobus Pharmaceuticals).

Parasite culture

P. falciparum clone 3D7 was routinely cultured in human O^+ erythrocytes (Interstate Blood Bank) at 2% hematocrit in RPMI 1640 medium supplemented with 0.37 mM hypoxanthine, 11 mM glucose, 27 mM sodium bicarbonate, 10 μg/mL gentamicin and

5 g/L Albumax I (Gibco). Cultures were incubated at 37 °C in a 5% CO_2 incubator and were synchronized by treatment with 5% (w/v) sorbitol.

Generation of plasmids and parasite transfection

Oligonucleotides used in plasmid construction and parasite line validation are listed in **Table 3-S1**. All nucleotide sequences were confirmed by DNA sequencing. PCR analyses were conducted on 10 ng of genomic DNA in 15 µL volumes with amplification by Taq polymerase (New England Biolabs). A list of the parasite lines generated in this study is provided in **Table 3-S2**.

Markerless deletion of the entire coding sequences of XL1, XL2 and XLH3 was accomplished by CRISPR/Cas9 editing. Cas9 sgRNAs targeting the respective coding sequences were selected from the database assembled by Ribeiro *et al*[36] and were cloned into the BtgZ1 site of pUF-Cas9-pre-sgRNA[37], which contains yeast DHOD as a selectable marker. Homology repair plasmids were constructed using ~250 nucleotides each of 5' and 3' UTR sequences. The 5' and 3' homology arms were cloned into *Xho*I/*Sal*I sites and *Eco*RI/*Bgl*II sites of pPM2GT[38], respectively. 25 µg each of the Cas9/sgRNA plasmid (two Cas9/sgRNA plasmids together were used at 12.5 µg each for XLH3) and the homology repair plasmid (linearized with *Bgl*I) were co-transfected into ring-stage *P. falciparum* by high-capacitance electroporation[39]. After 24 hours, parasites were selected with 2 µM DSM-1 for four days and then grown out without selection. Clonal lines were generated by limiting dilution. Loss of coding sequences was validated by PCR (Figure 3-S2 and Figure 3-S3).

Disruption of the XLH4 coding sequence and generation of C-terminal YFP fusions with XLH3 and 4 were accomplished by homologous recombination and selection-linked integration[26]. The sequence for the yellow fluorescent protein allele Citrine (lacking a stop codon) was inserted into the *Avr*II and *Sal*I sites in pSLI-2×FKBP-GFP[26], replacing L3-2xFKBP-L4-GFP, to yield pSLI-YFP. An ~800 bp homology sequence preceded by a stop codon was then inserted into the *Not*I and *Avr*II sites of pSLI-YFP to generate plasmids pSLI-XLH3-YFP, pSLI-XLH4-YFP, and pSLI-XLH4(GD)-YFP. Parasites were transfected by electroporation and after 48 hours were selected with 5 nM WR99210. Resistant parasites were then subjected to selection with 400 µg/mL G418 for up to 12 days to obtain parasites with episomal integration into the targeted genomic locus, which was confirmed by PCR (Figure 3-S3 and Figure 3-S4).

For XL2 complementation, a *piggybac* transposon[40] carrying a copy of the XL2 coding sequence, with transcription driven by the PfRab7 promoter, was constructed. First, the rab7 5' UTR (bases -1007 to -1) and the XL2 coding sequence (including a single intron and the stop codon) were amplified from genomic DNA. Both products were merged in an overlapping PCR reaction with oligos 1374/1377 and the resulting fragment was ligated into *Xma*I/*Not*I-digested pDD-mCherry-Rab7-DHOD[41]. QKO parasites were transfected by electroporation and after 48 hours were selected with 1.5 µM DSM-1. Presence of the XL2 coding sequence in drug-resistant parasites was confirmed by PCR (Figure 3-S6).

C4,C9-FA competition assay for inhibition of LPC hydrolysis *in situ*

Assays for inhibition of LPC hydrolysis in intact parasitized erythrocytes were conducted using a dual-fluorescent labeling strategy as previously described[15] and

modified as follows. Parasites were pre-labeled with 1 μM BODIPY-TR-ceramide (BTC) in complete RPMI for 1 hour. They were then washed into fatty acid-free (*i.e.*, incomplete) RPMI, aliquoted at 0.5 mL and 8% hematocrit into a 24-well plate, supplemented with 10 μM inhibitor or equivalent volume of DMSO, and incubated for 30 minutes at 37 °C in a CO_2 incubator. An equal volume of medium containing fatty acid free BSA, C4,C9-FA, LPC18:1 (or 50% ethanol for no-LPC controls), and 10 μM inhibitor (or DMSO for no-inhibitor controls), such that final concentrations were 2 mg/mL BSA, 30 μM C4,C9-FA, 30 μM LPC18:1 and 10 μM inhibitor. After 30 minutes, cultures were transferred to 9 mL of cold 0.03% saponin in PBS and parasites were isolated by centrifugation. Lipids were extracted as previously described[15], dissolved in chloroform, and spotted on a 10 × 10 cm glass HPTLC Silica Gel 60 plate (Millipore). BTC fluorescence was imaged on a Typhoon RGB imager (Cytiva) using a 633 nm laser and a 670/30 bandpass filter. Neutral lipids were resolved in heptane/diethyl ether/acetic acid at ratio of 40:60:1 and C4,C9-FA fluorescence was imaged using the 532 nm laser and a 570/20 bandpass filter. Fluorescence intensities for DAG, TAG and BTC were quantified using ImageQuantTL (Cytiva). BTC fluorescence intensities were used to normalize DAG and TAG intensities across samples.

MACS purification and TAMRA-FP analysis

Parasites were enriched from ~100 mL of culture containing synchronized schizonts (~36-44 h post-invasion) at ~10% parasitemia using a SuperMACS™ II Separator and a D Column (Miltenyi Biotec). Numbers of eluted cells were determined with a hemocytometer and parasitemia was calculated from a Giemsa-stained smear. Typical yields were 5 x 10^8 parasite-infected erythrocytes at 90-95% parasitemia. To

generate cell lysates, pellets were resuspended at 5 x 10^8 parasites/mL in cold PBS supplemented with 5 μM pepstatin A and 10 μM E64. The suspension was sonicated three times for eight seconds using a microtip at 30% maximum power. Hemozoin was removed by centrifugation at 12,000 x*g* at 4 °C. Lysates were aliquoted, snap frozen in liquid nitrogen, and stored at – 80 °C. Lysates of uninfected erythrocytes (uRBC) were generated in the same manner except that the MACS separation was omitted.

For serine hydrolase inhibitor profiling with the activity-based probe TAMRA-FP, 19.4 μL of MACS or uRBC lysate was mixed with 0.2 μL of 1 mM inhibitor (or DMSO for controls), 0.2 μL of 100 μM AA74-1 to selectively inhibit human APEH[42], and was incubated at 30 °C for 30 minutes. The reaction was added with 0.2 μL of 100 μM TAMRA-FP and incubated at 30 °C for 30 minutes. The reaction was quenched by adding 20 μL of 2X SDS-PAGE loading buffer and incubating at 95 °C for 5 minutes. Labeled proteins were resolved on 8.5 or 10% sodium dodecyl sulfate–polyacrylamide gels and imaged on a Typhoon RGB flatbed scanner using the 532 nm laser and a 570/20 bandpass filter.

Oleate alkyne competition assay for inhibition of LPC hydrolysis *in situ*

Synchronized parasite cultures with ~10% trophozoites were labeled with 1 μM BTC for 1 hour at 37 °C in a CO_2 incubator and then washed three times with incomplete RPMI. Cultures were resuspended in pre-warmed incomplete RPMI containing 3 mg/mL fatty acid-free BSA, 30 μM oleic acid alkyne and 30 μM LPC 18:1 (or 50% ethanol for no-LPC controls) and incubated for 40 minutes with gentle mixing on an orbital rotator at 37 °C in a CO_2 incubator. Labeled cultures were harvested and lipids were extracted as

described above for C4,C9-FA competition assays. Alkyne-labeled lipids were rendered fluorescent by Cu-catalyzed azide–alkyne cycloaddition of 3-azido-7-hydroxycoumarin as previously described[24]. Solvent was evaporated in a vacuum centrifuge and lipids were redissolved in ~10 µL chloroform. For TLC separation, 1 µL was spotted on a 10 cm × 10 cm glass HPTLC Silica Gel 60 plate (Millipore). BODIPY-TR-ceramide fluorescence was then recorded as described above for C4,C9-FA competition assays. Phospholipids were developed with 65:25:4:1 chloroform/methanol/water/acetic acid for about 4.5 cm. Plates were air dried and neutral lipids were resolved with 1:1 hexane/ethyl acetate. Plates were sprayed with 6 mL 4% (v/v) *N*,*N*-diisopropylethylamine in hexane prior to imaging. Fluorescence was imaged on an Azure C400 CCD camera imager using blue LED illumination (472 nm) for excitation and a 513/17 bandpass filter for emission. BTC, neutral and polar lipid fluorescence intensities were quantified using ImageQuantTL software (Cytiva) and lipid intensities were normalized across samples using BTC fluorescence.

In vitro LPC hydrolysis assays

Lysates of MACS-purified infected erythrocytes or of uRBC were serially 3-fold diluted with cold PBS. TopFluor LPC was added to 50 µM from a 2.5 mM DMSO stock and reactions were incubated at 30°C for 15 minutes. Reaction products were extracted by transferring 3 µL to 150 µL chloroform and vortexing for 20 seconds. 1 µL of the chloroform layer was spotted on a 10 × 10 cm aluminum HPTLC Silica Gel 60 plate (Millipore). TopFluor LPC and the hydrolysis product TopFluor oleic acid were resolved with 65:25:4:1 chloroform/methanol/water/acetic acid and imaged on a Typhoon RGB

scanner using a 488 nm laser and 525/20 bandpass filter. The relative fluorescence intensities of TopFluor LPC and TopFluor oleic acid were assessed by resolving equimolar mixtures using the TLC system described above and quantifying fluorescence intensities. The signal for TopFluor oleic acid was 1.25-fold higher than that for TopFluor LPC; therefore, a correction factor was applied. Percent hydrolysis was then calculated for each sample.

Growth in medium containing LPC as sole source of fatty acids

Synchronized ring-stage parasite cultures (0-16 h post-invasion) were washed three times with incomplete RPMI and resuspended at 3% parasitemia and 1% hematocrit in 1 mL of RMPI containing 3 mg/mL fatty acid BSA and 0-50 μM each of LPC 16:0 and 18:1 and placed in a 24-well plate. Parallel cultures for normalization were set up with either: 1) RMPI with 3 mg/mL BSA and 30 μM each of palmitic (16:0) and oleic (18:1) acids; and 2) RPMI with 5% Albumax I. Parasites were cultured for 60 hours at 37 °C in a 5% CO_2 incubator, at which point Giemsa-stained smears were prepared. Parasitemia was calculated from a minimum of 1000 cells.

Growth in medium containing human serum

Synchronized ring-stage parasite cultures (0-16 h post-invasion) at 2% parasitemia and 2% hematocrit were washed into complete RPMI containing either 0.5% Albumax I or 10% (v/v) pooled, heat-inactivated human serum (Interstate Blood Bank) and cultured at 37 °C in a 5% CO_2 incubator. Over an eight-day period, parasitemia was counted from

Giemsa-stained smears every two days and parasites were subcultured unless they were not thriving, in which case the medium was changed.

EC_{50} measurements

EC_{50} values for LPC 18:1 and AKU-010 were determined using a SYBR Green I assay as previously described[43]. For LPC, early ring stage parasites (0-8 hours post-invasion) were inoculated into in 96 well plates at 3% parasitemia, 1% hematocrit in complete RPMI containing 0.5% Albumax I. LPC 18:1 (1.9 to 240 μM) or 50% ethanol (final concentration 0.2%) were then added and cultures were incubated in a low-oxygen environment (5% O_2, 5% CO_2, and 90% N_2) at 37°C for 48 hours. No hemolysis was observed under these conditions. For AKU-010, parasites were inoculated in complete RPMI containing 0.5% (w/v) Albumax I or 10% (v/v) pooled human serum. AKU-010 (80 nM - 40 μM for Albumax and 10 nM - 20 μM for serum), DMSO (0.2% or 0.4%), or mefloquine (300 nM; positive control for parasite killing) were then added and cultures were incubated in 5% CO_2 incubator for 60 hours. Cultures were developed with SYBR Green I as previously described[43] and fluorescence was quantified on a Molecular Devices SpectraMax M5 microplate fluorometer. Fluorescence values were expressed as a fraction of the DMSO control and the EC_{50} values were determined using four-parameter sigmoidal non-linear regression.

ACKNOWLEDGMENTS

We are grateful to Tapio Nevalainen (University of Eastern Finland) for providing the monoacylglycerol lipase inhibitors described in Aaltonen *et al*[19] and to Josh Beck

(University of Iowa) for the CRISPR/Cas9 plasmids. M. K. discloses support for this work from National Institutes of Health grant AI133136 and from USDA National Institute of Food and Agriculture HATCH project VA-160082.

REFERENCES

1 WHO. World malaria report 2022. (2022).

2 Dhorda, M. *et al.* Artemisinin and multidrug-resistant *Plasmodium falciparum* - a threat for malaria control and elimination. *Current Opinion in Infectious Diseases* **34**, 432-439 (2021).

3 Vial, H. J. & Ancelin, M. L. Malaria lipids, in Malaria: parasite biology, biogenesis, protection. *American Association of Microbiology Press* (1998).

4 Palacpac, N. M. Q. *et al.* Developmental-stage-specific triacylglycerol biosynthesis, degradation and trafficking as lipid bodies in *Plasmodium falciparum*-infected erythrocytes. *Journal of cell science* **117**, 1469-1480 (2004).

5 Jackson, K. E. *et al.* Food vacuole-associated lipid bodies and heterogeneous lipid environments in the malaria parasite, *Plasmodium falciparum*. *Molecular Microbiology* **54**, 109-122 (2004).

6 Vaughan, A. M. *et al.* Type II fatty acid synthesis is essential only for malaria parasite late liver stage development. *Cellular Microbiology* **11**, 506-520 (2009).

7 Psychogios, N. *et al.* The human serum metabolome. *PLoS One* **6**, e16957 (2011).

8 Vial, H. J. *et al.* Phospholipid metabolism in *Plasmodium*-infected erythrocytes: guidelines for further studies using radioactive precursor incorporation. *Parasitology* **98**, 351-357 (1989).

9 Brancucci, N. M. B. *et al.* Lysophosphatidylcholine regulates sexual stage differentiation in the human malaria parasite *Plasmodium falciparum*. *Cell* **171**, 1532-1544 (2017).

10 Ramaprasad, A. *et al.* A choline-releasing glycerophosphodiesterase essential for phosphatidylcholine biosynthesis and blood stage development in the malaria parasite. *Elife* **11**, e82207 (2022).

11 Zidovetzki, R. *et al.* Inhibition of *Plasmodium falciparum* lysophospholipase by anti-malarial drugs and sulphydryl reagents. *Parasitology* **108** 249-255 (1994).

12 Aurrecoechea, C. *et al.* PlasmoDB: a functional genomic database for malaria parasites. *Nucleic Acids Research* **37**, D539-543 (2009).

13 Asad, M. *et al.* An essential vesicular-trafficking phospholipase mediates neutral lipid synthesis and contributes to hemozoin formation in *Plasmodium falciparum*. *BMC Biology* **19**, 159 (2021).

14 Sheokand, P. K. *et al.* GlmS mediated knock-down of a phospholipase expedite alternate pathway to generate phosphocholine required for phosphatidylcholine synthesis in *Plasmodium falciparum*. *Biochemical Journal* **478**, 3429-3444 (2021).

15 Dapper, C. *et al.* Leveraging a fluorescent fatty acid probe to discover cell-permeable inhibitors of *Plasmodium falciparum* glycerolipid biosynthesis. *Microbiology Spectrum* **10**, e0245622 (2022).

16 Nomura, D. K. *et al.* Activation of the endocannabinoid system by organophosphorus nerve agents. *Nature Chemical Biology* **4**, 373-378 (2008).

17 Elahi, R. *et al.* Functional annotation of serine hydrolases in the asexual erythrocytic stage of *Plasmodium falciparum*. *Scientific Reports* **9**, 17532 (2019).

18 Chang, J. W. *et al.* Highly selective inhibitors of monoacylglycerol lipase bearing a reactive group that is bioisosteric with endocannabinoid substrates. *Chemistry & Biology* **19**, 579-588 (2012).

19 Aaltonen, N. *et al.* Piperazine and piperidine triazole ureas as ultrapotent and highly selective inhibitors of monoacylglycerol lipase. *Chemistry & Biology* **20**, 379-390 (2013).
20 Patricelli, M. P. *et al.* Direct visualization of serine hydrolase activities in complex proteomes using fluorescent active site-directed probes. *Proteomics* **1**, 1067-1071 (2001).
21 Ribaut, C. *et al.* Concentration and purification by magnetic separation of the erythrocytic stages of all human *Plasmodium* species. *Malaria Journal* **7**, 45 (2008).
22 Spillman, N. J. *et al.* Exported epoxide hydrolases modulate erythrocyte vasoactive lipids during *Plasmodium falciparum* infection. *MBio* **7** (2016).
23 Zhang, X. *et al.* Rapid antigen diversification through mitotic recombination in the human malaria parasite *Plasmodium falciparum*. *PLoS Biology* **17**, e3000271 (2019).
24 Thiele, C. *et al.* Tracing fatty acid metabolism by click chemistry. *ACS Chemical Biology* **7**, 2004-2011 (2012).
25 Boddey, J. A. *et al.* Role of the *Plasmodium* export element in trafficking parasite proteins to the infected erythrocyte. *Traffic* **10**, 285-299 (2009).
26 Birnbaum, J. *et al.* A genetic system to study *Plasmodium falciparum* protein function. *Nature Methods* **14**, 450-456 (2017).
27 Soupene, E. *et al.* Mammalian acyl-CoA:lysophosphatidylcholine acyltransferase enzymes. *Proceedings of the National Academy of Sciences of the United States of America* **105**, 88-93 (2008).
28 Mi-Ichi, F. *et al.* Oleic acid is indispensable for intraerythrocytic proliferation of *Plasmodium falciparum*. *Parasitology* **134**, 1671-1677 (2007).
29 Mi-Ichi, F. *et al.* Intraerythrocytic *Plasmodium falciparum* utilize a broad range of serum-derived fatty acids with limited modification for their growth. *Parasitology* **133**, 399-410 (2006).
30 Sato, T. & Fujii, T. Changes in shape and osmotic resistance of human erythrocytes resulted from changes in the lysolecithin content of the membranes. *Chemical and Pharmaceutical Bulletin* **22**, 152-156 (1974).
31 Bierbaum, T. J. *et al.* A mechanism of erythrocyte lysis by lysophosphatidylcholine. *Biochimica et Biophysica Acta* **555**, 102-110 (1979).
32 Tellez, M. *et al.* The C-terminal domain of the *Plasmodium falciparum* acyl-CoA synthetases PfACS1 and PfACS3 functions as ligand for ankyrin. *Molecular and Biochemical Parasitology* **129**, 191-198 (2003).
33 Elmendorf, H. G. & Haldar, K. *Plasmodium falciparum* exports the Golgi marker sphingomyelin synthase into a tubovesicular network in the cytoplasm of mature erythrocytes. *Journal of Cell Biology* **124**, 449-462 (1994).
34 Tamez, P. A. *et al.* An erythrocyte vesicle protein exported by the malaria parasite promotes tubovesicular lipid import from the host cell surface. *PLoS Pathogens* **4**, e1000118 (2008).
35 Garcia-Gonzalo, F. R. & Izpisúa Belmonte, J. C. Albumin-associated lipids regulate human embryonic stem cell self-renewal. *PLoS One* **3**, e1384 (2008).

36 Ribeiro, J. M. *et al.* Guide RNA selection for CRISPR-Cas9 transfections in *Plasmodium falciparum*. *International Journal for Parasitology* **48**, 825-832 (2018).
37 Garten, M. *et al.* EXP2 is a nutrient-permeable channel in the vacuolar membrane of *Plasmodium* and is essential for protein export via PTEX. *Nature Microbiology* **3**, 1090-1098 (2018).
38 Klemba, M. *et al.* Trafficking of plasmepsin II to the food vacuole of the malaria parasite *Plasmodium falciparum*. *Journal of Cell Biology* **164**, 47-56 (2004).
39 Fidock, D. A. & Wellems, T. E. Transformation with human dihydrofolate reductase renders malaria parasites insensitive to WR99210 but does not affect the intrinsic activity of proguanil. *Proceedings of the National Academy of Sciences of the United States of America* **94**, 10931-10936 (1997).
40 Balu, B. *et al.* High-efficiency transformation of *Plasmodium falciparum* by the lepidopteran transposable element *piggyBac*. *Proceedings of the National Academy of Sciences of the United States of America* **102**, 16391-16396 (2005).
41 Krai, P. *et al.* Evidence for a Golgi-to-endosome protein sorting pathway in *Plasmodium falciparum*. *PLoS One* **9**, e89771 (2014).
42 Elahi, R. *et al.* Internalization of erythrocyte acylpeptide hydrolase is required for asexual replication of *Plasmodium falciparum*. *MSphere* **4** (2019).
43 Smilkstein, M. *et al.* Simple and inexpensive fluorescence-based technique for high-throughput antimalarial drug screening. *Antimicrobial agents and chemotherapy* **48**, 1803-1806 (2004).

SUPPLEMENTARY INFORMATION

Table 3-S1. Oligonucleotides used in this study. Abbreviations: HA, homology arm; SLI, selection-linked integration; YFP, yellow fluorescent protein; CDS, coding sequence; UTR, untranslated region; GD, gene disruption.

Oligo Number	Sequence	Function	Sequence
901	pSLI	Diagnostic PCR	ATCCATCTTGTTCAATCATTGGTCC
930	YFP	pSLI-YFP	GTACGCCTAGGGAAAATTTATATT TTCAAAGTATGAGTAAAG
931	YFP	pSLI-YFP	GTACGGTCGACTTTGTATAGTTCAT CCATGCCATG
1101	XL1, 5' UTR	HA1, CRISPR repair	GTGACACTATAGAACTCGAGATGA ATATTCATTTATTCTAAACCTGTG
1102	XL1, 5' UTR	HA1, CRISPR repair	GGGGATCCTCTAGAGTCGACCAAA TTATAAATAAAGTGCCTCTTTTCC
1103	XL1, 3' UTR	HA2, CRISPR repair	CGGGTACCGAGCTCGAATTCGTTG TTACAAATGTGTAACTGTTATAAT
1104	XL1, 3' UTR	HA2, CRISPR repair	ATAGGGAGACCGGCAGATCTAATA TATAACAATATGAATTCTTTTAAA G
1094	XL1, CDS	sgRNA	TAAGTATATAATATTAGAACATGT CAGTTCACGAAGTTTTAGAGCTAG AA
1095	XL1, CDS	sgRNA	TTCTAGCTCTAAAACTTCGTGAACT GACATGTTCTAATATTATATACTTA
1069	XL1, CDS	Diagnostic PCR, wild-type	TGACACTATAGAATACTCGCGGCC GCTAAGGTGGATGTATAGCTTTAA GAAC
1070	XL1, CDS	Diagnostic PCR, wild-type	TTGAAAATATAAATTTTCCCTAGG TACAAATATATTATTTATCCAGTCA G
1137	XL1, 3' UTR	Diagnostic PCR, CRISPR-edited	ATCTGATAAGTTCTCATCTTACAC
1151	XL1, 5' UTR	Diagnostic PCR, CRISPR-edited	TAAAGCAAAATAATTAAAACTTTA TAC
1105	XL2, 5' UTR	HA1, CRISPR repair	GTGACACTATAGAACTCGAGAACA TGAATGACACATATAGTTGTCC
1106	XL2, 5' UTR	HA1, CRISPR repair	GGGGATCCTCTAGAGTCGACGGTG AATGGATTAATATAAAGCAGTC
1107	XL2, 3' UTR	HA2, CRISPR repair	CGGGTACCGAGCTCGAATTCTTTC ATTCCGCTATAAAAAAATGTTATG

1108	XL2, 3’ UTR	HA2, CRISPR repair	ATAGGGAGACCGGCAGATCTGAATAACTTAATTAATAATATGCACTAG
1098	XL2, CDS	sgRNA	TAAGTATATAATATTTGCAGATGCACTTTTGAGGGGTTTTAGAGCTAGAA
1099	XL2, CDS	sgRNA	TTCTAGCTCTAAAACCCCTCAAAAGTGCATCTGCAAATATTATATACTTA
953	XL2, CDS	Diagnostic PCR, wild-type	TGACACTATAGAATACTCGCGGCCGCTAAAAGTCACAGATTAAAAGTTTAGTAC
954	XL2, CDS	Diagnostic PCR, wild-type	TTGAAAATATAAATTTTCCCTAGGTGGATATATATTATTAAGCCAATTAAC
1138	XL2, 5’ UTR	Diagnostic PCR, CRISPR-edited	AAAATAGTAACGTCTACTATTAAG
1140	XL2, 3’ UTR	Diagnostic PCR, CRISPR-edited	AACAAATGCATATTCATTAATTGCC
1376	XL2, CDS	XL2 complement	ATTGAAGGAAAATATGCTCAATTTTAGGAGGTGGAG
1377	XL2, CDS	XL2 complement	ATTATATAACTCGACGCGGCCGCTTATGGATATATATTATTAAGCCAATTA
1146	XLH3, 5’ UTR	HA1, CRISPR repair	CATACGATTTAGAACAAATAATAACAGTAATGAACTTAATAC
1147	XLH3, 5’ UTR	HA1, CRISPR repair	GGGGATCCTCTAGAGTCTTTATTCCATTAAATTTCCTATAC
1148	XLH3, 3’ UTR	HA2, CRISPR repair	CGGGTACCGAGCTCGCGTGTGCCTATTTTGTTATTAAAAG
1149	XLH3, 3’ UTR	HA2, CRISPR repair; diagnostic PCR	ATAGGGAGACCGGCAGGTATTTGGCTTTTACTTAATTTGC
1142	XLH3, CDS	sgRNA 1	TAAGTATATAATATTTTATCATGGTAGGCCCGAATGTTTTAGAGCTAGAA
1143	XLH3, CDS	sgRNA 1	TTCTAGCTCTAAAACATTCGGGCCTACCATGATAAAATATTATATACTTA
1144	XLH3, CDS	sgRNA 2	TAAGTATATAATATTTCATCATCCAGTTTAACCCAGTTTTAGAGCTAGAA
1145	XLH3, CDS	sgRNA 2	TTCTAGCTCTAAAACTGGGTTAAACTGGATGATGAAATATTATATACTTA

1071	XLH3, CDS	Diagnostic PCR, wild-type; pSLI-XLH3-YFP	TGACACTATAGAATACTCGCGGCC GCTAAGGTAGGACTCTAAAATATC CATGG
1072	XLH3, CDS	Diagnostic PCR, wild-type; pSLI-XLH3-YFP	TTGAAAATATAAATTTTCCCTAGG GCTAAATATATTATTAAGCCAATC AAC
1196	XLH3, 5' UTR	Diagnostic PCR, CRISPR-edited	GATACACACATATGTATAATATAC G
1215	XLH3, 3' UTR	Diagnostic PCR, CRISPR-edited	ATAGGCATTATTCTAAAATAGCAA C
1049	XLH3, CDS	Diagnostic PCR, wild-type and XLH3-YFP integration	GGATCGAGGGAAGGATTTCAGAAT TCGAAAACCTGTATTTTCAGAGCA ATGAAAAATTATATAATTCAAGAA AATA
1275	XLH4, CDS	pSLI-XLH4-GD	TGACACTATAGAATACTCGCGGCC GCTAAAACGAATTGAAAGAGTCGG AAAAG
1276	XLH4, CDS	pSLI-XLH4-GD	TTGAAAATATAAATTTTCCCTAGG TTCTCCACAATTACAATAATTACA AAC
1185	XLH4, 5' UTR	Diagnostic PCR, wild-type and DXLH4 integration	GTGACACTATAGAACTCGAGGTAT ATTGATGATATACATACGAC
1179	XLH4, CDS	pSLI-XLH4-YFP	TGACACTATAGAATACTCGCGGCC GCTAAGAGCATAACGAAAAATTGG CGAC
1180	XLH4, CDS	pSLI-XLH4-YFP	TTGAAAATATAAATTTTCCCTAGG ATGAAATATATTATTCAACCAATT CAC
1229	XLH4, CDS	Diagnostic PCR, wild-type and XLH4-YFP integration	GTGATGATAATATGATGGTTGATG
1230	XLH4, CDS	Diagnostic PCR, XLH4 wild-type	CACCCATAGATAACCCCATAA
1188	XLH4, 3' UTR	Diagnostic PCR, wild-type	ATAGGGAGACCGGCAGATCTCCAT TTAAATATATACCTAATTTGGG

1194	Pf3D7_1001300, CDS	Diagnostic PCR	GCTTAATTTATCTAATGGAATATTTG
1195	Pf3D7_1001300, CDS	Diagnostic PCR	ACAATATCATTAAGACAATCTATCC
1374	Rab7, 5' UTR	Promoter for XL2 complement	TCGACCTCGATATATCCCGGGGAAAAGTATACAATGACGCATGC
1375	Rab7, 5' UTR	Promoter for XL2 complement	TAAAATTGAGCATATTTTCCTTCAATATATTGTTCTTTTT

Table 3-S2. *P. falciparum* 3D7 lines generated in this study. Abbreviations: NC, not cloned, hDHFR, human dihydrofolate reductase; NPT, neomycin phosphotransferase; yDHOD, yeast dihydroorotate dehydrogenase

Genotype	Clone	Drug resistance
ΔXL1	27	none
ΔXL2	43	none
ΔXLH3	3	none
ΔXLH4	3	hDHFR, NPT
ΔXL1/2	51–5	none
ΔXL2/XLH4	NC	hDHFR, NPT
ΔXL1/2/XLH4	72	hDHFR, NPT
ΔXL1/2/XLH3/4 (QKO)	7	hDHFR, NPT
ΔXL1/2/XLH3/4 with XL2 complement	NC	hDHFR, NPT, yDHOD
XLH3-YFP	NC	hDHFR, NPT
XLH4-YFP	NC	hDHFR, NPT

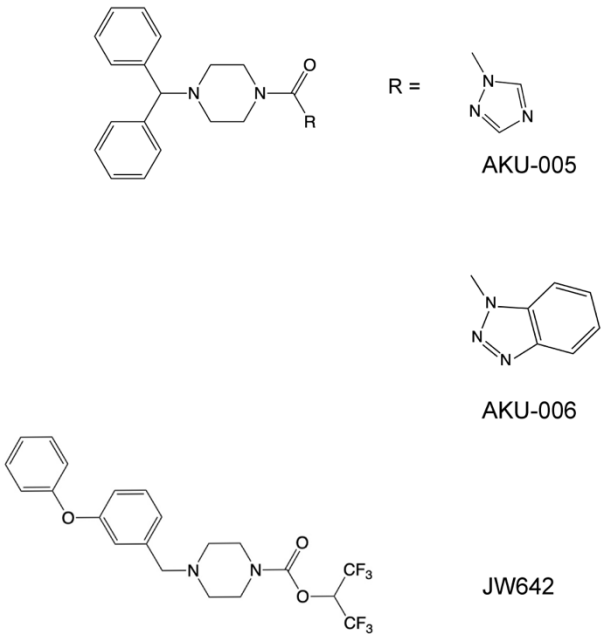

Figure 3-S1. Structures of inhibitors used for TAMRA-fluorophosphonate profiling of lysophospholipase activities.

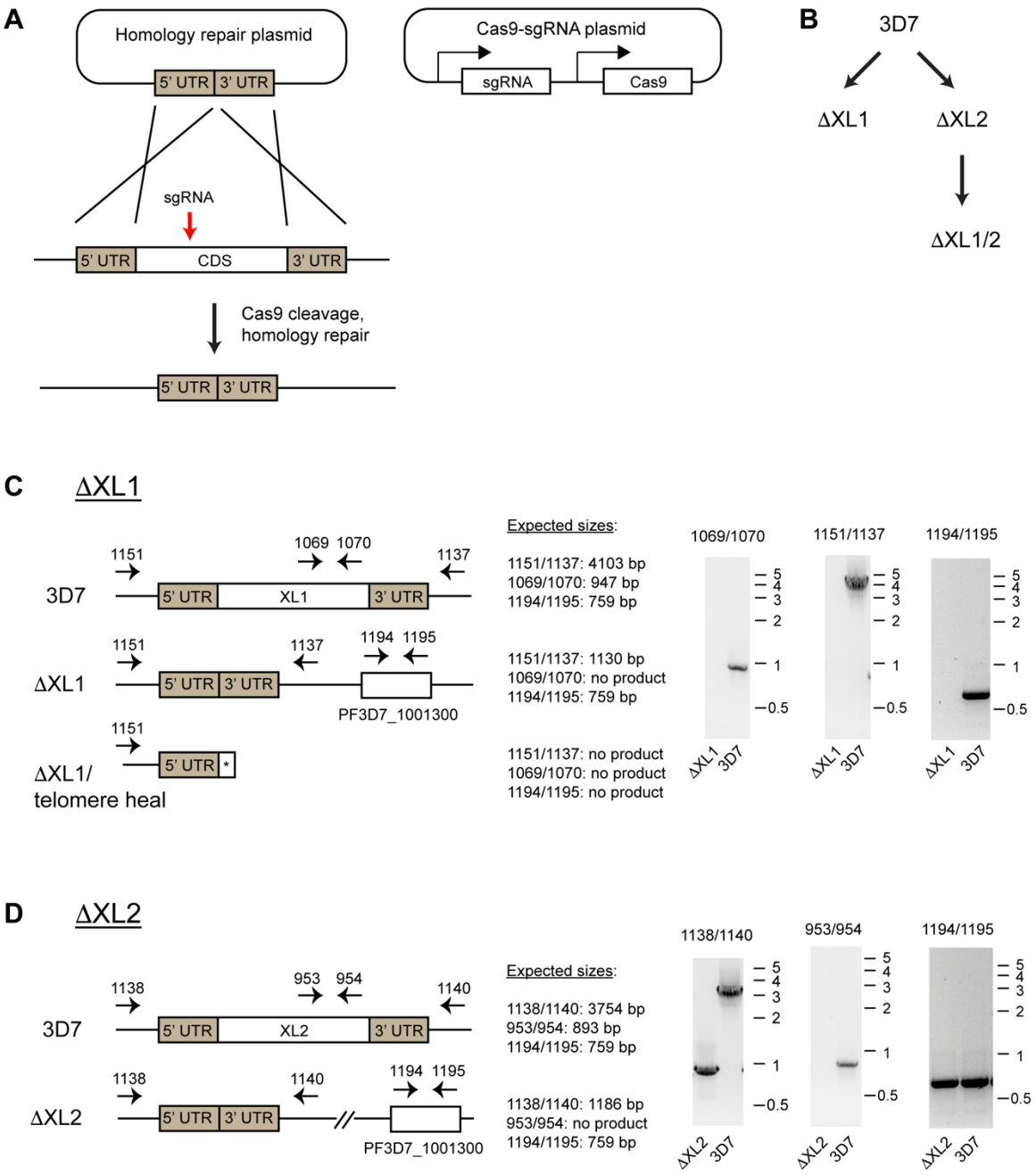

Figure 3-S2. Continued on next page.

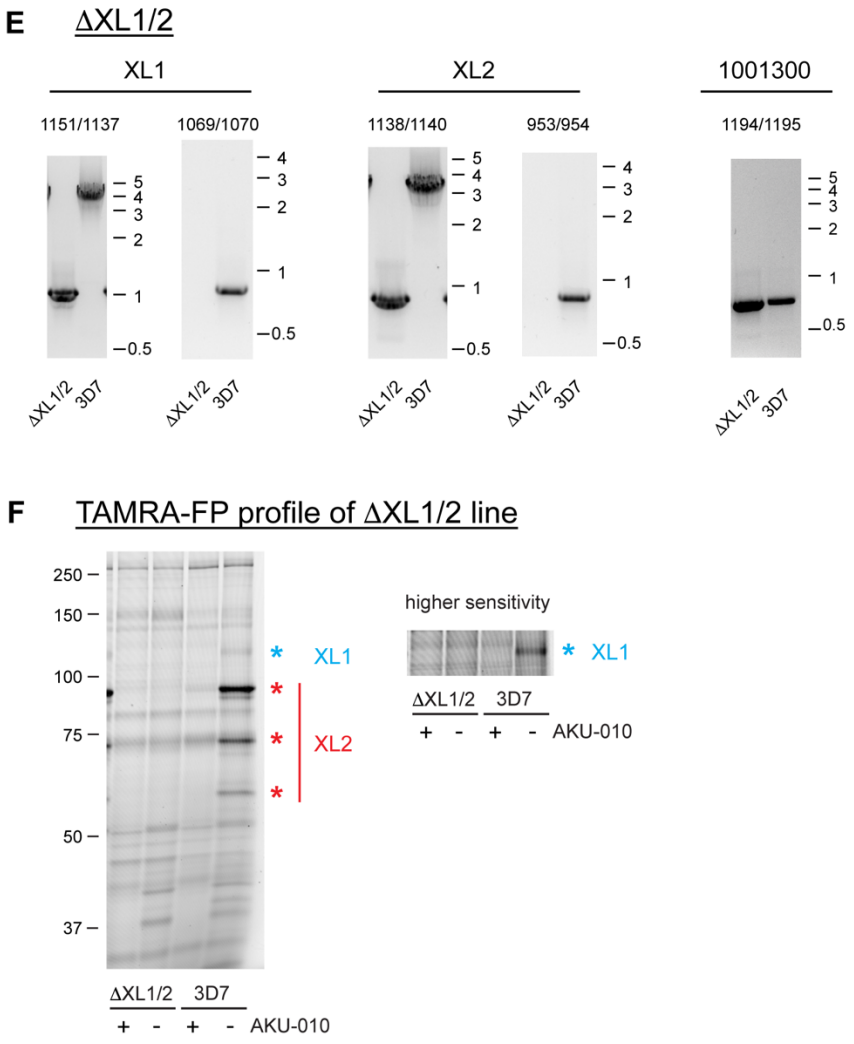

Figure 3-S2. Creation of XL1 and XL2 single and double knockout lines. (A) CRISPR-Cas9 strategy used for deletion of the entire coding sequences (CDS) of XL1 and XL2. UTR, untranslated region. The sgRNA targets a site in the CDS, shown schematically. (B) Lineage of single and double knockout lines. c-e: PCR analysis of knockout genotypes. Sizes of markers are indicated in kilobases. Introns in XL1, XL2 and PF3D7_1001300 are not shown for clarity. (C) Loss of XL1 occurred through "telomere healing", evidenced by the absence of PF3D7_1001300. (D) Deletion of the XL2 CDS occurred through the expected homology repair mechanism. (E) Deletion of the XL1 CDS in the DXL2 line occurred through the expected homology repair mechanism as indicated by the presence of PF3D7_1001300. (F) TAMRA-fluorophosphonate profiling of ΔXL1/2 and 3D7 lines. 1 µM AA74-1 was present to inhibit human APEH. The panel on the right side has been contrast-adjusted to visualize the lighter XL1 band. AKU-010 was added at 10 µM. Sizes of markers are indicated in kilodaltons. Curved lines in the images are Newton's rings, an interference pattern that occurs during fluorescence scanning when glass plates are closely apposed.

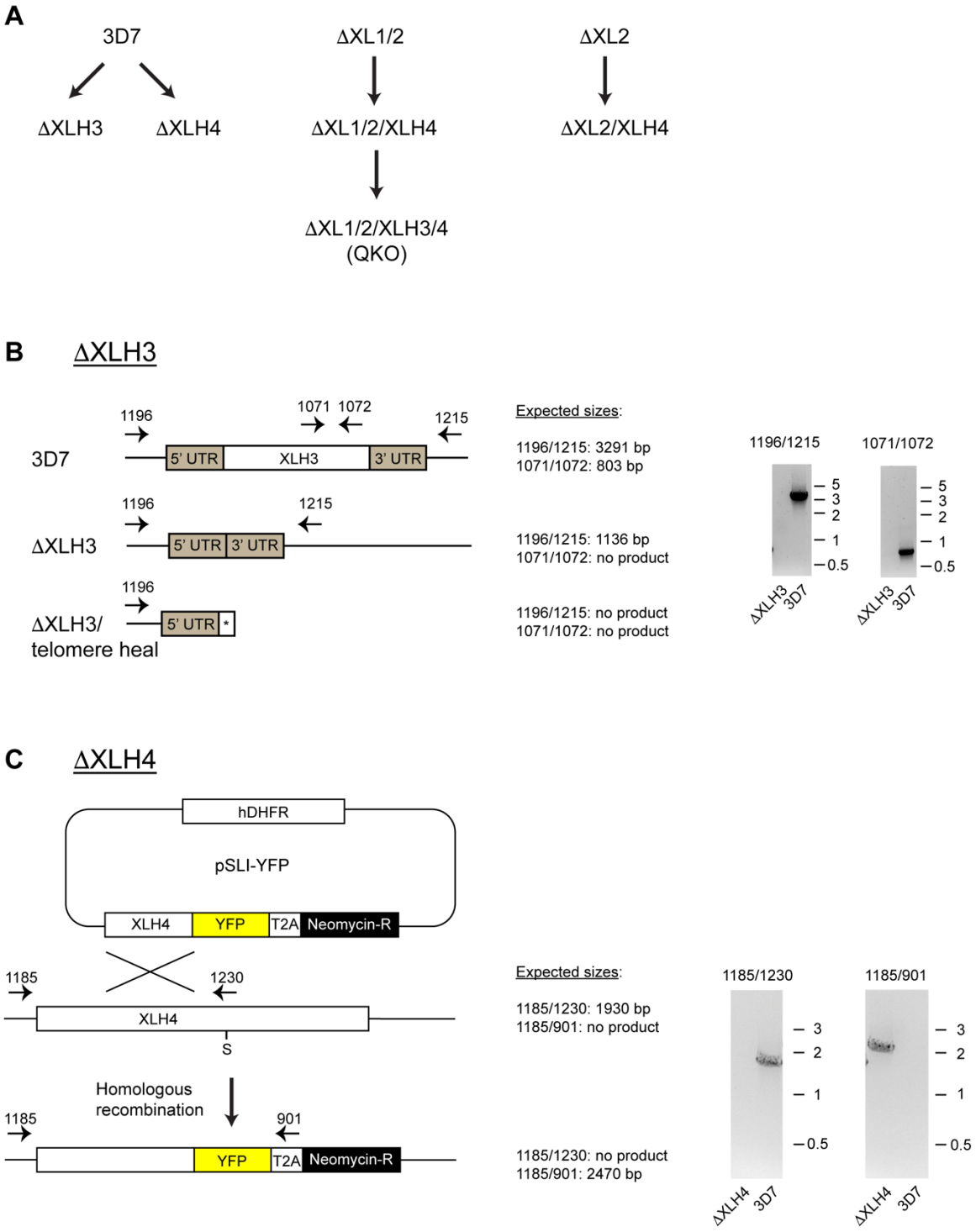

Figure 3-S3. Continued on next page.

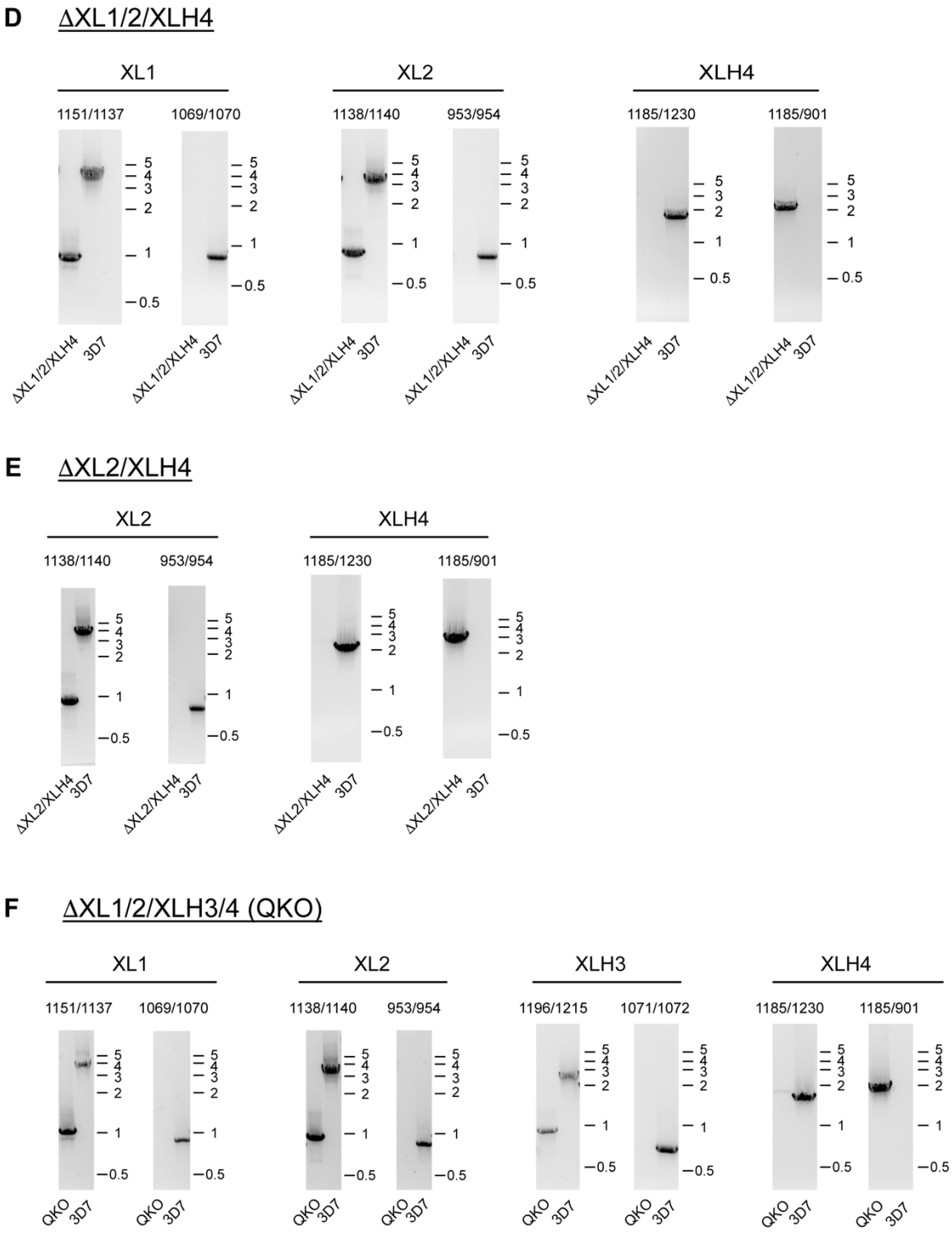

Figure 3-S3. Continued on next page.

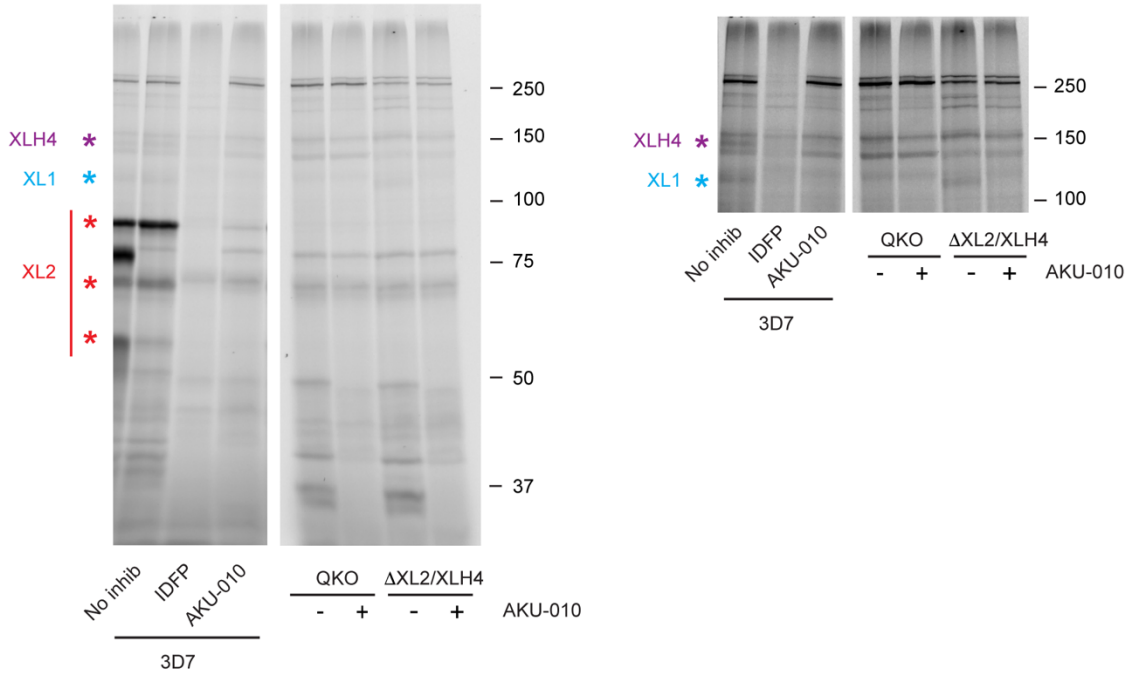

Figure 3-S3. Generation of XLH3 and 4 knockout lines. (A) Lineages of parasite lines involving disruption of XLH3 and XLH4. QKO, quadruple knockout. b-f: PCR genotyping of knockout lines. See Figure 3-S2 for positions of PCR primers used for XL1 and XL2 genotyping and expected sizes. Positions of markers are indicated in kilobases. (B) Generation of an XLH3 single knockout by markerless CRISPR-Cas9 editing. The Cas9 cleavage was repaired by telomere healing. (C) Disruption of the XLH4 coding sequence through homologous recombination and selection-linked integration. The position of the catalytic serine (S) is indicated. T2A, ribosome skip peptide. (D) Disruption of XLH4 on a ΔXL1/2 background. (E) Disruption of XLH4 on a ΔXL2 background. (F) Disruption of XLH3 on a ΔXL1/2/XLH4 background. XLH3 was repaired by recombination with the donor plasmid, not by telomere healing. QKO, quadruple knockout. (G) TAMRA-fluorophosphonate profiling of two independent XLH4-deficient lineages. 1 μM AA74-1 was present to inhibit human APEH. Panels on the right side have been contrast-adjusted to visualize the lighter XL1 and XLH4 bands. IDFP and AKU-010 were added at 10 μM. Sizes of markers are indicated in kilodaltons.

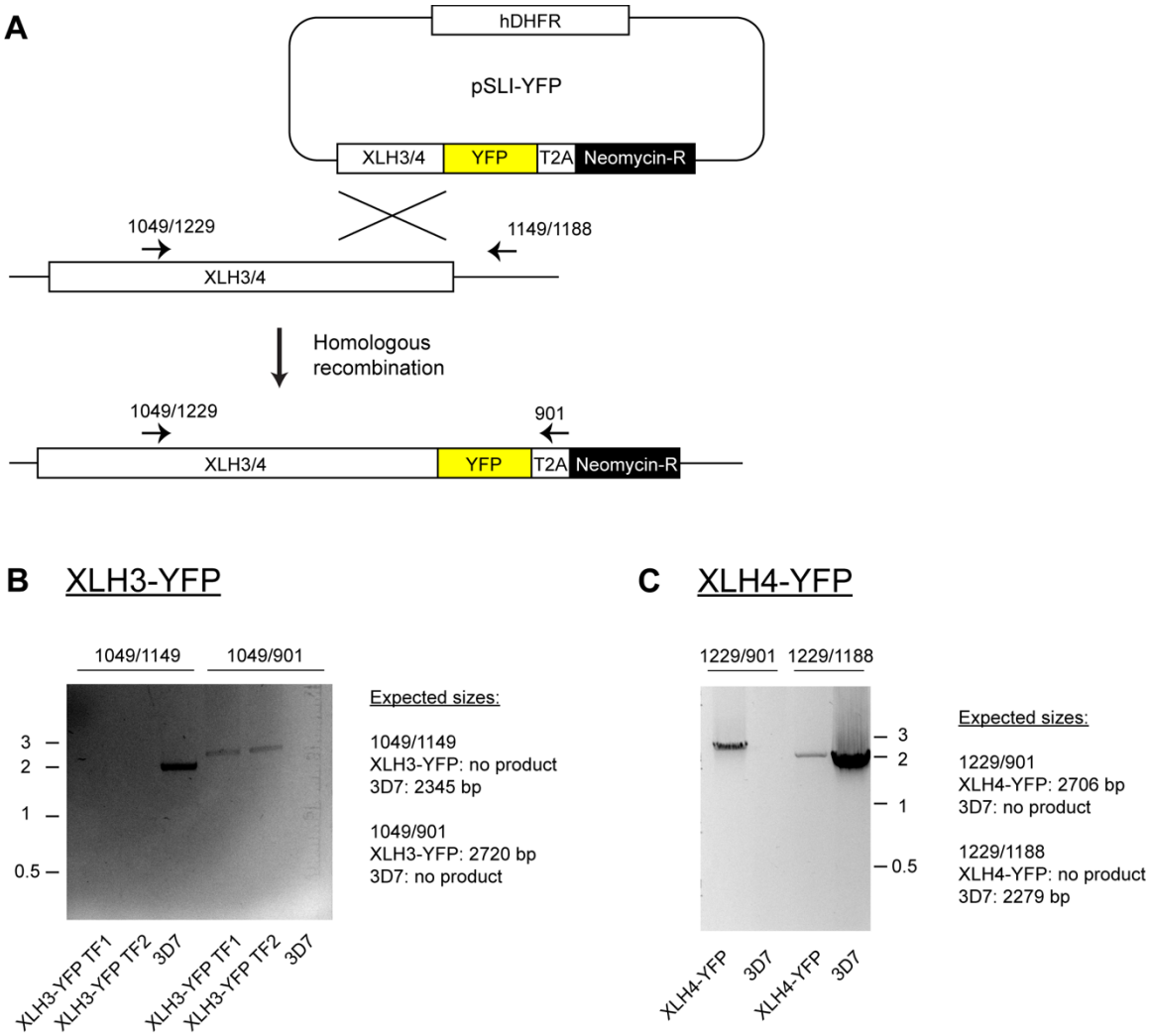

Figure 3-S4. Generation of parasite lines encoding C-terminal YFP fusions with endogenous XLH3 or XLH4. (A) Strategy for tagging of endogenous loci by homologous recombination and selection-linked integration. PCR primers used for genotyping are shown in the order XLH3/XLH4. (B) Genotyping of XLH3-YFP lines. Two independent transfections (TF1, TF2) were analyzed. (C) Genotyping of an XLH4-YFP line

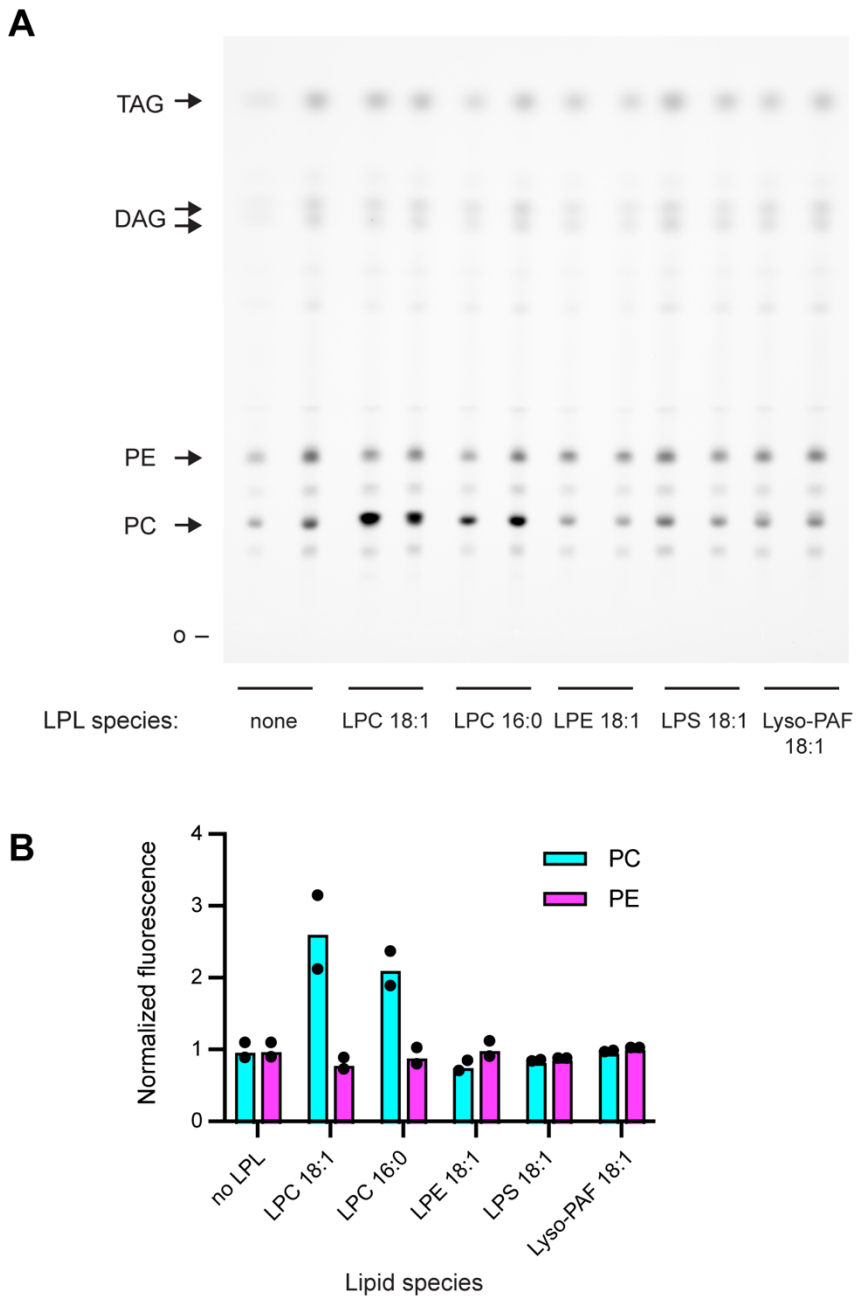

Figure 3-S5. LPC is required for enhanced PC synthesis during oleate alkyne labeling of QKO parasites. (A) TLC image of oleate alkyne labeling assays conducted with QKO parasites and the indicated lysophospholipids (30 μM). Duplicate cultures were labeled, extracted and spotted for each. o, origin. DAG is resolved into 1,2- and 1,3-isomers. Lyso-PAF, lyso-platelet activating factor, a non-hydrolyzable LPC analog. (B) Quantitation of PC and PE fluorescence intensities. Mean values and individual data points are shown. Fluorescence values were normalized with BTC fluorescence and the mean value for "no LPL" was set to 1.

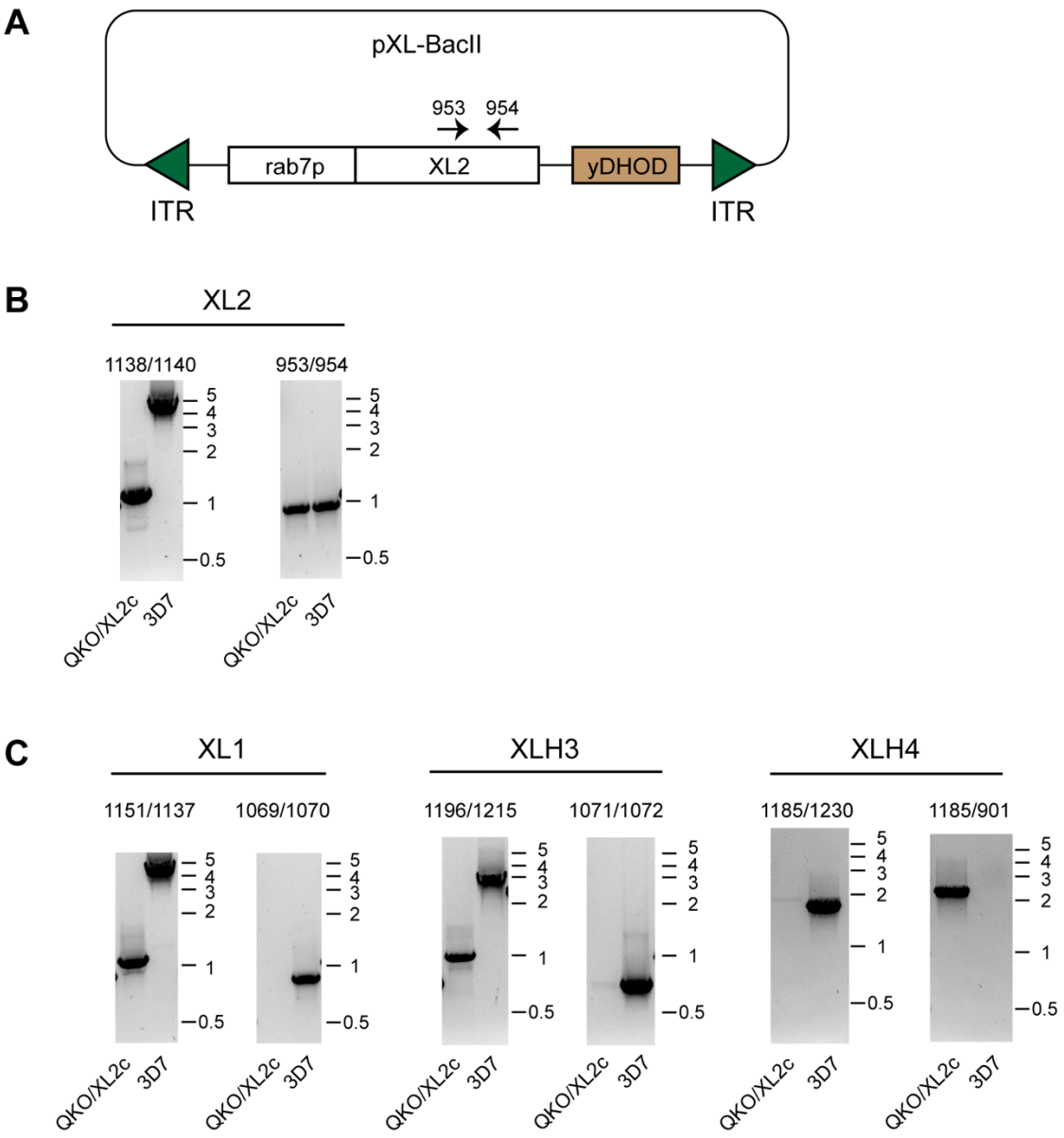

Figure 3-S6. Complementation of the QKO line with XL2. (A) Design of the piggybac transposon-based XL2 expression cassette for complementation of the QKO line (termed QKO/XL2c). The XL2 coding sequence retains the single intron from the genomic sequence (not shown). XL2 expression is driven by the PfRab7 promoter. A yeast dihydroorotate dehydrogenase (yDHOD) cassette confers resistance to DSM-1. ITR, inverted terminal repeat. (B) PCR gentotyping with XL2-specific primers confirms the absence of the genomic coding sequence (1138/1140) and the introduction of a transposon-derived coding sequence (953/954). (C) PCR gentotyping of XL1, XLH3 and XLH4 alleles confirms their knockout status. See Figure 3-S2 and 3-S3 for primer positions and expected sizes of PCR products.

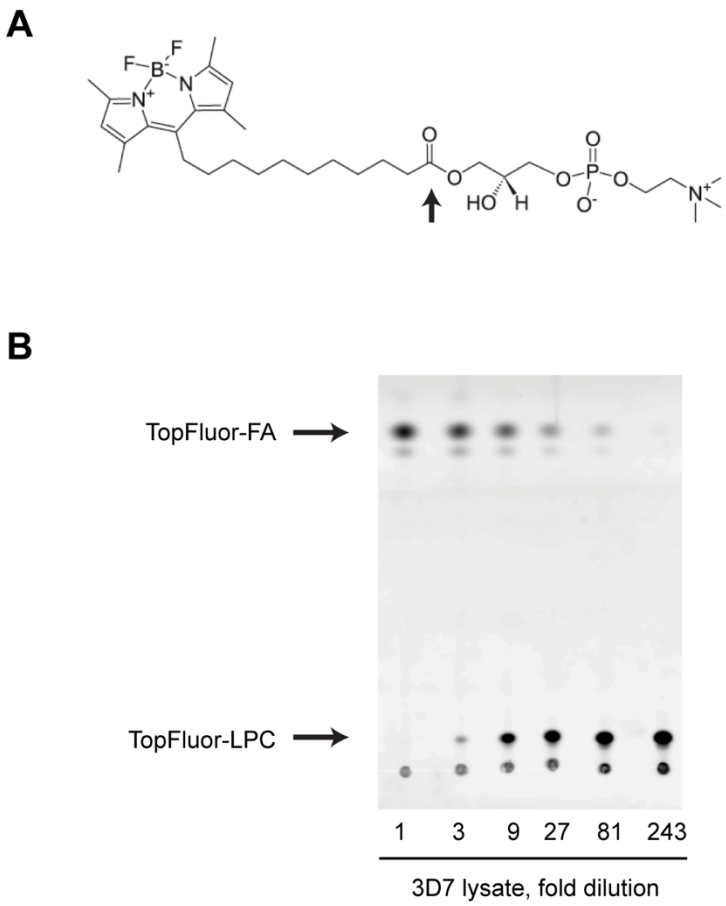

Figure 3-S7. *In vitro* assay for lysophospholipase activity in cell lysates. (A) Structure of the TopFluor-LPC substrate. The ester bond hydrolyzed by A1-type lysophospholipases is indicated with an arrow. (B) Resolution of TopFluor-LPC and the TopFluor-fatty acid (FA) hydrolysis product by thin layer chromatography. Serial dilution of a lysate of MACS-enriched 3D7 parasites is shown. Positions of TopFluor-LPC and TopFluor-FA standards are indicated with arrows.

Chapter 4

Plasmodium falciparum prodrug activation and resistance esterase is involved in lysophosphatidylcholine metabolism

Jiapeng Liu, Seema Dalal and Michael Klemba

Department of Biochemistry, Virginia Tech

Running Head: *P. falciparum* prodrug activation and resistance esterase

4.1 ABSTRACT

Understanding the metabolic processes will shed light on the treatment to malaria. Lysophosphatidylcholine (LPC) hydrolysis is important for asexual stage *Plasmodium falciparum* parasite growth by providing fatty acids (FAs) and choline for lipid synthesis. The *P. falciparum* genome encodes 17 putative lysophospholipases. Using chemical biology and genetic approaches, we have identified that red blood cell (RBC)-localized exported lipase (XL) 2 and cytosolic exported lipases homolog (XLH) 4 contribute to most LPC hydrolysis in the asexual stage. However, remaining LPC hydrolysis was observed in parasites without XLs and XLHs, which is likely due to the existence of other lysophospholipases. Lysophospholipases inhibitor AKU-010 can inhibit several serine hydrolases (SHs) besides XLs and XLHs, including an esterase the mutation of which can mediate drug resistance, termed *Plasmodium falciparum* prodrug activation and resistance esterase (PfPARE). Utilizing ΔPfPARE parasites and PfPARE conditional knockdown parasites on XL/XLH deficient background, we discovered that PfPARE contributes to parasite growth and LPC metabolism on XL/XLH deficient background, although the contribution of PfPARE is limited with the existence of XLs and XLHs. Parasites deficient in PfPARE, XLs and XLHs have little LPC hydrolysis and can hardly utilize LPC as FA source for growth. We also observed that PfPARE is membrane-bound, which is different to the previous discovery.

KEYWORDS: *Plasmodium*, malaria, serine hydrolase, PfPARE, esterase, lysophospholipase,

4.2 INTRODUCTION

We have applied chemical biology and genetic approaches to identify lysophospholipases involved in LPC hydrolysis (Chapter 3). We discovered that RBC-localized XL2 and cytosolic XLH4 contribute to most LPC hydrolysis in the asexual stage. However, parasites deficient in XLs and XLHs still exhibited a higher *in vitro* LPC hydrolysis than uninfected RBC (Figure 3-3G) and could still use LPC as sole source of FAs for growth (Figure 3-4A), which suggests that there are other enzymes besides XLs and XLHs contributing to LPC hydrolysis.

The 17 *P. falciparum* putative lysophospholipases can be roughly classified into 3 clusters: XL and XLH family with 4 members, patatin-like phospholipases with 4 members and another putative lysophospholipases family with 9 members (Plasmodb.org[1]). The putative 9-member lysophospholipases family includes PfPARE and another three members verified to have lysophospholipase A1 activity termed lysophospholipase (LPL) 1, 3 and 20[2-4]. Using activity-based protein profiling (ABPP) on XL/XLH deficient parasites via TAMRA-fluorophosphonate (TAMRA-FP)[5,6], we noticed that lysophospholipase inhibitor AKU-010 showed inhibition on at least another 4 targets (Figure 3-S3G), including PfPARE, a dispensable esterase the mutation of which mediates drug resistance[7-9].

We determined the impact of PfPARE on parasite growth and LPC metabolism using ΔPfPARE parasites and conditional knockdown parasites on XL/XLH deficient background. Loss of PfPARE on wild type (wt) background had no impact while loss of PfPARE on XL/XLH deficient background led to a slower growth. Parasites deficient in

PfPARE, XLs and XLHs exhibited little ability to release FA from LPC and couldn't grow in medium that LPC acts as the only FA source.

4.3 RESULTS

Loss of PfPARE led to a slower growth on XL/XLH deficient background but not on wild type background

We determined the effect of PfPARE on parasite growth. ΔPfPARE parasites[8] (a stop codon was inserted in front of the catalytic domain so that the catalytic activity of PfPARE was disrupted) exhibited no difference compared to wt parasites growing in Albumax (Figure 4-1A). We validated the activity of PfPARE in ΔPfPARE parasites was disrupted successfully using saponin treated parasites via TAMRA-FP[5,6], a fluorescent probe which can bind to the active site serine in SHs covalently (Figure 4-1A). We also generated PfPARE conditional knockdown parasites on XL/XLH deficient background using TetR-DOZI approach[10] (Figure 2-4C and 4-S1). PfPARE knockdown parasites on XL/XLH deficient background exhibited slower growth 6 days after removing the ligand, although no change on parasite growth was observed before day 6 probably due to the residual activity of PfPARE (Figure 4-1B). We validated that the expression of PfPARE was knocked down successfully 6 days after removing the ligand using activity-based protein profiling (ABPP) on parasite-invaded RBCs (about 90% parasitemia, Figure 4-1B). We reasoned that PfPARE had impact on parasite growth on XL/XLH deficient background but not on wt background because only a small amount of choline was present due to limited LPC hydrolysis in parasites deficient in XLs and XLHs. We complemented

parasites with choline and discovered that the growth of parasites deficient in PfPARE, XLs and XLHs was recovered (Figure 4-1C).

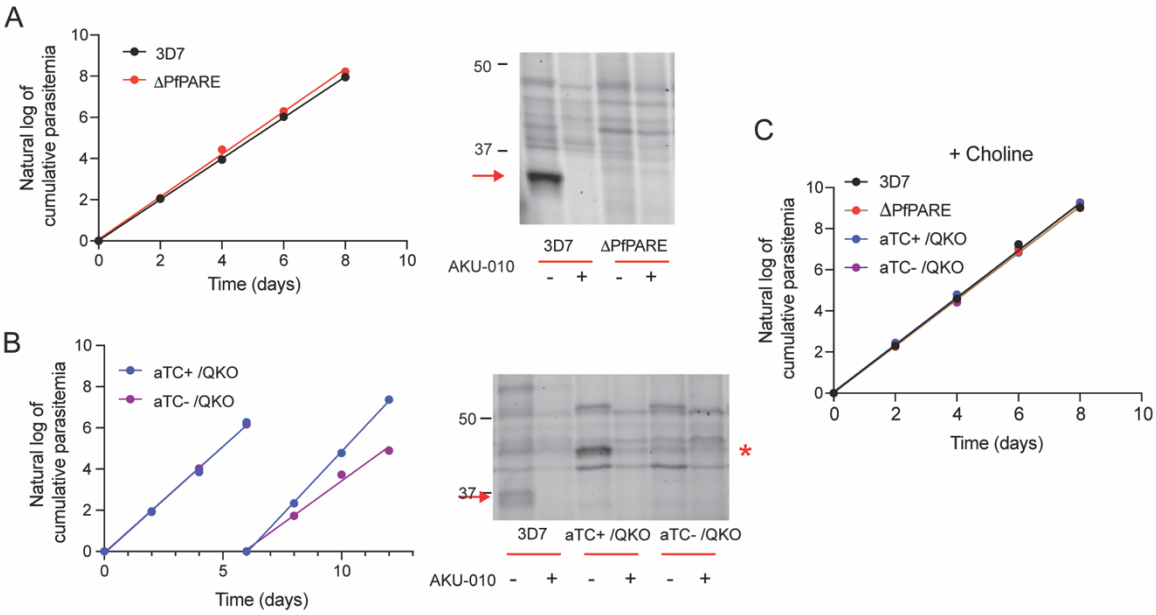

Figure 4-1. Loss of PfPARE leads to a slower growth on XL/XLH deficient background but not on wild type background. (A) ΔPfPARE parasites have a similar growth rate as 3D7. Left, growth curve of ΔPfPARE and 3D7 parasites. Right, TAMRA-FP profiling of saponin treated parasites reveals the expression of PfPARE was disrupted successfully. AKU-010 was used to inhibit PfPARE and was added at 10 µM. Red arrow indicates PfPARE. (B) PfPARE has impact on parasite growth on XL/XLH deficient background. Left, growth curve of PfPARE TetR-DOZI parasites on XL/XLH deficient background after removing the ligand anhydrotetracycline. Right, TAMRA-FP profiling of parasite-invaded RBC reveals the expression of PfPARE was knocked down successfully 11 days after removing the ligand. 3-human influenza hemagglutinin (3HA) tagging of PfPARE results in a mass increase. AKU-010 was used to inhibit PfPARE and was added at 10 µM. Red arrow indicates PfPARE. Red asterisk indicates PfPARE-3HA. aTC, anhydrotetracycline. (C) Choline addition recovers the slow growth caused by the loss of PfPARE, XLs and XLHs. Choline was added at 2 mM. aTC+ /QKO and aTC- /QKO represent PfPARE TetR-DOZI parasites on XL/XLH deficient background with or without aTC, respectively.

Parasites loss of PfPARE and XLs/XLHs had little ability to release FA from LPC and are not able to proliferate in medium that LPC acts as the sole FA source

We verified PfPARE having impact on parasite LPC metabolism using competitive FA uptake assay. Firstly, we applied an *in situ* competitive oleic acid alkyne uptake assay (Figure 3-2D), which was designed based on the result that unlabeled FA liberated from LPC could compete with oleic acid alkyne for the incorporation into parasite lipids and led to a reduction of labeled FA in parasite lipids. ΔPfPARE parasites exhibited no significant difference with 3D7 (Figure 4-2A), which indicated that the contribution of PfPARE on LPC hydrolysis is limited. This was not surprising because we have verified that most LPC hydrolysis in the asexual stage is conducted by XL2 and XLH4 (Chapter 3). We assumed that *in situ* competitive oleic acid alkyne uptake assay might not be sensitive enough to detect remaining LPC hydrolysis in XL/XLH deficient parasites since the relative fluorescence of "+ LPC to – LPC" is about 1 in neutral lipids. Instead, we applied an *in situ* competitive fluorescent FA uptake assay to detect remaining LPC hydrolysis (Figure 3-1A and 4-2B). ΔPfPARE parasites exhibited no difference from 3D7 (Figure 4-2B). We observed LPC addition reduced near 70% fluorescence in parasite triacylglycerol (TAG) in XL/XLH deficient background while only about 20% in parasites deficient in PfPARE and XLs/XLHs, which suggests that PfPARE is important for releasing FA from LPC in parasites deficient in XLs/XLHs. Combined with the observation that LPC addition reduced near 98% fluorescence in wt parasites, there was little FA releases from LPC in parasites without PfPARE and XL/XLHs.

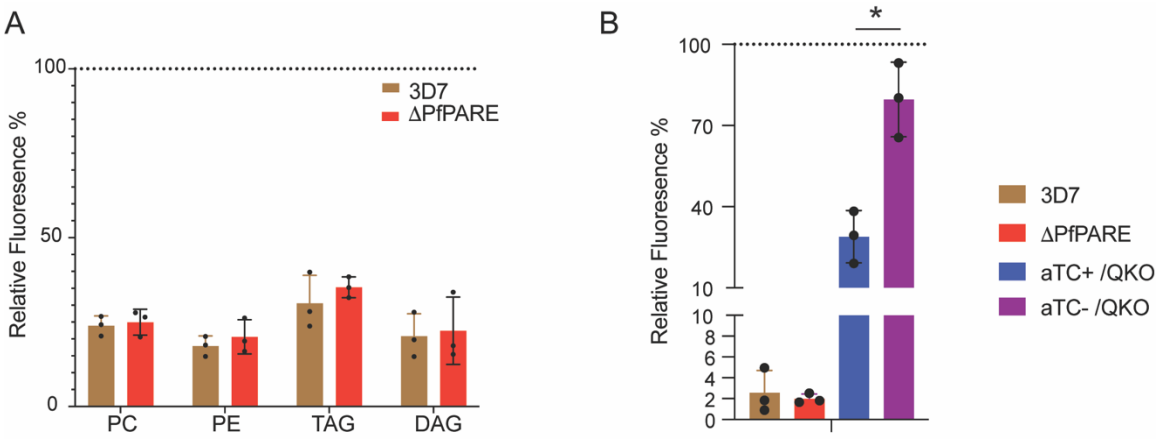

Figure 4-2. PfPARE contributes to LPC metabolism. (A) Oleate acid alkyne profiling of ΔPfPARE and 3D7 parasites. Means and standard deviations are from three independent experiments. Significance relative to 3D7 was assessed within lipid groups using a two-tailed Welch's *t*-test. no asterisk, $p \geq 0.05$. (B) TAG C1,C12-FA profiling of 3D7, ΔPfPARE and PfPARE TetR-DOZI parasites on XL/XLH deficient background with and without ligand. Means and standard deviations are from three independent experiments. Significance between "aTC+ /QKO" and "aTC- /QKO" group was assessed using a two-tailed Welch's *t*-test. *, p <0.01. aTC+ /QKO and aTC- /QKO represent PfPARE TetR-DOZI parasites on XL/XLH deficient background with or without aTC, respectively.

We then determined the effect of PfPARE on parasites using LPC as sole FA source for growth. ΔPfPARE parasites behaved similar with wt parasites (Figure 4-3), while loss of PfPARE on XL/XLH deficient background rendered parasites unable to utilize LPC for proliferation (less than 0.5% parasitemias were observed for all LPC concentrations). These results verified that PfPARE contributes to LPC metabolism in the asexual stage, although its contribution is limited.

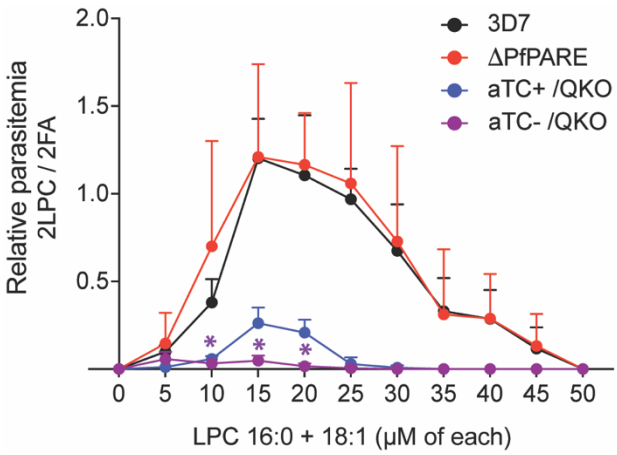

Figure 4-3. Parasites deficient in PfPARE and XLs/XLHs are not able to use LPC as a sole source of fatty acids for growth. Parasites were grown for one generation in a minimal-lipid medium containing either two LPC ("2LPC") or two fatty acid species ("2FA"), Means and standard deviations are shown for three biological replicates. Significance between "aTC+ /QKO" and "aTC- /QKO" group was assessed using a two-tailed Welch's *t*-test. *, p <0.05. aTC+ /QKO and aTC- /QKO represent PfPARE TetR-DOZI parasites on XL/XLH deficient background with or without aTC, respectively.

PfPARE locates to parasite membranes

We detected the cellular location of PfPARE using microscopy on yellow fluorescent protein (YFP)-tagged parasites (Figure 4-4). Different to previous study[8], we observed PfPARE locates to the membranes instead of the cytosol. PfPARE is mainly accumulated to the periphery of the parasite. It can also be detected on the membrane in the parasite.

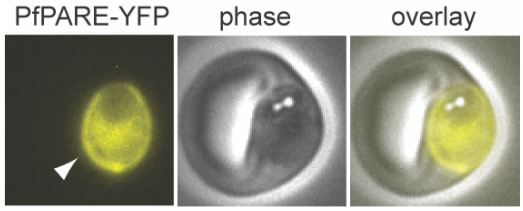

Figure 4-4. PfPARE locates to the membranes at the periphery of the parasite and in the parasite. White arrow indicates the signal of PfPARE at the periphery of the parasite.

4.4 DISCUSSION

Determining the function of *P. falciparum* proteins will expand our knowledge on parasite life processes and provide new insights on the treatment to malaria. We focused on PfPARE, an esterase the mutation of which can mediate drug resistance and showed that PfPARE is involved in LPC metabolism. Parasites deficient in PfPARE, XLs and XLHs contains little ability to release FA from LPC and cannot utilize LPC as sole FA source for growth.

During the development of asexual stage *P. falciparum* parasites, a near 6-fold increase of phospholipids in mature parasite-invaded RBCs was observed compared to the uninvaded RBCs[11] because of the expansion of parasite membranes and biosynthesis of parasitophorous vacuole membrane (PVM) and various organelles. Besides, parasites also produce a large quantity of neutral lipids and store them in the lipid droplet[12,13]. Thus, parasites exert a great demand for FAs. However, FA *de novo* synthesis by the parasites can meet little on the total demand of the FAs in the asexual stage[14,15] and parasites have to obtain the FA from the host[16,17]. Parasites mainly use two sources of FAs, free FAs from host plasma or FA hydrolyzed from LPC by lysophospholipase A1[18,19]. We demonstrated XL2 and XLH4 have the major contribution to asexual stage LPC hydrolysis in Chapter 3. However, we observed remaining LPC hydrolysis in the parasites after loss of XLs/XLHs, which may be contributed by other lysophospholipases. We verified that PfPARE contribute to parasite releasing FA from LPC using *in situ* assays, although the contribution of PfPARE on LPC hydrolysis is limited and can be only detected on XL/XLH deficient background. Together, our study suggests that in *P. falciparum* infected-RBCs, most exogenous LPC is hydrolyzed in the RBCs by XL2. The remaining LPC that escapes from

hydrolysis may be hydrolyzed further by PfPARE at the points of contact between host cell and parasite membranes[20,21]. Then LPC that comes into the parasite will be hydrolyzed to release FA by cytosolic XLH4, which may also be facilitated by the membrane-bound PfPARE. We also showed parasites deficient in PfPARE, XLs and XLHs can hardly release FA from LPC and are not able to use LPC as sole FA source for growth, which suggests that the contribution of LPL1, 3, 20 on releasing FA from LPC may be trivial.

The contribution of PfPARE on parasite growth is also limited on wt background. However, in XL/XLH-deficient parasites, because the amount of choline is low due to the lack of LPC hydrolysis, the effect of PfPARE on parasite growth can be detected, which can be complemented by addition of choline to the parasites.

PfPARE may have other functions on releasing FA from LPC. A homolog of PfPARE, termed *Plasmodium falciparum* monoacylglycerol lipase-like protein (PfMAGLLP, 53% identity), was verified to exhibit monoacylglycerol lipase (MAGL) activity[22]. We also showed PfPARE can be inhibited by a series human MAGL inhibitor previously[5]. Together with the enzymatic function prediction according to Plasmodb.org[1], PfPARE may have MAGL activity. LPC may be hydrolyzed by phospholipase Cs that generate phosphocholine and monoacylglycerol (MAG). At least one phospholipase C termed *Plasmodium falciparum* neutral sphingomyelinase (PfNSM) was found to be able to hydrolyze LPC[23]. PfPARE may be able to hydrolyze MAG which is generated from LPC hydrolysis by phospholipase C to release FA. Besides, we recently found that parasites can also scavenge FA from MAG, which may be contributed by PfPARE.

Although we and others[8] showed that PfPARE is dispensable for asexual stage parasite growth, it may have important roles in other stages. PfPARE has a much higher

expression in gametocytes than the asexual stage, especially in stage V gametocytes[24]. Besides, the expression of PfPARE in female gametocytes is more than 40-fold higher than in male gametocytes[25]. These suggest that PfPARE may be important in gametocyte development and sex determination. Determining the functions of PfPARE through life cycle will expand our understanding on *Plasmodium* biology.

4.5 MATERIALS AND METHODS

Reagents

BODIPY^{TM} 500/510 C_1, C_{12} (C1,C12-FA) and saponin were purchased from ThermoFisher. The origin of other reagents can be found from Chapter 2 and 3.

Parasite culture, generation of plasmids, parasite transfection and growth assay in Albumax can be found from Chapter 2.

Growth in medium containing choline

Anhydrotetracycline was removed more than 10 days before the assay started. Growth assays were conducted the same way as growth assay in Albumax (Chapter 3) excepted 2mM choline chloride was added to medium.

Generation of saponin-treated parasite lysate

About 100 mL synchronized schizont stage parasites (~36-44 h post-invasion) with ~10% parasitemia was pelleted, treated with 40 mL 0.03% (w/v) saponin in cold phosphate buffered saline (PBS) and incubated on ice for 10 minutes. The suspension was pelleted,

washed with PBS and stored at – 80 °C. Parasite yield was determined with a hemocytometer. The pellet was resuspended with cold PBS containing 5 μM pepstatin A and 10 μM E-64 to a density of 5 x 10^8 parasites/mL. The parasite suspension was sonicated three times for eight seconds using a microtip at 30% maximum power. The suspension was centrifuged at 12,000 x*g* at 4 °C. The supernatant was aliquoted, snap frozen in liquid nitrogen and stored at – 80 °C.

MACS purification, TAMRA-FP analysis, oleate acid alkyne competition assay for inhibition of LPC hydrolysis *in situ* and growth in medium containing LPC as sole source of fatty acids can be found from Chapter 3.

C1,C12-FA competition assay for assessing LPC hydrolysis *in situ*

Assays were modified from C4,C9-FA competition assay for inhibition of LPC hydrolysis *in situ* (Chapter 3). Briefly, parasites were labeled with 1 μM BODIPY-TR-ceramide (BTC) in complete RPMI for 1 hour. Parasites were then washed with fatty acid-free RPMI medium for 3 times and incubated with pre-warmed incomplete RPMI containing 3 mg/mL fatty acid-free BSA, 30 μM C1,C12-FA and 30 μM LPC 18:1 (or 50% ethanol for no-LPC controls) for 40 minutes with gentle mixing on an orbital rotator at 37 °C in a CO_2 incubator. Reactions were harvested and lipids were extracted and analyzed as C4,C9-FA competition assay.

ACKNOWLEDGMENTS

We are grateful to Dr. Daniel Goldberg (Washington University in St. Louis) for providing ΔPfPARE parasites[8], Dr. Josh Beck (University of Iowa) for the CRISPR/Cas9 plasmids, Dr. Sean Prigge (Johns Hopkins University) for the TetR-DOZI plasmids and Dr. Tapio Nevalainen (University of Eastern Finland) for providing AKU-010 inhibitor. M. K. discloses support for this work USDA National Institute of Food and Agriculture HATCH project VA-160082.

REFERENCES

1 Aurrecoechea, C. *et al.* PlasmoDB: a functional genomic database for malaria parasites. *Nucleic Acids Research* **37**, D539-D543 (2009).

2 Asad, M. *et al.* An essential vesicular-trafficking phospholipase mediates neutral lipid synthesis and contributes to hemozoin formation in *Plasmodium falciparum*. *BMC Biology* **19**, 1-22 (2021).

3 Sheokand, P. K. *et al.* GlmS mediated knock-down of a phospholipase expedite alternate pathway to generate phosphocholine required for phosphatidylcholine synthesis in *Plasmodium falciparum*. *Biochemical Journal* **478**, 3429-3444 (2021).

4 Sheokand, P. K. *et al.* A *Plasmodium falciparum* lysophospholipase regulates host fatty acid flux via parasite lipid storage to enable controlled asexual schizogony. *Cell Reports* (2023).

5 Elahi, R. *et al.* Functional annotation of serine hydrolases in the asexual erythrocytic stage of *Plasmodium falciparum*. *Scientific reports* **9**, 1-11 (2019).

6 Patricelli, M. P. *et al.* Direct visualization of serine hydrolase activities in complex proteomes using fluorescent active site-directed probes. *Proteomics* **1**, 1067-1071 (2001).

7 Butler, J. H. *et al.* Resistance to some but not other dimeric lindenane sesquiterpenoid esters is mediated by mutations in a *Plasmodium falciparum* esterase. *ACS Infectious Diseases* **6**, 2994-3003 (2020).

8 Istvan, E. S. *et al.* Esterase mutation is a mechanism of resistance to antimalarial compounds. *Nature communications* **8**, 1-8 (2017).

9 Sindhe, K. M. *et al. Plasmodium falciparum* resistance to a lead benzoxaborole due to blocked compound activation and altered ubiquitination or sumoylation. *MBio* **11**, e02640-02619 (2020).

10 Rajaram, K. *et al.* Redesigned TetR-aptamer system to control gene expression in *Plasmodium falciparum*. *MSphere* **5**, e00457-00420 (2020).

11 Vial, H. J. & Ancelin, M. L. Malaria lipids, in Malaria: parasite biology, biogenesis, protection. *American Association of Microbiology Press* (1998).

12 Palacpac, N. M. Q. *et al.* Developmental-stage-specific triacylglycerol biosynthesis, degradation and trafficking as lipid bodies in *Plasmodium falciparum*-infected erythrocytes. *Journal of Cell Science* **117**, 1469-1480 (2004).

13 Gulati, S. *et al.* Profiling the Essential Nature of Lipid Metabolism in Asexual Blood and Gametocyte Stages of *Plasmodium falciparum*. *Cell Host & Microbe* **18**, 371-381 (2015).

14 Vaughan, A. M. *et al.* Type II fatty acid synthesis is essential only for malaria parasite late liver stage development. *Cellular Microbiology* **11**, 506-520 (2009).

15 van Schaijk, B. C. *et al.* Type II fatty acid biosynthesis is essential for *Plasmodium falciparum* sporozoite development in the midgut of *Anopheles* mosquitoes. *Eukaryotic Cell* **13**, 550-559 (2014).

16 Vial, H. J. & Ancelin, M. L. Malarial lipids. *Intracellular Parasites*, 259-306 (1992).

17 Vial, H. J. *et al.* Phospholipid Biosynthesis in Synchronous *Plasmodium falciparum* Cultures 1. *The Journal of protozoology* **29**, 258-263 (1982).

18 Vial, H. *et al.* Phospholipid metabolism in *Plasmodium*-infected erythrocytes: guidelines for further studies using radioactive precursor incorporation. *Parasitology* **98**, 351-357 (1989).
19 Brancucci, N. M. *et al.* Lysophosphatidylcholine regulates sexual stage differentiation in the human malaria parasite *Plasmodium falciparum*. *Cell* **171**, 1532-1544. e1515 (2017).
20 Elmendorf, H. G. & Haldar, K. *Plasmodium falciparum* exports the Golgi marker sphingomyelin synthase into a tubovesicular network in the cytoplasm of mature erythrocytes. *Journal of Cell Biology* **124**, 449-462 (1994).
21 Tamez, P. A. *et al.* An erythrocyte vesicle protein exported by the malaria parasite promotes tubovesicular lipid import from the host cell surface. *PLoS Pathogens* **4**, e1000118 (2008).
22 Yoo, E. *et al.* The Antimalarial Natural Product Salinipostin A Identifies Essential α/β Serine Hydrolases Involved in Lipid Metabolism in *P. falciparum* Parasites. *Cell Chemical Biology* **27**, 143-157.e145 (2020).
23 Hanada, K. *et al. Plasmodium falciparum* phospholipase C hydrolyzing sphingomyelin and lysocholinephospholipids is a possible target for malaria chemotherapy. *The Journal of experimental medicine* **195**, 23-34 (2002).
24 López-Barragán, M. J. *et al.* Directional gene expression and antisense transcripts in sexual and asexual stages of *Plasmodium falciparum*. *BMC Genomics* **12**, 587 (2011).
25 Lasonder, E. *et al.* Integrated transcriptomic and proteomic analyses of *P. falciparum* gametocytes: molecular insight into sex-specific processes and translational repression. *Nucleic Acids Research* **44**, 6087-6101 (2016).

SUPPLEMENTARY INFORMATION

Table 4-S1. Oligonucleotides used in this study for plasmid construction and diagnostic PCR. Abbreviations: CDS, coding sequence; HA, homology arm; pKD, homology repair plasmid used to generate TetR-DOZI parasite; UTR, untranslated region.

Oligo Number	Sequence	Function	Sequence
1381	PfPARE, CDS	sgRNA	TAAGTATATAATATTTACTTGTTC TTCTTGTTTGGGTTTTAGAGCTAG AA
1382	PfPARE, CDS	sgRNA	TTCTAGCTCTAAAACCCAAACAA GAAGAACAAGTAAATATTATATA CTTA
1387	PfPARE, 3' CDS	HA1, CRISPR repair	GATATCGTCCACCTGGATATCTT TACGTCTTACTCCTGGTTTACG
1388	PfPARE, 3' CDS	HA1, CRISPR repair	CATAAGGATAGACGTCTACTTGT TCTTCCTGCTTAGGGGTATGGAC AGCTAGCCATG
1389	PfPARE, 3' UTR	HA2, CRISPR repair	CCCTTTCCGGGCGCGCCTTTAAT GAAGCGTATTATACTGACG
1390	PfPARE, 3' UTR	HA2, CRISPR repair	GATATCCAGGTGGACGATATCGG AAGAATGGATTAAGAGAAAAAG
1413	PfPARE, CDS	Diagnostic PCR	AGCTGGTATGATATCTATAGATG AG
1407	pKD	Diagnostic PCR	CCAGACAGTGGGCCCTTATGCG
1214	pKD	Diagnostic PCR	ATTATTATATTTAACTATATACTA TGG
1414	PfPARE, 3' UTR	Diagnostic PCR	CAATTTTGTATACACAAAATAAG TTGC

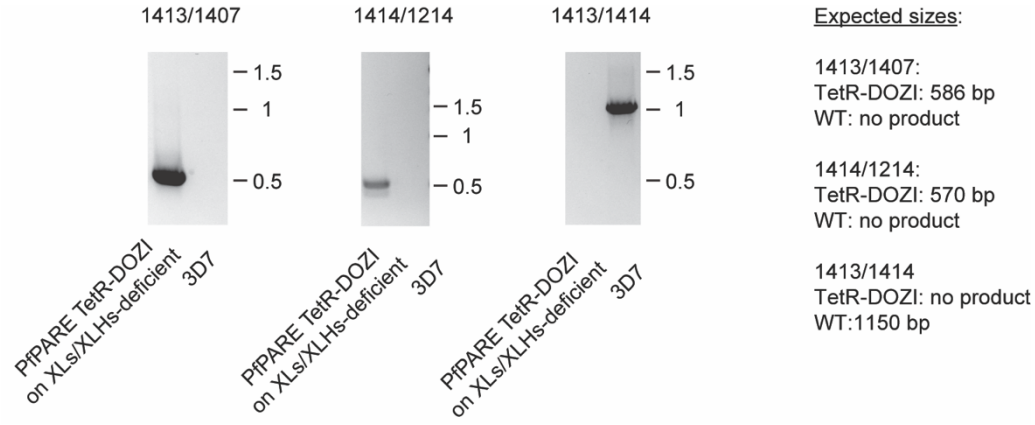

Figure 4-S1. Generation of PfPARE conditional knockdown parasites through TetR-DOZI method. PCR analysis of PfPARE TetR-DOZI on XLs/XLHs deficient background and wt parasites. Primer 1413/1407 are used for integration check on 3'CDS, primer 1414/1214 are used for integration check on 3'UTR and primer 1413/1414 are used for wt check. Sizes of markers are indicated in kilobases.

CHAPTER 5

Summary and Conclusion

5.1 SUMMARY AND FUTURE DIRECTIONS

The deadliest human malaria parasite *Plasmodium falciparum* causes nearly a half million deaths annually[1]. New druggable target identification and drug development are urgently needed to deal with the malaria issue. The *P. falciparum* genome contains more than 50 serine hydrolases (SHs)[2], which use nucleophile serine to catalyze hydrolysis reaction. However, most of them remained uncharacterized. Determining the essentially and characterize their functions will shed light on future drug development to treat malaria. To address this issue, we focused on a likely essential depalmitoylase in the asexual stage termed PfABHD17A and enzymes important for releasing fatty acids (FAs) from lysophosphatidylcholine (LPC) including exported lipases (XLs), exported lipases homolog (XLHs) and *P. falciparum* prodrug activation and resistance esterase (PfPARE). We demonstrated that these SHs are important for parasite growth in the asexual stage.

We identified essential metabolic SHs in the asexual stage based on our previous proteomic study[2] and a mutagenesis study on identifying essential genes in the asexual stage[3]. PfABHD17A, a human depalmitoylase homolog, is identified as essential for it was refractory to gene disruption. Although the essentiality verification through conditional knockdown parasites was not successful, we conducted an inhibitor screen and verified the function of PfABHD17A through chemical biology approach. Human depalmitoylase inhibitor ML211 inhibits PfABHD17A and merozoite invasion, combined with the location of PfABHD17A on the rhoptries and the depalmitoylase activity of PfABHD17A *in vitro*, we suggest that PfABHD17A is essential in merozoite invasion for regulating palmitoylation status of rhoptry proteins.

Asexual stage *P. falciparum* parasites have to acquire FAs from the host to support their survival[4,5]. Two forms of FAs can by uptake by the parasites: free FAs in the plasma or the FAs hydrolyzed from LPC[6,7]. LPC hydrolysis is also important for parasites by providing parasites

choline for phospholipid synthesis and regulates sexual differentiation[7]. However, enzymes responsible for the hydrolysis of LPC are unknown. Understanding how LPC is hydrolyzed by the parasites will not only fill the knowledge gap in LPC metabolism but may also identify new druggable targets to treat malaria.

Combined chemical biology and genetic approaches, we successfully identified enzymes responsible for LPC hydrolysis from 17 putative *P. falciparum* lysophospholipases (Plasmodb.org[8]). Using an assay to assess *in situ* LPC hydrolysis, we identified a series of structurally-related serine hydrolase inhibitors which can provide an inhibitory signature of key parasite lysophospholipases. By competitive activity-based profiling of the serine hydrolases inhibitors, we identified that a family of four lysophospholipases termed exported lipases (XLs) and exported lipases homologs (XLHs) are candidates in LPC hydrolysis. We generated a series of knockout parasite lines on XLs/XLHs and discovered that red blood cell (RBC)-localized XL2 and parasite-localized XLH4 contributed to most LPC hydrolysis in the asexual stage. Parasites deficient in XL2 and XLH4 exhibited defect in using LPC for growth and detoxified from the accumulated LPC. Besides, parasites deficient in XL2 and XLH4 or treated by lysophospholipases inhibitor are not able to grow in human serum. Our study not only discovered the process of how parasites hydrolyzing exogenous LPC to acquire FAs for its own lipid synthesis, but also provided the basis for targeting enzymes involved in LPC hydrolysis to treat malaria.

XL/XLH deficient parasites exhibited a great decrease in LPC hydrolysis. However, there was remaining LPC hydrolysis in XL/XLH deficient parasites probably caused by other putative lysophospholipases. We focused on PfPARE, a target of lysophospholipases inhibitor and homolog of enzymes exhibiting lysophospholipase activity[9-11]. Via conditional knockdown parasites, we showed that parasite membrane located PfPARE contributes to parasite growth and

LPC metabolism in the asexual stage on XL/XLH deficient background, although loss of PfPARE on wild type parasites has little effect. Parasites loss of XLs, XLHs and PfPARE exhibited little ability to release FA from LPC and cannot grow using LPC as sole FA source for growth.

Our study suggests that PfABHD17A is essential in merozoite invasion. However, the substrates of PfABHD17A need to be further identified and the regulation of PfABHD17A on the substrates need to be validated. Using acyl-biotin exchange and metabolic labeling via clickable palmitic acid analog which were established to identify palmitoylated proteins in asexual stage parasites[12], we will be able to identify and verify the substrates of PfABHD17A. Giving the existence of rhoptry in sporozoites, PfABHD17A may be also important in sporozoites. The *P. falciparum* genome includes only 4 ABHD17s but not the other homologs of the current known human depalmitoylases acyl-protein thioesterases (APTs), palmitoyl-protein thioesterases (PPTs) and alpha/beta hydrolase domain containing 10 (ABHD10), which suggests that PfABHD17s may be the only enzymes having depalmitoylase activity. Although PfABHD17B/C/D is dispensable in the asexual stage, they may be essential in other stages. PfABHD17B/D have much higher expression in gametocytes and the mosquito stage than the asexual stage[13,14], which suggests they may have important functions in gametocyte or mosquito stage development.

We discovered that XLs, XLHs and PfPARE are important for LPC metabolism in the asexual stage and verified that parasites deficient in XLs/XLHs and PfPARE can hardly grow in medium that LPC act as the sole source of FAs. We observed that phosphatidylcholine (PC) is hyperproduced for about 10-fold in parasites having little LPC hydrolysis. The most reasonable explanation for this is that PC is derived from direct acylation from LPC to PC. At least LPC acyltransferase (LPCAT) 1 and a trifunctional enzyme containing LPCAT activity termed peroxiredoxin 6 were verified to be expressed in RBCs[15,16]. However, we validated that RBC LPC

acylation contributes little to the PC hyperproduction in XL and XLH deficient parasites. Thus, the LPCAT is encoded by the parasite genome. The *P. falciparum* genome encodes one homolog (PF3D7_0914200) of human LPCATs. However, our preliminary data showed that this putative LPCAT is not responsible for PC hyperproduction when LPC hydrolysis is deficient in the parasite.

The effect of XLs/XLHs and PfPARE on gametocytogenesis and gametocyte development need to be further determined. LPC depletion, in which LPC hydrolysis but not the role as signaling molecule triggers the sexual commitment of asexual stage parasites[7], thus loss of enzymes responsible for LPC hydrolysis may has a similar effect as loss of LPC, that loss of XLs/XLHs and PfPARE may promote gametocytogenesis. Although XLH3 has little impact in the asexual stage, it has a much higher expression in gametocytes and was detected in early phase of gametocytogenesis[13,17], which suggests that XLH3 may influence gametocytogenesis and gametocyte development. The expression of PfPARE is much higher in gametocytes than the asexual stage, especially in stage V gametocytes[13] and the expression of PfPARE in female gametocytes is more than 40-fold higher than that in male gametocytes[18], which indicate that PfPARE may be important in gametocyte development and sex determination.

Although we have characterized the functions of several SHs in the asexual stage, a large number of SHs still remain understudied. Understanding their functions may provide new solutions to deal with the malaria issue.

REFERENCES

1 WHO. World malaria report 2022. (2022).

2 Elahi, R. *et al.* Functional annotation of serine hydrolases in the asexual erythrocytic stage of *Plasmodium falciparum*. *Scientific reports* **9**, 1-11 (2019).

3 Zhang, M. *et al.* Uncovering the essential genes of the human malaria parasite *Plasmodium falciparum* by saturation mutagenesis. *Science* **360**, eaap7847 (2018).

4 Vial, H. J. & Ancelin, M. L. Malarial lipids. *Intracellular Parasites*, 259-306 (1992).

5 Vial, H. J. *et al.* Phospholipid Biosynthesis in Synchronous *Plasmodium falciparum* Cultures 1. *The Journal of protozoology* **29**, 258-263 (1982).

6 Vial, H. *et al.* Phospholipid metabolism in *Plasmodium*-infected erythrocytes: guidelines for further studies using radioactive precursor incorporation. *Parasitology* **98**, 351-357 (1989).

7 Brancucci, N. M. *et al.* Lysophosphatidylcholine regulates sexual stage differentiation in the human malaria parasite *Plasmodium falciparum*. *Cell* **171**, 1532-1544. e1515 (2017).

8 Aurrecoechea, C. *et al.* PlasmoDB: a functional genomic database for malaria parasites. *Nucleic Acids Research* **37**, D539-D543 (2009).

9 Asad, M. *et al.* An essential vesicular-trafficking phospholipase mediates neutral lipid synthesis and contributes to hemozoin formation in *Plasmodium falciparum*. *BMC Biology* **19**, 1-22 (2021).

10 Sheokand, P. K. *et al.* GlmS mediated knock-down of a phospholipase expedite alternate pathway to generate phosphocholine required for phosphatidylcholine synthesis in *Plasmodium falciparum*. *Biochemical Journal* **478**, 3429-3444 (2021).

11 Sheokand, P. K. *et al.* A *Plasmodium falciparum* lysophospholipase regulates host fatty acid flux via parasite lipid storage to enable controlled asexual schizogony. *Cell Reports* (2023).

12 Jones, M. L. *et al.* Analysis of protein palmitoylation reveals a pervasive role in *Plasmodium* development and pathogenesis. *Cell Host & Microbe* **12**, 246-258 (2012).

13 López-Barragán, M. J. *et al.* Directional gene expression and antisense transcripts in sexual and asexual stages of *Plasmodium falciparum*. *BMC Genomics* **12**, 587 (2011).

14 Zanghì, G. *et al.* A Specific PfEMP1 Is Expressed in *P. falciparum* Sporozoites and Plays a Role in Hepatocyte Infection. *Cell Reports* **22**, 2951-2963 (2018).

15 Soupene, E. *et al.* Mammalian acyl-CoA: lysophosphatidylcholine acyltransferase enzymes. *Proceedings of the National Academy of Sciences of the United States of America* **105**, 88-93 (2008).

16 Wagner, M. P. *et al.* Human peroxiredoxin 6 is essential for malaria parasites and provides a host-based drug target. *Cell Reports* **39**, 110923 (2022).

17 Silvestrini, F. *et al.* Protein export marks the early phase of gametocytogenesis of the human malaria parasite *Plasmodium falciparum*. *Molecular and Cellular Proteomics* **9**, 1437-1448 (2010).

18 Lasonder, E. *et al.* Integrated transcriptomic and proteomic analyses of *P. falciparum* gametocytes: molecular insight into sex-specific processes and translational repression. *Nucleic Acids Research* **44**, 6087-6101 (2016).